Looking through the Noise

Improved algorithms for genetic variant detection

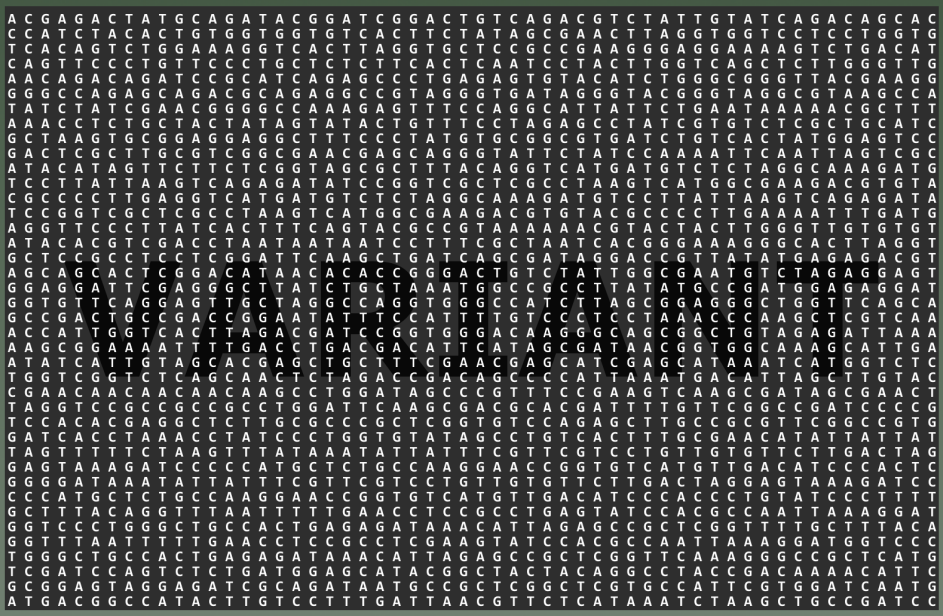

Leonard F. Johansson

Looking through the Noise

Improved algorithms for genetic variant detection

Leonard F. Johansson

Leonard Fredericus Johansson. **Looking through the noise: improved algorithms for genetic variation detection.** Thesis, University of Groningen, with summary in English and Dutch.

The research presented in this thesis was mainly performed at the Department of Genetics, University Medical Center Groningen, University of Groningen, Groningen, the Netherlands. Part of the work in this thesis was financially supported by ZONMW, grant no 40-41200-98-9159, Netherlands CardioVascular Research Initiative (CVON2011–19; Genius), and the Netherlands Organization or Scientific Research (NOW) VIDI grant number 917.164.455 received by Morris A. Swertz.

Printing of this thesis was financially supported by Rijksuniversiteit Groningen, University Medical Center Groningen.

Cover design and layout by L.F. Johansson. The front cover shows a variant that can only be seen when looking through the noise created by the four DNA nucleotides A, C, G and T.

Printed by XX, XX.

© 2019 L.F. Johansson. All rights reserved. No part of this book may be reproduced or transmitted in any form or by any means without permission of the author.

ISBN: XXX-XX-XXX-XXXX-X ISBN (electronic version): XXX-XX-XXX-XXXX-X

umcg

rijksuniversiteit groningen

rijksuniversiteit
groningen

Looking through the noise improved algorithms for genetic variation detection

Proefschrift

ter verkrijging van de graad van doctor aan de
Rijksuniversiteit Groningen
op gezag van de
rector magnificus prof. dr. E. Sterken
en volgens besluit van het College voor Promoties.

De openbare verdediging zal plaatsvinden op

maandag X X 201X om XX.XX uur

door

Leonard Fredericus Johansson

geboren op 29 mei 1980
te Hefshuizen

Promotor
Prof. dr. R.H. Sijmons
Copromotores
Prof. dr. M.A. Swertz
Dr. B. Raddatz
Beoordelingscommissie
Prof. dr. XX
Prof. dr. XX
Prof. dr. XX

Paranimfen
XX
XX

Contents

Chapter 1

Introduction

1.1 A short history on chromosomes and DNA

In 1865 the Augustinian friar and scientist Gregor Mendel was the first to give a systematic account of the heredity of traits following specific laws [135]. In the following decades it was discovered that during cell division a substance in the cell nucleus, dubbed *chromatin* (stainable substance) by German biologist Walther Flemming, was divided over the two halves of the cells during a process that Flemming called *mitosen*, or mitosis [183, 65, 40]. A few years later, in 1890, German histologist Richard Altmann noted the presence of granules in cells that he believed were elementary organisms enclosed within cells, features later renamed 'mitochondria' by German microbiologist Carl Benda [4, 12]. In 1888, German anatomist Wilhelm Waldeyer was the first to use the term chromosomen – chromosomes, meaning colored bodies – to describe the individual pieces of chromatin thread [225, 40]. In the last decade of the 19th century, the German biologist August Weismann proposed that the chromosomes were the bearers of hereditary material, which he called keimplasma, or germ plasm [232]. At the time he was unaware of Mendel's work. However, after its rediscovery at the turn of the century, the cytologists Walter Sutton, from the United States of America, and Theodor Boveri, from Germany, both showed that chromosomes follow Mendelian laws [206, 23, 24, 42].

The chromosome theory of heredity quickly became the leading theory in the field that became known as genetics, a term introduced by the English biologist William Bateson in 1905 [100]. Around the same time, he and his colleagues observed coupling between different traits in pea plants [224, 123], leading the British biologist Thomas Morgan, upon further Drosophila studies, to state that 'we find "associations of factors" that are located near together in the chromosomes' [140]. This led to the theory of linkage a few years later [139]. It was several more decades before the normal human chromosome number was correctly defined as 46 by Indonesian cytogeneticist Joe Hin Tjio in 1956 [210]. After that it took only a few more years, until 1959, for French scientists Lejeune, Gauthier and Turpin to connect Down syndrome to the presence of a small extra chromosome [109]. One year later, the Philadelphia-based researchers Hungerford and Nowell discovered a small abnormal chromosome present in people with human chronic myelogenous leukemia, demonstrating the use of cytogenic techniques in diagnosis of hematological diseases [153]. This chromosome was later named the 'Philadelphia chromosome' and shown to be the product of translocation between chromosomes 9 and 22 [172]. In the meantime, based on work by British physicist Maurice Wilkins and chemist Rosalind Franklin, American biologist James Watson and British physicist Francis Crick created the

double-helix DNA model containing the four nucleotides – Adenine, Cytosine, Guanine and Thymine – which are paired A=T and G≡C [229, 235, 68]. Several years later Crick and his team inferred – without being able to sequence – the triplet DNA-protein translation code [41, 240]. However, it was not until the following decade, when British Chemist Frederick Sanger invented DNA sequencing methods, that the DNA sequence itself could be read [179, 180]. In 1963, it was discovered that apart from the nucleus, mitochondria also contained DNA [145]. In 1983, Huntington's disease was the first human disease to be linked to a specific genomic marker [83]. In the following years more diseases were linked to genomic markers and genetic diagnostics expanded from analysis of chromosomes to inclusion of DNA analysis. After the invention of Polymerase Chain Reaction (PCR), DNA analysis became much easier [175, 174] and at the turn of the 21st century scientists were able to create a draft sequence of the human genome [105, 219].

The introduction of so-called next-generation sequencing in 2005 ushered in the start of yet another era [131]. Sequencing costs decreased rapidly to the point that a whole genome can now be sequenced for less than 1000 dollars [77], opening up new possibilities for human genome analysis and bringing the fields of cytogenetics and molecular genetics closer together[1].

1.2 Human genome variation

With improving genomic analysis techniques came increasing knowledge about the composition of the human genome. When comparing any two individuals, their six billion base pair human genome will show many differences, or DNA variants. On average, everyone has around three million DNA variants that differ from the major allele present in the population, of which 10.000-11.000 are non-synonymous variants that change the triplet code and result in an amino-acid change of a protein [54]. Most of those variations do not cause disease but, as will be discussed in section 1.6, some variants are associated with or can contribute to a congenital disorder or a predisposition for the development of a disease. Several types of DNA variants can be distinguished. The smallest are Single Nucleotide Variants (SNVs) and indels: insertions or deletions of one or more bases (Figure 1.1A-D). When a larger stretch of DNA is lost or duplicated, the variant is considered to be structural variation

[1]Paragraph 1.1 suggests a logical and continuous timeline between discoveries. However, many of those discoveries were heavily contested and others were made by several research groups independently around the same time. This means that the history told in this paragraph could just as well have contained other names. Their omission is not meant to discredit their scientific contribution, but this introduction is too short to give a more nuanced vision of the scientific progress in genetics.

(SV) and the term Copy Number Variation (CNV) is used (Figure 1.1E-H). The size threshold to distinguish a large indel from a small CNV is arbitrary, and different definitions are used in literature. While 1 kb was traditionally used as the lower threshold for CNVs, variants larger than 50 bp are now labelled as CNVs [167, 208, 234]. In formal notation, duplication is regarded as a tandem duplication, i.e. insertion of a duplicate sequence, following directly 3'of the original copy (figure 1.1F), leaving the formal term 'insertions' to signify all other nucleotide insertions [48] (Figure 1.1D and H). However, in practice, the term duplication is used in a broader sense for copy number gains that can also include translocational insertions [97, 86]. One subset of duplications is repeat expansions in which a repeated nucleotide sequence is extended. An example of this is the CAG repeat that is extended in Huntington disease [173]. Another type of SV are translocations, in which terminal parts of chromosomes are exchanged (figure 1.1I). In reciprocal translocations both derivative chromosomes are present without an apparent net loss or gain of chromosomal content, but in so-called unbalanced translocations, the translocation results in loss of part of one chromosome and gain of part of another chromosome [128]. In Robertsonian translocations, two acrocentric chromosomes are connected at the centromere [169] (Figure 1.1J). A further type of DNA variation are inversions in which a nucleotide sequence is replaced by its reverse complement sequence [204, 48] (Figure 1.1K). While reciprocal translocations and inversions are balanced events in principle, deletions or insertions are often present around the breakpoints in both types of variations [204, 191]. A further type of chromosomal variation are aneuploidies, in which whole chromosomes are lost or gained (and can be considered as whole chromosome CNVs), such as in Down syndrome (Figure 1.1L).

1.3 Conventional techniques for variant detection

Over the years many different techniques have been developed to detect and chart the DNA constitution. The earliest was karyotyping, the technique used by Tjio and Levan, in which metaphase spreads are made that enable analysis of chromosomes using a microscope [210]. The development of chromosome staining techniques, such as Q,- C-, G- and R-banding, increased the resolution to a maximum of 5 Mb and enabled detection of smaller aberrations as well as more-specific determination of known variations [85, 120]. In situ hybridization techniques using radio- or fluorescent-labelled probes enabled detection of the presence and localization of specific parts of chromosomes [71, 11, 111]. It is particularly the latter, Fluorescence In Situ Hybridization (FISH), that paved the way for subchromosomal structural analysis, making

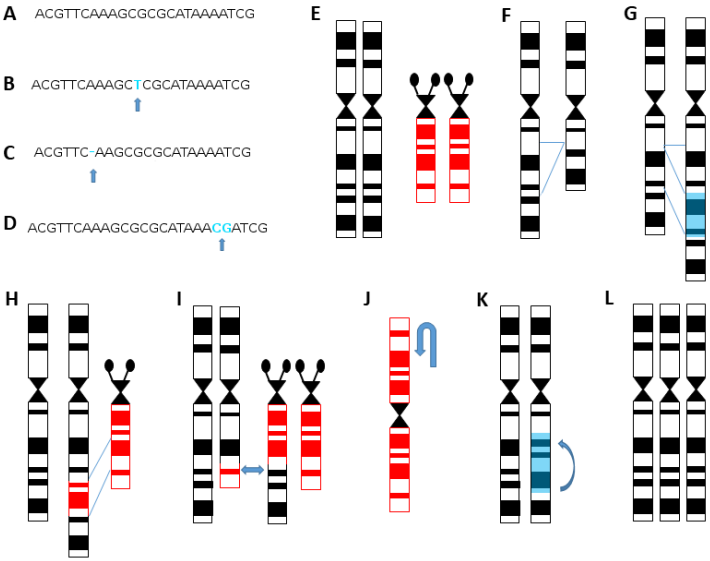

Figure 1.1: Human genome variation types: A) genomic base sequence, B) Single nucleotide variant, C) Indel: one base deletion, D) Indel: two base insertion, E) Two sets of chromosomes, F) CNV: Deletion, G) CNV: duplication, H) CNV: insertion, I) Reciprocal translocation, J) Robertsonian translocation, K) Inversion, L) Aneuploidy: trisomy

it possible to detect microdeletions of several hundreds of kilobases (kb) [43]. Further developments of this technique, such as fiber-FISH, increased the resolution to 50 kb using mechanically stretched chromosomes [166]. While these molecular techniques greatly advanced cytogenetics, analysis of solid tumors remained difficult because often no high-quality metaphases can be produced. Comparative Genomic Hybridization (CGH), an adaptation of FISH procedures, in which all patient DNA is fluorescently labelled and hybridized together with differently labelled reference DNA to high quality metaphases of a normal cell line enabled evaluation of aneuploidies, unbalanced translocations and CNVs [96]. In other words, all types of variations resulting in loss or gain of chromosomal material could be detected genome-wide to a maximum resolution of 10 Mb for deletions and 2 Mb for amplifications, without the need of patient metaphase spreads [103]. The same principle was used in array-CGH but, instead of metaphase spreads, a series of probes were used

as the hybridization target, making it possible to detect CNVs smaller than 1 kb depending on the number and placing of the probes [163, 164]. Using knowledge gained by earlier sequencing projects, it became possible to target specific SNPs, enabling the array to be used not only for CNV detection, but also as a genotyping tool [227]. A targeted technique to further enhance the resolution for CNV detection is Multiplex-Ligation Probe Amplification (MLPA), in which several targeted stretches of DNA are amplified in one experiment, after which a relative comparison is done within a series of samples. Depending on the included targets, deletions or duplications of single exons can be detected [185].

Where cytogenetics and molecular cytogenetics focused on the detection of structural variations, including copy-neutral variations and aneuploidies (figure 1.1E-L), molecular genetics focused on the detection of the nucleotide sequence, searching for SNVs, indels and repeat expansions (figure 1.1A-D). Often, Sanger sequencing was the method of choice here. However, only a short stretch of DNA of a single sample can be analyzed in a single experiment using this technique.

Variants are not always expected to be present in all cells from all tissues, as is the case with genetic mosaicism, including mitochondrial heteroplasmy, as well as in cancer. In karyotyping or FISH, a separate analysis is performed for each cell. By analyzing a large number of metaphases or nuclei, mosaicisms can be detected or excluded with high probability in the tissue studied [91, 9, 238]. Several DNA-based methods are also able to assess the presence of low fractions of a certain type of DNA in a larger pool. Real-time quantitative PCR measures fluorescence after each PCR cycle, then, through comparison with samples having a known concentration, fractions of targeted DNA stretches can be calculated for a sample [87]. Quantitative fluorescent (QF-)PCR measures the DNA concentration after a fixed number of PCR cycles [223]. A more recent addition is digital droplet PCR (ddPCR), where DNA fragments are encapsulated in oil droplets. For each droplet it is determined if a specific DNA sequence is present or not. Because tens of thousands droplets can be assessed in a single experiment, this technique has a high sensitivity for low-abundance variations [89]. It is no coincidence that so many techniques have been developed for DNA analysis, as each technique has distinct strengths and weaknesses. In karyotyping at low resolution, chromosome specific analysis can be done for the whole genome of a single cell. FISH increases resolution, but only gives information about targeted regions, while array gives high resolution whole genome information, but can't distinguish alleles and thus misses copy neutral structural variations. MLPA and Sanger sequencing have even higher resolution – the latter up to a single base pair – but, in a single experiment, are limited to analysis of a small part of

the genome. Therefore, using these conventional techniques to find all types of variations present in a single sample requires many different experiments.

1.4 Next-generation sequencing

In the mid-2000s, massive parallel sequencing was developed. With the introduction of this method, there was an immediate 50,000 fold drop in sequencing costs, resulting in the label 'next-generation sequencing' (NGS) [77]. NGS can be used for DNA as well as RNA sequencing. While the term NGS might suggest a single technique, it is in fact an umbrella-term encompassing many different technologies that sequence many DNA or RNA fragments in parallel and infer a read of the nucleotide sequence of each fragment. The first NGS platform available was developed by 454 Life Sciences using a pyrosequencing strategy [132]. Solexa then introduced NGS using reversible dye terminator chemistry [16] and Ion Torrent a non-optical system based on pH changes on nucleotide incorporation [171]. With these technologies being acquired by Roche, Illumina and Life Technologies, three strong contenders entered the short-read sequencing market. Other platforms focus on sequencing long single DNA molecules, such as Pacific Biosystems [57] and Oxford NanoPore [37], making use of real-time measurements of fluorescent signals and changes in current, respectively. Other contenders have since entered and left the NGS market, all using different chemistry and measurement tools. Because of this, technical bias is different from one technique to the other, although some genomic regions still remain a challenge for all platforms.

Although the exact methods used differ between different NGS techniques, their general approach is similar, as shown in figure 1.2, although the strong and weak points vary between the platforms. For NGS DNA analysis, various input materials can be used. Some contain fragmented DNA, such as blood plasma or formalin-fixed paraffin-embedded (FFPE) material (figure 1.2A), while others containing high quality DNA, for example white blood cells, bone marrow or cultured cells (figure 1.2B). The first step in all DNA NGS procedures is to isolate DNA from the material. In the materials where the DNA is already fragmented, short DNA fragments are isolated (figure 1.2C).

Source materials containing higher quality DNA can give rise to longer DNA-fragments (figure 1.2D) or even very long DNA fragments, if DNA breakage is prevented during isolation (figure 1.2E). The short-read sequencing methods work best when using relatively short DNA fragments. For these techniques, DNA needs to be fragmented if the input fragments are too long

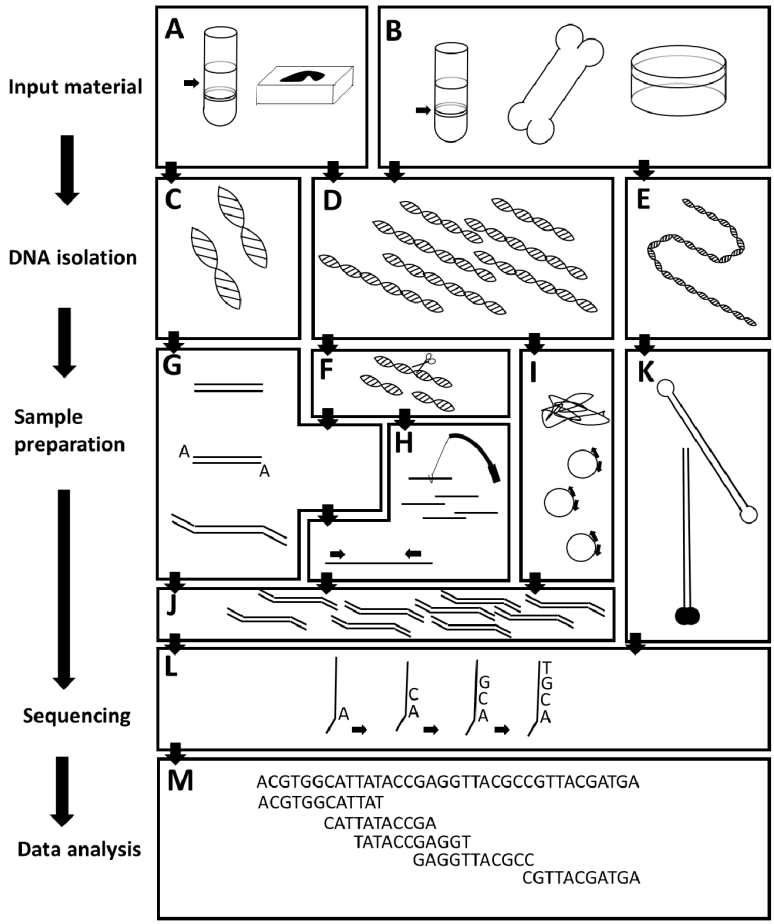

Figure 1.2: DNA Next-generation sequencing workflows. A) Sources of fragmented DNA, such as blood plasma or FFPE material, B) sources of high quality DNA, such as white blood cells, bone marrow cells or cultured cells, C) isolated fragmented DNA, D) isolated high-quality DNA, E) isolated long fragments of DNA, F) DNA fragmentation, G) sample preparation (end-repair, dA-tailing and adapter ligation), H) enrichment via capturing or amplicon sequencing), I) alternative sample preparation, such as Targeted Locus Amplification or ATAC-seq, J) PCR, K) long-read sequencing sample preparation, L) sequencing of the DNA, M) data analysis to transform sequenced DNA into sequence reads and subsequently into sample-specific genomic sequences.

(figure 1.2F). The most basic short-read strategy is whole genome sequencing (WGS). Sample preparation consists of adding so-called 'adapters' to DNA-fragments, thus making the fragments suitable for sequencing (figure 1.2G). If only a part of the genome needs to be sequenced, the DNA can be enriched for the sequences of interest (figure 1.2H). Various methods can be used to reach this goal, such as DNA capturing, in which short RNA or DNA sequences complementary to the region of interest called 'baits' are used to fish out specific parts of the genome. A second method is amplicon sequencing. Here, similar to Sanger sequencing, two primers are used that bind to their complementary sequence and copy the genomic sequence in between the primers. Such enrichment techniques are used in, for instance, whole exome sequencing (WES) and gene panels that target specific genes of interest. In addition to these 'standard' sample preparation methods, alternative sample preparations can be performed that have a different perspective on the genome (figure 1.2I), for instance using proximity ligation [200], targeted locus amplification [47], or chromatin-immunoprecipitation or by enzymatic digestion [93].

The final step in the sample preparation is PCR amplification to produce sufficient fragments of the DNA of interest to be sequenced (figure 1.2J). Alternatively, long-read sample preparation methods can be used (figure 1.2K). The bases of the DNA fragments are subsequently read by the sequencer (figure 1.2L). Data analysis is then carried to determine the nucleotide sequence of the DNA fragments, and the genomic sequence of the sample can be inferred through further processing, for instance through alignment of sequenced reads to a reference genome (figure 1.2M). Once the genomic sequence is inferred as far as possible, the presence or absence of variants can be de determined and interpreted in the context of a scientific or diagnostic question. An important step in variant calling and interpretation is to distinguish true positive and negative results from false ones. Knowing where variants can be missed, or where artefacts are more likely to occur, can be important for making a correct interpretation. Moreover, if the cause of artefacts is known, analysis procedures can be adapted to counteract sources of bias and create a more optimal balance between sensitivity and specificity.

1.5 Technical bias and error rates

Where conventional techniques have proven their worth in genetic diagnostics, NGS procedures and analysis still need to be optimized, and refining the methods to improve their sensitivity and specificity remains a challenge. The aim of the different NGS techniques is to measure the exact nucleotide sequences

of the DNA fragments. However, technical bias and sequencing errors create noise, resulting in some of the nucleotides in a sequence read being called incorrectly. This error rate is much higher for long-read technologies than for short-read sequencing. Depending on the chemistry and platform used, error rates range from 0.1% to 15% [77]. These error rates are presented as base quality scores and, when several reads are combined to infer a genotype, as a genotype quality score [149]. However, it has been shown that discordance rates between short-read samples that have been analyzed twice are higher than would be expected using the genotype quality scores [226, 182], which suggests that error rates are higher than the sequence data lead us to believe. Whereas some of the sequencing errors are random, each type of sequencer, as well as each experimental design, has its own systematic biases that occur at specific sequence patterns, inverted repeats or homopolymers [144, 182]. Because some of the errors are made during PCR amplification, base quality scores are not always sufficient to determine the chance that a specific base is called correctly for a sequenced DNA fragment. This is especially important when the aberration of interest is expected to occur in only a subset of the analyzed DNA fragments, as is the case for germline and somatic mosaic variants and for non-invasive prenatal testing (NIPT), where fetal DNA is analyzed in the presence of maternal DNA, because fewer sequence reads will be present to support a genotype call. An important contributor to the creation of bias during PCR is the GC percentage in the DNA fragment. If a high (>65%) or low (<12%) percentage of guanine or cytosine bases are present, the DNA fragments are barely amplified during PCR, with the amplification efficiency gradually increasing with GC percentages closer to 50% [1]. With each PCR cycle needed in the experiment, the GC bias will grow, although this bias can also occur during PCR-steps that are part of the sequencing procedure itself [170]. The severity of this bias can differ between samples and experiments. An extra effect of using many PCR cycles in sample preparation is that the number of reads originating from the same DNA fragment, called duplicate reads, will grow. This can lead to a risk of overestimating the effective coverage and sensitivity as well as the chance of amplifying errors occurring during extension in early PCR cycles, thus reducing specificity.

For WGS, fewer PCR cycles are usually needed in the sample preparation, leading to a relatively even coverage between different genomic regions. However, targeted techniques such as WES and targeted NGS (tNGS) that rely on selective amplification of genomic regions of interest require PCR during sample preparation. In general, the rule applies that the lower the amount of input material or the smaller the targeted region, the more PCR cycles are needed, up to more than 30 cycles for some procedures. At 30 PCR cycles, over a billion copies of the same original DNA fragment are generated. In

contrast, after 10 PCR cycles, just over one thousand copies are present. When randomly sheared DNA fragments are amplified and sequenced, duplicate reads can, to a certain extent, be identified based on the fact that they have an (almost) identical sequence. However, in amplicon-based sequencing, which uses primers to amplify a region of interest, it is expected that different original DNA fragments give rise to reads with the same sequence. This makes it more difficult to distinguish those reads from each other, unless separate molecular identifiers are used.

But, even when all technical bias is corrected for, not all parts of the genome are accessible, especially in short-read sequencing. Many parts of the genome are not unique, for instance genes that have pseudogenes [129]. When a DNA-fragment originating from such a region is sequenced, there is no way to determine from the sequenced read itself if it is informative for the region of interest or for the other region that has the same sequence.

1.6 DNA variant detection in genome diagnostics

In current genome diagnostics many of the DNA variant detection methods described in sections 1.3 and 1.4 are used. The types of variations that are searched for, as shown in figure 1.1, are different for different diagnostic questions. Moreover, the variants being examined can be present in only some of the cells – and therefore only part of the DNA analyzed – as discussed earlier. In the paragraphs below I discuss three important types of variants that need specific analysis and interpretation approaches: germline variants, somatic variants and variants found in prenatal testing.

1.6.1 Germline variants

Germline variants are present at the formation of the zygote and, in principle, are present in all cells, including the germline [81]. For genetic analysis, white blood cells or fibroblasts provide a source of high-quality DNA. Germline variants can be transmitted from parent to child and can therefore result in multiple affected relatives within a family. Depending on the nature of the variants, a disease phenotype may develop during childhood, or adulthood, or even not at all. For Mendelian diseases the inheritance pattern for variants in autosomal chromosomes (i.e. chromosomes 1-22) can be autosomal dominant (AD) or autosomal recessive (AR). In AD inheritance, a variant in only one of the alleles can result in the disease phenotype. In AR inheritance, both parents transmit a pathogenic variant. Variants present in sex-chromosomes or mitochondria have different inheritance patterns. Because men carry one copy of each sex chromosome, a sex-chromosome-related recessive trait will

result in a phenotype when a single copy of the causal variant is present. Mitochondria are always transmitted from mother to child, leading to phenotypes caused by mitochondrial variants only being inherited through the maternal line.

One example of an AD hereditary disease is Lynch syndrome, one of the most common cancer predisposition syndromes. In Lynch syndrome, SNVs, indels, intragenic deletions or duplications cause a deficiency in the mismatch repair system that significantly increases the risk of developing cancer compared to the general population, although, as in other cancer-predisposing syndromes, not all carriers of pathogenic variants develop cancer [212, 207]. It is estimated that around 1 in 300 people carry a pathogenic variant in one of the genes associated with Lynch syndrome [27]. One of the most common AR disorders is cystic fibrosis, which leads to dysfunctional chloride channels that cause thickened mucus and affects around 1 in 3500 individuals in Europe [241, 187]. Children with cystic fibrosis often inherit a non-functional allele of the *CFTR* gene from both of their parents, who themselves don't present with the disease phenotype because they have a functional copy of the gene. An example of a common recessive X-linked trait is red-green color-blindness, which affects 1 in 12 males and 1 in 200 females in populations with Northern-European ancestry [168]. The prevalence of mitochondrial diseases is highly dependent on the population and is associated with, among other conditions, neurological diseases and ataxia [34].

It is also possible that variants appear de novo during de formation of the gametes. De novo means that a variant is found in an individual even though neither of the parents carry this variant. Such a variant can arise through mistakes in copying DNA for SNVs and indels, through errors in crossing over for SVs, or through non-disjunction for aneuploidies. Examples of syndromes caused by SVs are Down syndrome (trisomy 21), Klinefelter syndrome (XXY), Turner syndrome (X0), Di-George syndrome (del 22q11) and the 1q21.1 microduplication syndrome.

1.6.2 Somatic variants

When a DNA variant is not present in the zygote but rather originates from a later cell division, it is called a somatic variant. If such a variant originates during embryonic development, it will be present in many cells; if it occurs later in life, it may be present in a small number of cells [67]. Some of the syndromes mentioned in the previous paragraph, Down syndrome and Turner syndrome for instance, can have their origin not only in germ cells, but also be the result of somatic mosaics. Mosaics may not lead to a clinical abnormal phenotype, depending on the distribution of the somatic variants over cells

and tissues. Low level mosaics in parents that include their germ cells may be difficult to distinguish from de novo cases discussed in the previous section. Mosaics may also arise through a germline variation with a rescued cell-line in which the variation is eliminated [49, 92].

Some disorders such as segmental neurofibromatosis [197] or McCune-Albright syndrome [52], in which parts of the body are affected while other parts are unaffected, are caused by mosaics. In cancer, somatic variants are the main cause of tumorigenesis. A tumor can develop when a gene variant causes uncontrolled cell division, as is the case with the Philadelphia chromosome [98], or fails to lead the cell into appropriate cell-death, as is the case with variations affecting the *MYC* gene [51]. A cell that develops such a variant can then grow into a clonal population, which can later on develop into further subclones, together constituting the tumor cells [152, 146, 133]. In advanced disease stages, some variants can be present in a high percentage of cells. However, in earlier stages, after treatment or when a new variant has arisen in a subclone, it can be the case that only a small percentage of the cells analyzed carry the variant. In addition, tumor samples sent in for analysis typically contain both tumor cells and normal cells (e.g. lymphocytes or stromal cells), which adds to the mosaic nature of gene variants in these samples.

Somatic variants in tumor or hematological cells can consist of all the variant types described in section 1.2. However, while large structural variants, including aneuploidies, are rare events when looking at germline variants, they are more prevalent in cancer cells, where complex aberrant karyotypes are also seen. The main challenge for somatic variant detection in tumors is the possible presence of a wide variety of DNA variants and, sometimes balanced, chromosomal aberrations in a low percentage of the cells or DNA to be analyzed. In addition, the material containing the variations, such as bone marrow or tumor material, is harder to come by and often of lower quality than that used for germline variation detection.

1.6.3 Prenatal testing

Genetic variants can also be detected prenatally. Conventionally, such tests are offered to pregnant women at an elevated risk of carrying a child with a chromosomal abnormalities, most notably Down syndrome, Patau syndrome (trisomy 13) and Edwards syndrome (trisomy 18), and for hereditary disease-causing-gene variants previously identified in one or both of the parents. Conventional invasive prenatal tests are performed using cells from the fetus or from extra-fetal tissue that shares genetic origin with the fetus: amniotic fluid cells (fetal and extra-fetal origin) or chorionic villi cells (extra-fetal, placen-

tal). The main problem with the frequently used types of invasive procedures – amniocentesis and chorionic villi biopsy – is a risk of a procedure-related miscarriage of 0.3% and 0.5%, respectively [17]. Fortunately, the mother's blood can also be used as a source of short fragments of extra-fetal DNA [122]. This so-called cell-free fetal DNA (cffDNA) circulates through the blood stream of a pregnant woman, next to a greater fraction cell-free DNA (cfDNA) originating from her own cells. On average only around 12% of the cfDNA is cffDNA, though it can be much lower [6]. The cfDNA, including the cffDNA, can be isolated from blood plasma to enable non-invasive prenatal testing (NIPT). Because no invasive procedures are needed in NIPT, there is no risk of inducing a miscarriage. For this reason, NIPT has quickly become a mainstream genetic test. In the Netherlands NIPT has been offered to women with a high risk of carrying a child with a trisomy 13, 18 or 21 since 2014 and to all pregnant women since 2017 [38]. However, because a mosaic of cffDNA and maternal cfDNA is present, similar technical challenges have to be overcome to those faced in somatic variant testing.

1.7 Aims of this thesis

As we have seen throughout the introduction, many different DNA variants can be present in a single sample. However, technical bias, size of the variation, copy-neutrality of variations, mixed cell-populations or DNA samples and the biological origin of analyzed DNA fragments can all create noise in the analysis process. The task of the clinical genetics laboratory is to look through this noise to detect and interpret the presence or absence of relevant variants. When using conventional techniques, many independent tests are needed to overcome different types of noise or to change resolution, sensitivity, number of variants analyzed and the ability to detect balanced variants or not. NGS has the potential to replace all these tests. However, not all types of variants are easy to detect. By using efficient sample preparation and analysis algorithms that can distinguish artefacts from variants, NGS is able to challenge conventional techniques and may become the method of choice for all diagnostic questions related to the detection of DNA variants. The studies in this thesis aim to improve NGS DNA analysis for detection of germline SNVs, indels and CNVs, somatic translocations and trisomy detection through NIPT, as well as interpretation of analysis outcomes. In this thesis, I introduce new tools, methods and algorithms for NGS DNA analysis and interpretation and, in some cases, use them in a practical application (figure 1.3).

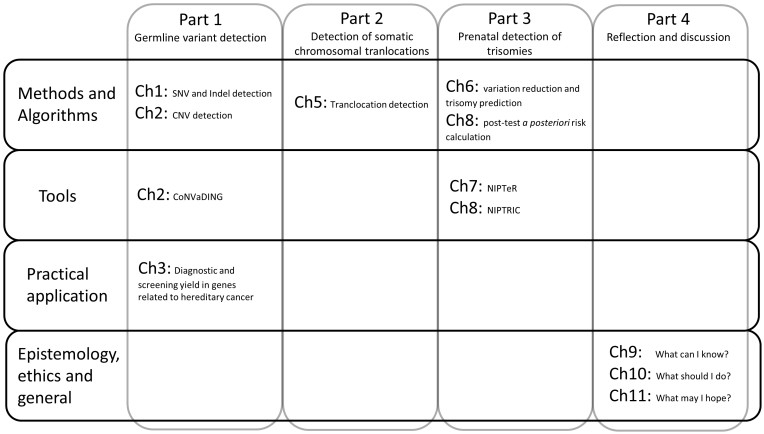

Figure 1.3: Overview of the topics addressed in the thesis chapters.

1.7.1 PART 1: Germline variant detection (chapters 2, 3 and 4)

The most prevalent germline variants – SNVs, indels and small CNVs – were conventionally analyzed mainly using Sanger sequencing for SNV and indel detection and MLPA to detect CNVs. However, only a short stretch of DNA can be analyzed in each measurement using these techniques, limiting the number of genes that can by analyzed in a single experiment. In chapter 2 we set out to implement tNGS as a stand-alone diagnostic test to enable analysis of a large set of genes in a single test and replace Sanger sequencing in clinical diagnostics. For this we developed, validated and established quality criteria for a tNGS genepanel to detect SNVs and indels with high sensitivity and specificity in 48 genes involved in cardiomyopathies, ultimately demonstrating that tNGS is a technique suitable for diagnostic use. In chapter 3 we further expand the application of tNGS and enable simultaneous detection of CNVs up to the single exon level, next to SNVs and indels. Because it is likely in tNGS that CNV breakpoints are located outside targeted regions, CNVs can only be inferred through analysis of read depth. However, laboratory-induced variability of read depth is larger than biological variability. To look through the experimental noise and detect (single-exon) CNV in tNGS data, we introduce new algorithms with strict quality control that we implement in the open-source tool CoNVaDING (Copy Number Variation Detection In Next-generation sequencing Gene panels). In chapter 4 we set out to use

the tools and methods developed in the previous chapters in the context of hereditary cancer, for which we have analyzed 85 genes in 2,090 patients and 1,326 individuals from the general Dutch population. The first goal here was to determine the diagnostic yield, focusing on genes with a relation to the cancer type warranting referral. The second goal was to determine the findings if, in addition to these genes, we search for pathogenic or likely pathogenic variants in genes without such a relation (secondary findings), and how often variants leading to a cancer predisposition occur in the general Dutch population.

1.7.2 PART 2: Detection of somatic chromosomal translocations (chapter 5)

The second part of this thesis consists of a single chapter that focuses on somatic translocation detection. In current hematological malignancy diagnostics SVs, including translocations, are detected using various conventional techniques. Using karyotyping, large rearrangements are detected on a single-cell basis. However, this technique is unable to detect some so-called cryptic translocations. FISH and RT-PCR are needed to detect those, but these techniques can only target one SV or fusion-gene at a time. In chapter 5 we aim to develop an NGS-based technique to target 18 genes and detect translocations involving one of those genes commonly involved in acute leukemia, regardless of their translocation partner, to be suitable for use as a first-line screening tool in diagnostics. For this we make use of Targeted Locus Amplification (TLA) [47] to create a multiplex TLA acute leukemia gene panel. In addition to the genes themselves, our panel captures DNA physically close to the targeted genes, which enables the capture and detection of chromosomal translocation partners even if they are not in the targeted panel. We develop analysis and interpretation strategies and demonstrate for several targeted genes that the panel detects translocations involving those genes at 10% aberrant cells. We conclude that multiplex TLA is a promising technique that it needs further optimization before it can replace conventional methods.

1.7.3 PART 3: Prenatal detection of trisomies (chapters 6, 7 and 8)

Part three of this thesis is dedicated to NIPT. Where conventional methods for prenatal trisomy detection, such as karyotyping, FISH, QF-PCR or array, rely on invasive procedures, NIPT can be performed using ultralow-coverage NGS data. Using a basic sample preparation with as few PCR cycles as possible, the short cfDNA fragments are made available for sequencing. Several algorithms

are described in the literature to analyze such ultralow-coverage NGS data to predict the presence of a trisomy [35, 63, 188]. These strategies rely on the comparison of the sample of interest to a group of non-trisomy control samples to determine if significantly more sequence reads are present that originate from DNA fragments of the potential trisomic chromosome. Because cffDNA is mixed with maternal DNA, a trisomy will only cause a small increase in the fraction of reads of the chromosome involved. Therefore it is important to make the variability in chromosomal fractions as small as possible between samples. In chapter 6 we introduce novel algorithms to analyze ultralow-coverage NGS data and obtain a higher sensitivity for trisomy detection than found using earlier described calculations. In addition, we create a quality metric that can be used to detect if the available reference samples are suitable for comparison with the sample analyzed. In chapter 7 we describe NIPTeR, an open-source R package that makes the algorithms developed in chapter 6 available along with the algorithms described in the literature for analysis of NIPT data. Two women receiving a similar test result from NIPT do not necessarily have a similar risk of carrying a child with a trisomy. In chapter 8 we focus on the clinical interpretation of the NIPT result, taking into account not only biological and technical characteristics of the test, but also the population to which the woman being tested belongs. Including these pre-test conditions in the interpretation might result in different risk profiles for women from different risk-groups who have the same raw test result. We created algorithms to calculate such a personalized post-test risk for a specific fetal trisomy and made these available in NIPTRIC, an online calculator.

1.7.4 PART 4: Reflection and discussion (Chapters 9, 10 and 11)

Inspired by the three questions posed by Immanuël Kant in his Kritik der reinen Vernunft published in 1781/1787: "what can we know?", "what should I do?" and "what may I hope?" [99][p. 728], in part four of this thesis I reflect on and discuss the methods, tools and algorithms described in this thesis. In chapter 9 I look back on the chapters from an epistemological point of view. In genetic diagnostics we infer the genetic or genomic constitution of a person through a measurement outcome. I elaborate on the concept of noise that I define as 'everything that, from a certain perspective, blocks the path between reality and measurement outcome'. Throughout this thesis we are battling four types of such noise: biological noise, laboratory-induced noise, sequencing noise and data analysis noise. The variants of interest are hidden behind this noise, but through innovative perspectives we are better able to look through the noise and correctly interpret measurement outcomes.

In chapter 10 I make an ethical reflection on the technologies introduced in this thesis. I use the theories of Peter-Paul Verbeek who states that artefacts are morally charged and mediate human action [220][p 21]. I try to uncover intended and unintended moral consequences of the availability of the methods, tools and algorithms presented in this thesis.

In chapter 11 I address the last question of Kant: 'what may I hope?' and put the work presented in this thesis in broader perspective in the general discussion and to give future perspectives on developments in NGS DNA analysis.

Chapter 2

Targeted Next-Generation Sequencing can Replace Sanger Sequencing in Clinical Diagnostics

Human Mutation 2013;34(7):1035-42.
DOI: 10.1002/humu.22332
PubMed ID: 23568810

L.F. Johansson[1,2,*], F. van Dijk[1,2,*], E.N. de Boer[1], K.K. van Dijk-Bos[1], L.G. Boven[1], M.P. van den Berg[2], K.Y. van Spaendonck-Zwarts[1], J. Peter van Tintelen[1], R.H. Sijmons[1], J.D. Jongbloed[1], R.J. Sinke[1]

1. University of Groningen, University Medical Center Groningen, Department of Genetics, Groningen, The Netherlands
2. University of Groningen, University Medical Center Groningen, Department of Cardiology, Groningen, The Netherlands

Received 2013 Jan 9; Accepted revised manuscript 2013 Apr 2; Published online 2013 Apr 4.

* Contributed equally

Abstract

Mutation detection through exome sequencing allows simultaneous analysis of all coding sequences of genes. However, it cannot yet replace Sanger sequencing (SS) in diagnostics because of incomplete representation and coverage of exons leading tomissing clinically relevant mutations. Targeted next-generation sequencing (NGS), in which a selected fraction of genes is sequenced, may circumvent these shortcomings. We aimed to determine whether the sensitivity and specificity of targeted NGS is equal to those of SS. We constructed a targeted enrichment kit that includes 48 genes associated with hereditary cardiomyopathies. In total, 84 individuals with cardiomyopathies were sequenced using 151 bp paired-end reads on an Illumina MiSeq sequencer. The reproducibility was tested by repeating the entire procedure for five patients. The coverage of $\geq$30 reads per nucleotide, our major quality criterion, was 99% and in total ~21,000 variants were identified. Confirmation with SS was performed for 168 variants (155 substitutions, 13 indels). All were confirmed, including a deletion of 18 bp and an insertion of 6 bp. The reproducibility was nearly 100%. We demonstrate that targeted NGS of a disease-specific subset of genes is equal to the quality of SS and it can therefore be reliably implemented as a stand-alone diagnostic test.

2.1 Introduction

Next-generation sequencing (NGS) techniques have significantly increased the possibilities of genome analysis. If we focus on diagnostic applications, mutation analysis through exome sequencing (ES) allows for the simultaneous

analysis of all coding sequences of genes. One of the first clinical applications of ES was the detection of disease-associated mutations in rare Mendelian diseases, such as Miller syndrome [147], Sensenbrenner syndrome [74], and Schinzel–Giedion syndrome [90]. The advantage of ES is that it does not require a priori knowledge of gene(s) responsible for a disorder using it as a genetic discovery panel. In diagnostics, ES is already used to screen for de novo pathogenic mutations in intellectual disability [46] explained by more than 1,000 different genes. In addition, ES can be used more targeted by analyzing only a panel of genes that may be involved in a particular disease. However, in routine diagnostics, detecting mutations via conventional Sanger sequencing (SS) is still the standard, despite the practical difficulties of keeping up with the ever-increasing numbers of test requests and of disease-associated genes. For instance, hereditary cardiomyopathies can be explained by 40-60 different genes [**?**, 151] and effective analysis of all these genes by SS in a diagnostic setting is not feasible. In practice, it is limited to no more than 10 genes. In contrast, ES would allow the simultaneous analysis of all coding genes through enrichment for these coding regions before sequencing. However, in its current state, ES cannot be used as a reliable substitute for SS in diagnostics. A major shortcoming is incomplete representation and coverage of exons, leading to clinically relevant mutations being missed [74, 205]. Here, amore dedicated targeted enrichment appears to be the method of choice, not only because it allows focusing on the genes relevant for a particular disorder, but also because its highly effective enrichment provides a superior quality of representation and coverage. In addition, focusing on only the genes relevant for a particular disorder minimizes the problems associated with unsolicited findings. Targeted NGS is faster and cheaper than ES, especially for the analysis of certain distinct disease phenotypes. Various enrichment methods have been developed in the last few years, such as solid phase-based microarrays, micro-droplet-based PCR (Rain Dance Technologies, Lexington, MA), amplicon-based or solution phase-based methods such as Sure Select Targeted enrichment and Illumina TruSeq Customenrichment. Different types of platformshave also been developed for high-throughput sequencing. Recently, even bench-top instruments have become available, such as Ion Torrent PGM (Life Technologies Ltd, Paisley, UK), 454 GS Roche Junior (Roche Applied Science, Indianapolis, IN), and the Illumina MiSeq (Illumina, SanDiego,CA) [124]. These are the size of a modern laser printer and offer modest set-up and running costs; they are particularly suited to small projects and allow a fast throughput. The aim of our study was to validate targeted NGS for application in clinical diagnostics and to assess its sensitivity and specificity relative to SS. We therefore developed a SureSelect targeted enrichment kit (Agilent Technologies, Inc., Santa Clara, CA)

for diagnostic testing of patients with hereditary cardiomyopathies. Hereditary cardiomyopathies are highly heterogeneous disorders, and include dilated (DCM), hypertrophic (HCM), and arrhythmogenic right ventricular cardiomyopathies (ARVC), which are leading causes of heart failure and sudden death. Approximately 30%–50% of DCM cases are familial, but with significant genetic and phenotypic heterogeneity [165]. Particularly for DCM, for which more than 50 cardiomyopathy-related genes have been identified, targeted resequencing would be a much better diagnostic platform than SS. The use of a MiSeq bench-top machine would also enable short turn-around times in the laboratory. We compared the outcome of our targeted NGS experiments with results from SS, and discuss our findings in the light of validation, clinical laboratory implementation, and quality assessment in general.

2.2 Material and Methods

2.2.1 Design of the Study

Our study was divided into two parts: a validation phase and an application phase. (1) Validation phase in which:

- sequencing quality of the targeted NGS kit was measured in terms of representation and coverage;
- sequencing reliability was measured in terms of sensitivity compared with SS results for at least six out of 14 different cardiomyopathy-related genes.

(2) Application phase in which:

- novel variants identified by our targeted NGS approach were confirmed by SS to assess the specificity;
- tests for reproducibility were performed. We set the following thresholds for accepting targeted NGS to replace SS in a diagnostic setting:
- Sequencing quality: coverage of at least$\times$30 for each nucleotide, based on a normal binomial contribution, a minimum number of four reads for a call, a 20% allele frequency resulting in a sensitivity of 99.96% for a heterozygote.
- Sequence reliability in validation and application phase: 100% sensitivity for at least 75 variants, including substitutions and indels. The specificity should be at least 98%, that is, amaximum of 2% false-positive variants.

- Reproducibility: 98%, so that a maximum of 2% difference in the variants within one sample was allowed when repeating the entire procedure.

2.2.2 Patients/Samples

For the validation phase, we selected DNA samples of 24 patients diagnosed with dilated or arrhythmogenic cardiomyopathies. These patients had previously been analyzed by SS for up to six out of 14 disease genes (*DES*, *DSC2*, *DSG2*, *LMNA*, *MYBPC3*, *MYH7*, *PKP2*, *PLN*, *RBM20*, *SCN5A*, *TMEM43*, *TNNC1*, *TNNT2*, and *TNNI3*). Here, SS resulted in the identification of a disease-associated mutation in seven out of the 24 patients and a total of 90 variants. Subsequently, for the application phase, we selected a further 60 DNA samples of unrelated cardiomyopathy patients, for whom no causative mutation had been found by routine diagnostic testing by SS. All samples (n = 84) were subjected to targeted NGS (described below). In addition, the entire procedure was repeated for five out of the total of 84 patient samples to test the reproducibility of our method.

2.2.3 Targeted Enrichment Kit Design

The biotinylated cRNA probe solution was manufactured by Agilent Technologies and provided as capture probes. We selected 48 genes known to be involved in isolated forms of cardiomyopathy or in disorders of which cardiomyopathy is a major part of the disease spectrum (mostly neuromuscular disorders) but in which mutations in isolated cardiomyopathy forms have been reported as well. The sequences corresponding to these 48 cardiomyopathy genes (Table 2.1) were uploaded to the Web-based probe design tool eArray (Agilent Technologies, Inc.); in total 1,134 targets with a size of 323,651 bp. The coordinates of the sequence data are based on NCBI build 37 (UCSC hg19). For the probe design, we set the following parameters: 120 bp bait length, per target spaced every 60 bp, centered, two times tiling, and targets to include sequences 40 bp before and after each exon.

Table 2.1: List of genes included in the targeted SureSelect Enrichment Kit

Gene	Chromosome	Basepair position (start-end)[1]	Total number of basepairs covered by baits	Number of exons covered
LMNA	1	156084670-156108971	3,010	12
TNNT2	1	201328298-201346845	2,339	17
PSEN2	1	227058923-227083365	2,701	12
ACTN2	1	236849934-236925959	4,365	21
RYR2	1	237205782-237996012	23,329	105
TTN	2	179391699-179672188	125,455	316
DES	2	220283145-220290507	2,011	8
TMEM43	3	14166654-14183335	2.163	12
SCN5A	3	38595730-38674890	7,117	27
MYL3	3	46899317-46904920[2]	X	7
TNNC1	3	52485251-52488071	966	6
MYOZ2	4	120056899-120107411	1,504	6
SGCD	5	155753727-156186441	2,467	9
DSP	6	7542109-7586986	11,371	24
LAMA4	6	112430565-112575868	9,125	39
PLN	6	118879948-118880328[2]	381	1
TBX20	7	35242002-35293271	1,988	8
PRKAG2	7	151254178-151573745	3,059	16
MYPN	10	69881155-69970283	5,515	19
MYOZ1	10	75391372-75401555	2,021	6
VCL	10	75757926-75878001	5,199	22
LDB3	10	88428388-88492804	4,519	16
ANKDR1	10	92672493-92681072	2,018	9
RMB20	10	112404173-112595790	4,951	15
BAG3	10	121411148-121437369	2,583	4
CSRP3	11	19204110-19223629	1,249	6
MYBPC3	11	47352917-47374293	6,858	33
CRYAB	11	111779310-111782513	931	3
ABCC9	12	21953938-22089668	7,928	39
PKP2	12	32945260-33049705	3,824	14
MYL2	12	111348584-111358444	1,291	7
MYH6	14	23851159-23877526	9,061	39
MYH7	14	23881907-23904910	9,361	41
PSEN1	14	73614463-73686082	2,464	11
ATC1	15	3508225-35087049	1,931	6
TPM1	15	63334989-63363411	2,576	14
TCAP	17	37821573-37822407	669	2
JUP	17	39911956-39928146	3,278	13
DSC2	18	28647949-28682428	2,706	17
DSG2	18	29078175-29126804	8,751	15
CALR3	19	16589835-16606980	1,942	9
TNNI3	19	55663096-55668997	1,340	8
JPH2	20	42743396-42789087	2,032	4
DMD	X	31139907-33357766	19,354	85
GLA	X	100652739-100663041	1,978	7
LAMP2	X	119565097-119603064	2,215	10
EMD	X	153607805-153609597	1,245	6
TAZ	X	153640141-153649402	1,782	11

[1] Basepair position according to NCBI build 37 [2] The original article mistakenly states the start position twice

2.2.4 Sample Preparation

Sample preparation was performed according to the manufacturer's instructions (SureSelect XT Custom 1kb-499kb library, Cat. No. 5190–4806, SureSelect Library prep kit; Agilent Technologies, Inc.). In brief, the quality of each sample was checked on a Nanodrop machine (Thermo Scientific,Waltham, MA) and, before fragmentation by electrophoresis, on a 0.7% agarose gel. Next, 3 µg of each genomic DNA sample was fragmented by Adaptive Focused Acoustics (Covaris S220 one channel, runtime 80 sec, peak power 140.0W, duty factor 10.0%, cycles/burst 200 cycles; Covaris,Woburn, MA), purified according to the QIAquick protocol and eluted in 20 µl (MinElute PCR purification kit, Cat. No. 28006, PCR purification kit, Cat. No. 28106; Qiagen, Hilden, Germany). After end-repair, A-tailing and adapter ligation size se-

lection of the fragments (335– 365 bp) was performed on a LabChip XT DNA Assay (750 chip; Caliper Life Sciences, Hopkinton, MA). After each step, DNA fragments were purified (QIAquick protocol). The resulting DNA fraction was amplified (11 cycles at a concentration of 5 ng/µl) by PCR amplification (Herculase II Fusion Enzyme with dNTP Combo 200 RXN kit, Cat. No. 600677; Agilent Technologies, Inc.) and purified again. The concentration and length of the DNA fragments of each sample were measured with an Experion^{TM} DNA chip (Experion DNA 12K Reagents and Supplies, Cat. No. 700–7165 and Experion DNA chips, Cat. No. 700–7163; Bio-Rad Laboratories Ltd., Hemel Hempstead, Herts, UK).

2.2.5 Capturing/Enrichment

Target enrichment was performed according to the manufacturer's instructions (SureSelect XT Custom 1kb-499kb library Cat. No. 5190–4806, Agilent Target Enrichment kit and Agilent SureSelect MPCapture Library kit; Agilent Technologies, Inc.). Briefly, samples were diluted or concentrated to 500 ng in 3.4 µl milliQ/elution buffer using a Speedvac machine (Savant SpeedVac SPD101B; Thermo Scientific) at a maximum temperature of 40 °C. Capture probes were mixed with RNase block solution and kept on ice. Each genomic DNA fragment library was mixed with SureSelect BlockMix, heated for 5 min at 95 °C, and kept at 65 °C. While maintaining the sample at 65 °C, hybridization buffer was added and the sample was incubated at this temperature for at least 5 min. The capture library mix was added and the sample incubated for 2 min. Then, the hybridization mixture was added to the capture probes, followed by the addition of the DNA fragment library. Solution hybridization was performed for 24 hr at 65 °C. After hybridization, the captured targets were pulled down by biotinylated probe/target hybrids using streptavidin-coated magnetic beads (Dynabeads MyOne Streptavidine T1; LifeTechnologiesLtd.). The magnetic beads were prewashed three times and resuspended in binding buffer. Next, the captured target solution was added to the beads and incubated for 30 min at room temperature. After purification, the captured DNA was eluted from the streptavidin beads and purified again. Finally, fragments were amplified by 14 cycles of PCR using the complete sample as a template. During the amplification step barcoding index tags were ligated to the fragments. The concentration and length of the DNA fragments of each sample were measured with an Experion^{TM} DNA chip (Experion DNA 12K Reagents and Supplies, Cat.No. 700–7165 and Experion DNA chips, Cat.No. 700–7163; Bio-Rad Laboratories Ltd.). The concentration of each sample was adjusted to 10 nmol/l, and 12 samples were pooled. According to the expected number of sequenced basepairs (1

$\times$ 109) and the size of the enrichment kit (323,651 bp) running equimolar pools of 12 samples resulted in a theoretical coverage of 257.5 for all targets.

2.2.6 Sequencing

A sample sheet was prepared on the MiSeq sequencer (Illumina) to provide run details. A standard flow-cell was inserted into the flow-cell chamber. The pooled sample was diluted with chilled HT1 buffer to a concentration of 2 nmol/l and an equal amount of 0.2N NaOH to denaturate the sample was added and incubated for five minutes. A PhiX sample at 2 nmol/l was denatured in the same way. Both the sample and the PhiX were diluted to 8 pmol/l and 1% PhiX was added to the sample. Then, 600 µl of the spiked sample with a final concentration of 8 pmol/l was pipetted into the sample well on the MiSeq consumable cartridge before loading in the cooling section of the MiSeq machine. Sequencing was performed on a MiSeq sequencer using 151 bp paired-end reads, including an index run according to the manufacturer's instructions (MiSeq System user guide part #15027617 Rev. C April 2012, MiSeq Reagent kit 300 cycles, Box1 [ref 15026431] and Box2 [ref 15026432]).

2.2.7 Data Analysis and Variant Annotation

Data analysis was performed using the MiSeq reporter program (Illumina) to generate fastq.gz output files. These were unpacked to create fastQ files. In the NextGENe software (v2.2.1; Softgenetics, State College, PA), we performed the following six steps:

1. the fastQ output file was converted into a FASTA file to eliminate reads that were not "paired" and that did notmeet the criteria of the default settings; it was also checked for "Paired Reads Data";

2. duplicate reads were removed;

3. reads from the converted unique FASTA file were aligned to the reference genome (Human_v37.2). The default settings were extra checked for load-paired end, library size range 200–500 bases, and allowing one mismatch or using seeds. After alignment a *.pjt file was created and opened in the NextGENe Viewer;

4. a mutation report was created using the coordinates from the targeted enrichment kit as a *.bed file to enable calling of SNPs and indels in the regions of interest. Data analyses were limited to $\pm$20 bp of exon-flanking intronic sequences;

5. an expression report was created from which the mean, minimal, and maximal coverage per target and targeted nucleotide was calculated. The coverage was defined as the average number of reads representing a given nucleotide in the reconstructed sequence;

6. a mutation report (*.vcf file) was created annotating all variants.

To interpret the data, additional custom-filtering criteria were imposed to minimize false-positive rates. Variants were filtered for those that are novel (not present in dbSNP133, downloadedApril 1, 2011; or 1000 Genomes databases, downloaded May 25, 2011) and were called pathogenic in case of a truncating variant or a missense variant when it was in silico predicted to be pathogenic, described as pathogenic in the literature or showed cosegregation in affected family members.

2.2.8 Validation of Mutations by Sanger Sequencing

Sequencing analysis of a subset of coding exons and flanking intronic sequences in which a novel variation was identified by NGS was carried out using flanking intronic primers (primer sequences are available upon request). The forward primer was designedwith a PT1 tail (5'-TGTAAAACGACGGCCAGT-3') and the reverse primer was designed with a PT2 tail (5'-CAGGAAACAGCTATGACC-3'). PCR was performed in a total volume of 10 µl containing 5 µl AmpliTaq Gold ®Fast PCR Master Mix (Applied Biosystems), 1.5µl of each primer with a concentration of 0.5 pmol/µl(Eurogentec, Serian, Belgium), and 2 µl genomic DNA in a concentration of 40 ng/µl. Samples were PCR amplified according to our standard diagnostic protocols (available upon request). To rule out sample switches during the procedure we performed a concordance check for 12 highly heterogeneous SNP's for which Sanger sequencing of the respective amplicons is performed in parallel.

2.3 Results

2.3.1 Validation Phase

Sequencing quality

The two validation runs, which contained 12 patient samples each, produced totals of 16,414,062 and 15,186,556 reads, respectively, which were aligned and met the Q30 quality criteria meaning that only reads were included in which the error probability for each base has a likelihood of 1/1,000. The

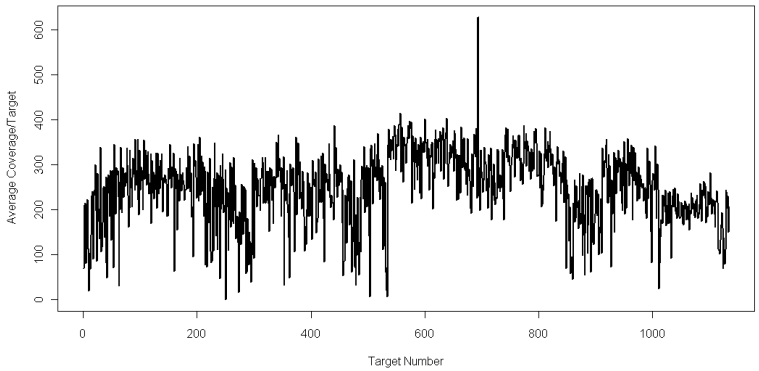

Figure 2.1: Average coverage obtained from 22 different samples of all exon (1,133 exons) and exon/intron junctions ($\pm$20 bp) of 48 genes potentially involved in cardiomyopathy. 99% of the targets show an average coverage of $\geq$30$\times$

pooling was proportional, resulting in a standard deviation between the 12 samples within one run of 0.99% and 0.75%, respectively. The coverage statistics were comparable between both runs (Table 2.2) as well as in subsequent runs (data not shown). The mean coverage per target was 246 and 251 reads, respectively, which is in accordance with our theoretical calculated coverage of 257.5. In 1,084 of the 1,134 targets, the minimal coverage was at least 30 reads in more than 22 out of 24 patients (Fig. 2.1). The validation runs had 99.4% to 99.1% mean coverage >30 of all targets, respectively. For 50 targets, the coverage of at least one basepair position was less than 30 reads in more than two out of the 24 patients. Of these 50 targets, a total of 4,398 bp had a coverage lower than 30 reads. When investigated in more detail, the coverage within such targets varied significantly and in most of these only a few basepairs were covered below 30, resulting in 67 different regionswith a coverage below 30. One example of such a target is shown in Figure 2.2.

Specificity and sensitivity of targeted NGS: confirmation of SS variants

In previous SS analyses, a total of 90 variants in 14 different genes had been identified in the 24 patients used for validation (2 runs). All these variants were also detected with our targeted NGS approach applying the Agilent SureSelect kit (Fig. 2.3) and resulting in no false negatives. This included

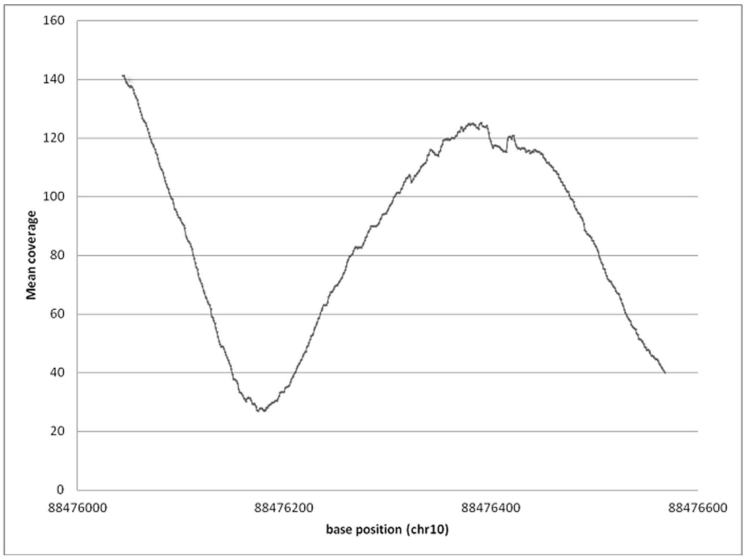

Figure 2.2: Coverage of one target, exon 9 of the *LBD3* gene on chromosome 10 (NCBI build 37, UCSC hg19), representing one region with a coverage $\leq$30 in one patient.

Table 2.2: Overview of the Sequence Performance for the Validation Runs

	Run 1	Run 2	Average of both runs
Cluster density (k/mm^2)	1,289	1,119	1,204
% Cluster PF	89.3	94.6	92.0
Q30	80.3	83.9	82.1
Total reads	17,168,243	15,788,049	16,478,146
Matched reads	16,414,062	15,186,556	15,800,309
% reads in .fasta file aligned	96	96	96
Mean mean coverage targets	246	251	248
Mean min coverage targets	166	179	173
Mean max coverage targets	299	297	298
%Targets Mean $<$30	0.6	0.9	0.7
%Targets Mean $>$30	99.4	99.1	99.3
%Targets Min $<$30	2.6	2.5	2.6
%Targets Min $>$30	97.4	97.5	97.4
%Targets Max $<$30	0.4	0.7	0.5
%Targets Max $>$30	99.6	99.3	99.5

84 substitutions and six indels (four deletions, two insertions). No additional variants were identified in these genes, comprising 55,784 bp. We therefore concluded that for these 24 samples there was full concordance with the SS results.

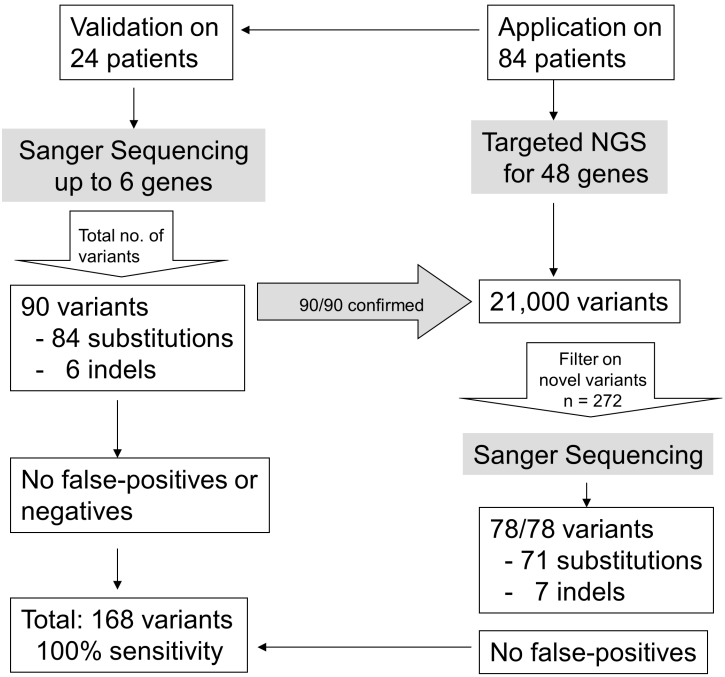

Figure 2.3: Summary of the results of our confirmation analyses.

2.3.2 Application Phase

Sequence specificity of targeted NGS: confirmation of NGS variants

Using targeted NGS of 48 genes, approximately 21,000 variants were identified in 84 unique patients (Fig. 2.3), including the 90 variants that had been previously detected with SS. Of these variants, 272 were novel (245 substitutions, 27 indels). On average, we identified three novel variants per patient. For validationwith SS, 78 out of the 272 novel variants were selected, including detected indels (n = 7). The largest deletion comprised 18 bp and the largest insertion 8 bp. Notably, of the 71 substitutions, one was initially not confirmed by SS. This could be explained by the presence of a SNP in the primer binding site of the forward primer. A subsequent SS experiment, in which an alternative set of primers was used, did confirm the presence of this variant. In summary, a total of 168 variants were confirmed with

SS. Based on these data, we reached a 100% sensitivity (at 95% confidence 97.76%–100%) [216] with the NGS targeted approach.

Diagnostic yield

Applying this targeted NGS strategy, our first results indicate that the diagnostic yield is significantly improved from 15% to about 40%,mostly for DCM. However, this is based on small numbers of samples and the increase in yield may be even higher if this strategy is applied on a regular basis for larger series. Where regular routine diagnostics involves stepwise testing of up to about 10 different genes (which can easily take more than 1 year to complete), using targeted NGS of entire gene-panels on the MiSeq sequencer could theoretically provide reporting times of no more than 2 weeks. At this stage, we are aiming for reporting times of 4–6 weeks, a huge improvement compared with current diagnostic services.

2.3.3 Reproducibility of Targeted NGS

The entire procedure was performed twice for five samples, including sequencing in different runs. On average, 231 variants (198– 268) were detected per sample, and on average, 10 unique variants (8–14) were differently reported between the two analyses of identical samples. In total, 1,007 variants were detected and 51 of these were differently reported in the two separate analyses of the same sample resulting in a nonconcordance rate of 0.00315% according to the number of sequenced bp (five times 323,651 bp of the targeted NGS kit). These differences can be attributed to three underlying causes: (1) in 12 out of 51 cases this was due to coverage differences, which meant variants were either not reported because of a too low coverage or reported when the coverage was just above threshold levels using the default settings; (2) in 24 out of 51 cases this was explained by alignment problems due to poly-T/A stretches, resulting in different annotating of the same variant; and (3) 15 out of 51 were due to differences in heterozygote levels, which meant variants that were present in $<$20% of reads were not reported. Variants that fall within the first two categories are "true variants" that were either missed or reported as the result of analysis software settings or limitations. In contrast, variants in the third category most likely represent recurring technical artefacts, as all were repeatedly reported in a significant number of patients and in different runs, but were nonetheless not reported in the dbSNP and/or 1000 Genomes databases. Considering the artefacts as potential false positives the technical specificity is 0.0009269%. In our future bioinformatic analyses, we will filter for the variants of the third category during our selection for potentially

interesting variants, in addition to other filtering steps.

2.4 Discussion

We present the validation of a targeted resequencing method for cardiomyopathy-associated genes and our results support its implementation in routine diagnostics. In this study, all the 168 variants identified by our NGS-approach were confirmed with SS (Fig. 2.3). The variants included deletions up to 18 bp and insertions up to 8 bp. No false-negative or false-positive results were obtained for variants selected for confirmation. We therefore conclude that, at a coverage of at least 30 times per nucleotide, the performance of our procedure is comparable with SS. ES is likely to become the most commonly used tool for identifying genes in Mendelian diseases in the coming years [76]. This approach has been shown to be successful in cases of rare monogenetic disorders [74, 90, ?] and of intellectual disability [221]. However, as demonstrated by Gilissen et al. (2012)[76], 2128 (5.7%) of 37,424 disease-causing variant positions from the Human Genome Mutation Database are not covered with the 50Mb SureSelect ES kit (Agilent Technologies, Inc.). From our experience, we know that all the 48 genes we targeted are covered by probes in the 50Mb ES kit. However, the coverage performance varied significantly between exons within a gene and between different genes, and for some regions the coverage was $<$20 times, too low for reliable variant detection. This is exemplified by the *TTN* gene. Recently, Herman et al. (2012)[88] showed that *TTN* truncating mutations are a common cause of DCM, occurring in approximately 25% of familial cases of idiopathic DCM and in 18% of sporadic cases. From our ES data, we have calculated the average coverage per target for the coding regions of *TTN*. We found that 7% of the targets sequenced had an average coverage of $\leq$20 times (around 25 exons) and among those, 12 exons showed an average coverage of $\leq$10 times. It is therefore very likely we would miss clinically relevant variants in these regions of low coverage. In contrast, the targeted region of the *TTN* gene in our designed kit shows a 100% coverage for all exons and the respective nucleotides were all covered $\geq$30 times, with a high reproducibility between different samples. We therefore decided to continue developing our targeted resequencing method to overcome the shortcomings of incomplete representation and coverage of exons in ES experiments. The first prerequisite for high sensitivity of a NGS method is the development of a well-designed enrichment kit. We chose to use the SureSelect kit (Agilent Technologies, Inc.) as the e-Array programme used for kit design offered flexibility in optimizing the respective probe design. The number of tilings

of each target can be chosen and extra baits can be added for GC-rich targets to increase coverage. A theoretical 100% representation was reached for all of our targets. Based on our data, the theoretical representation given by e-Array is indicative for the actual coverage. Because the cost of a targeted custom-made enrichment kit is rather high, a good prediction of the coverage is an advantage before ordering such a kit for diagnostic use. The second prerequisite is high coverage of preferably all the targets. Setting the threshold at a coverage $\geq$30, we found only 50 targets out of the 1,134 with less coverage of the nucleotides, mostly in a part of the respective targets. We therefore decided that, parallel to targeted NGS, we will perform SS for targets with a low coverage from those genes of which the clinical relevance is uncontested (e.g., *MYH7*, *TNNI3* or *MYBPC3* for HCM; *LMNA*, *MYH7* or *MYBPC3* for DCM; and *PKP2* for ARVC) to ensure complete coverage of the respective amplicons (see Table 2.3 for general recommendations).

Table 2.3: Resulting Diagnostic Workflow and Implementation Guidelines

Workflow	Recommendations
Enrichtment kit construction	Theoretically 100% horizontal and vertical coverage of all targets
Sample preparation	
Days 1-3	Automated, that is, using a Bravo or Caliper robot (Agilent Technologies, Inc./Caliper Life Sciences, Hopkinton, MA)
Sample Enrichment	Bar-coding samples to a theoretical mean coverage of 250 for all targets resulting in a coverage of at least 30 per nucleotide in p8% of targets
Days 4-6	Avaiding sample-mix-up by spiking unique DNA sequences before the procedure or including a limited SNP analysis for each individual patient
Sequencing on bench-top machine	80% of the reads with Q30
Days 7-8	
Data analysis	
Days 8-10	Minimal coverage of 30 per nucleotide In house (control) variant database for filtering A predifined variant filtering precedure, preferably automated in software programmes like the NGS bench lab from CARTAGENIA (Leuven, Belgium)[1]
Confirmation with Sanger Sequencing	
Days 11-20	Obsolete at a coverage of >30 per nucleotide Coverage of targets structurally below 20: Sanger sequencing in parallel with NGS Incidental coverage below 20: Sanger sequencing depending on the target's clinical relevance Coverage between 20 and 30: visual inspection, Sanger sequencing of novel variants
Total turn-around time	21 days

Valencia et al. (2012)[213] developed a SureSelect enrichment kit for congenital muscular dystrophy for 321 targets (12 genes) and 95% of them had a coverage of at least 20. According to their data, the coverage was below 20 times for two genes due to a high GC content. In contrast, our kit represents amuch better coverage (99% covered more than 30 times). There are several explanations for this difference, for instance the tiling of the baits, differences in the overall GC content, or the number of pooled patients, which make a good comparison difficult. In our approach, 12 samples were

[1] Basepair position according to NCBI build 37

pooled based on the size of the enrichment kit to reach a coverage of at least 30 times per basepair for most of the targets. Because no false-positive or -negative results were detected, this would seem to be a safe threshold. One could even consider whether more than 12 patients could be pooled or the coverage threshold reduced to >20 times instead of >30 times. In Table 2.3, we give some general recommendations on the clinical laboratory implementation and quality assessment of targeted resequencing methods. These recommendations are in line with the general guidelines for assuring the quality of NGS in clinical laboratory practice formulated by the national workgroup of the US Centers for Disease Control and Prevention [72]. A 100% sensitivity (95% confidence: 97.76%–100%) was reached with our approach and a specificity of nearly 100% (0.00315% false positive). Gowrisankar et al. (2010)[78] reported a false-positive rate of 0.011 ±0.002%, close to 100% specificity for 41,475 bp using an Illumina GAII sequencing machine and targeted resequencing of 19 DCM genes. However, four out of the 160 basepair substitutions and three out of 31 indels were missed, including one 18 bp duplication. The basepair substitutions were missed because of insufficient coverage (<30 times), whereas the indels were likely missed due to sequencing of short read lengths (36 bp). In our approach, 151 bp reads were used and we were able to detect an 18 bp deletion, the largest indel detected in our study. In total, 17 indels detected were confirmed with SS, but it is debatable how many and which type of indels should be confirmed by SS for proper validation. Depending on the gene panel to be sequenced, it seems obvious to choose patients with the largest known indels for validation. Gowrisankar et al. (2010)[78] recently reported an 18 bp duplication and Herman et al. (2012)[88] a 13 bp deletion in the titin gene, which seem to be the largest indels associated with cardiomyopathies so far. As indels of that size were detected in our procedure, we are convinced we can retain 100% sensitivity. Moreover, according to our results, we would have missed one variant with SS due to a SNP in the primer sequence. This suggests that resequencing after hybridization-based enrichment of targets may even outperform SS. The importance of longer read lengths was underscored by the results of Voelkerding et al. (2010)[222]. They performed SureSelect enrichment for 12 genes responsible for congenital muscular dystrophy in combination with sequencing on a SOLiD machine. Two out of the 34 identified variants were not confirmed with SS because of sequence read misalignment between two closely related genes. As a probe based method, not only targeted sequences but also highly homologous pseudogenes and other homologous sequences, such as those present in gene families and domain analogs will be captured [39]. Highly homologous sequences coalign to the reference sequence. However, it is uncertain to what extent regions of high-homology may negatively af-

fect the sensitivity and specificity. In general, construction of a unique tiled bait library using differences in the neighboring intron sequences and eventually longer paired end reads can reduce this problem. The reproducibility of our procedure was tested by repeating the procedure for five samples. The 99.99685% concordance of all detected variants demonstrates the high performance of our targeted enrichment and MiSeq resequencing method. Apart from low coverage an alignment problem due to poly A/T stretches resulted in discrepancies. However, these variants will not result in false positives. Discrepancies due to differences in the heterozygote level of 20% might be considered as technical false positives (0.0009269%). However, according to our analyses criteria we would have filtered these variants out. In summary, the differences seen between the separate analyses of the five repeated samples were due to bioinformatic threshold and annotation settings and not due to technical limitations. Variants with an allelic imbalance need careful follow up. This is in line with the first report on a MiSeq-based sequencing method in which drafting genomic sequences of E. coli resulted in an error rate of 0.1 substitutions per 100 bases and a near absence of indel errors[124]. This, together with the almost 100% sensitivity and specificity of our results, raises the question whether a variant still needs to be confirmed with SS, as is often daily practice in clinical diagnostics at the moment. Zhang et al. (2012)[243] felt it was necessary for two reasons: first, to remove incorrect calls due to experimental errors, and second, to confirm a diagnosis. However, as they discussed, confirmation becomes burdensome or impossible when a large number of novel variants need to be confirmed and this would result in long turn-around times. We therefore propose to refrain from confirming results with SS as long as the coverage is >30 times per nucleotide. In addition, targets that are not covered or badly covered can either be excluded from the final report or SS of these targets can be performed in parallel. At a coverage between 30 and 20 times, visual inspection of the regions is recommended (see Table 2.3 for general recommendations).

2.5 Conclusion

Our data convincingly demonstrate that targeted NGS of a disease-specific subset of genes can be reliably implemented as a stand-alone diagnostic test.

2.6 Acknowledgments

We thank Jackie Senior for editorial advice.

Disclosure Statement

The authors declare no conflict of interest.

Chapter 3

CoNVaDING: Single Exon Variation Detection in Targeted NGS Data

Human Mutation 2016;37(5):457-464.
DOI: 10.1002/humu.22969
PubMed ID: 26864275

L.F. Johansson[1,2,*], F. van Dijk[1,2,*], E.N. de Boer[1], K.K. van Dijk-Bos[1], J.D. Jongbloed[1], A.H. van der Hout[1], H. Westers[1], R.J. Sinke[1], M.A. Swertz[1,2], R.H. Sijmons[1],B. Sikkema-Raddatz[1]

1. University of Groningen, University Medical Center Groningen, Department of Genetics, Groningen, The Netherlands
2. University of Groningen, University Medical Center Groningen, Genomics Coordination Center, Groningen, The Netherlands

Received 2015 Nov 26; Accepted revised manuscript 2016 Jan 27; Published online 2016 Feb 10.

* Contributed equally

Abstract

We have developed a tool for detecting single exon copy-number variations (CNVs) in targeted next-generation sequencing data: CoNVaDING (Copy Number Variation Detection In Next-generation sequencing Gene panels). CoNVaDING includes a stringent quality control (QC) metric, that excludes or flags low-quality exons. Since this QC shows exactly which exons can be reliably analyzed and which exons are in need of an alternative analysis method, CoNVaDING is not only useful for CNV detection in a research setting, but also in clinical diagnostics. During the validation phase, CoNVaDING detected all known CNVs in high-quality targets in 320 samples analyzed, giving 100% sensitivity and 99.998% specificity for 308,574 exons. CoNVaDING outperforms existing tools by exhibiting a higher sensitivity and specificity and by precisely identifying low-quality samples and regions.

3.1 Introduction

Several methods for detecting exon deletion and duplication using next-generation sequencing (NGS) have been reported for whole genome [244, 75, 66] and whole gene sequencing data [**?**]. With the exception of those using read depth approaches, these methods rely on information from sequence reads spanning the breakpoints. For targeted NGS data, however, only a read depth approach can be successfully applied [208]. Existing tools using this approach are XHMM [69], CoNIFER [101], CONTRA [115], and CODEX [94]. All four consider all control samples equally informative even though there are sample to sample variations caused by differences in PCR

and capturing efficiency, which lead to variations in coverage patterns that complicate the determination of expected read depths [1][244]. In the four existing tools, this increases the risk of false- negative (FN) or false-positive (FP) results for exons with a high read depth variation, giving either a low sensitivity and specificity for single exon copy-number variation (CNV) detection or limiting the analysis to detection of variations that span multiple exons. This has meant that, until now, additional experiments were needed to identify single exon CNVs, including multiplex ligation-dependent probe amplification (MLPA) [185], Q-PCR [56], or array comparative hybridization [218]. These additional experiments are, however, costly and usually only applied to genes known to frequently harbor deletions or duplications. To overcome this limitation, we have developed CoNVaDING, an analysis tool that not only detects single (and multiple) exon CNVs with high sensitivity and specificity, but also provides quality metrics for each sample that distinguish high-quality samples and targets from low-quality ones with a high risk of producing FP or FN results.

3.2 Material and Methods

3.2.1 General Workflow CoNVaDING

The CoNVaDING analysis consists of several steps to determine whether a deletion or duplication is present. CoNVaDING focuses on specified target regions (Fig. 3.1A) and utilizes control samples captured with the same gene panel for a read depth comparison. A strategy unique for CoNVaDING is that out of a set of available control samples, it selects only samples with a coverage pattern that is most similar to that of the sample analyzed (Fig. 3.1C). The selected control samples are therefore most informative for this specific sample. CoNVaDING then normalizes the data in two different ways in parallel in order to enable comparison between the sample and the control samples. The first normalization uses all targets or all autosomal targets within the sample (Fig. 3.1B) and the second uses all targets of the same gene (Fig. 3.1D). Based on the normalized data, the ratio of the normalized average read depth of the sample to that of the controlsanda distribution analysis using a Z-score are calculated for each target (Fig. 3.1E). Based on the calculated ratio and distributions, a prediction is made for each target to determine whether a CNV is present or not (Fig. 3.1F). The mathematical formulas used are described in the Supplemental methods.

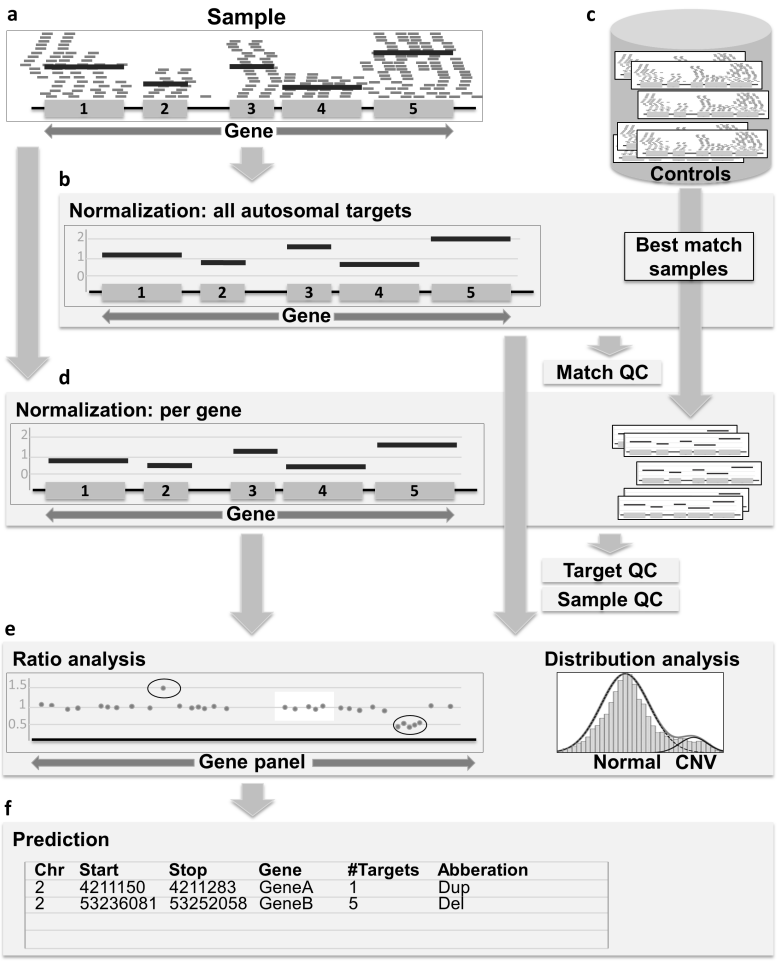

Figure 3.1: Caption next page.

Figure 3.1: (Previous page.) CoNVaDING workflow. A: For each specified target region, the average coverage is calculated for the analyzed sample. B: The sample is normalized using the average coverages of all autosomal targets. C: Out of a set of possible control samples, the samples showing the most similar coverage pattern are selected as control samples. The Match QC shows how well the control samples match the analyzed sample. D: All targets are alternatively normalized using the average coverages of targets belonging to the same gene. E: Based on the normalizations, a ratio and a distribution analysis are performed, showing the relative difference of the average coverages of the targets of the sample compared with those of the control samples. Target QC and Sample QC metrics are calculated showing the variability of each target and the complete sample. F: Based on the ratio and distribution analysis, a copy-number variation (CNV) prediction is made.

3.2.2 Input Data

CoNVaDING analysis starts with a list of targets that specify chromosome, start and stop position of the target and the exact gene the target belongs to. For each sample and the possible control samples, a BAM file containing aligned reads is also needed [113]. Typically, targets specify the exonic regions ofwhich the gene panel consists of, or a subset thereof. After an optional removal of sequence duplicates, for each BAMfile, of all targets in the sample and in the possible control samples, the average depth of coverage is calculated (Fig. 3.1A).

3.2.3 Control Group Selection

CoNVaDING makes use of a set of possible control samples that should be produced using the same type of sample preparation and sequencing as the test sample. The control samples with the most similar overall coverage patterns are selected using a "match score" for each possible control sample. This match score is calculated by first correcting all samples for total read number difference, that is, dividing the average depth of coverage of the target by the mean average depth of coverage of all (autosomal) targets (typeAnormalization) (Fig. 3.1B). Subsequently, the absolute difference between the sample and each possible control sample is calculated for each target. For each possible control sample, the absolute differences are sorted from smallest to largest and the average absolute difference of the center 95% targets, the match score, is calculated. A lower match score indicates a more similar overall coverage pattern and thus a more suitable control sample. The control samples with the lowest match scores are selected for further analysis (Fig. 3.1C). A minimum of 30 control samples is needed for analysis. An

example of the characteristics of the selected control groups for two samples is shown in Figure 3.2.

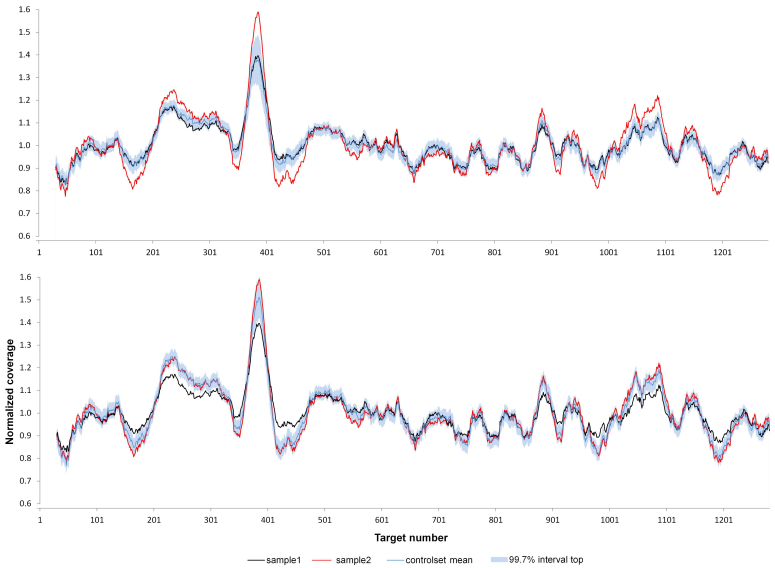

Figure 3.2: Both graphs show the moving average of the normalized coverage over 30 targets of two test samples (sample 1 [black continuous line] and sample 2 [red line line]) and the mean control group value of the 30 best matching normalized control samples (blue line line) with the 99.7% confidence interval (light blue area area). In graph (A), the best-fitting control samples for sample 1 are selected as control group and in graph (B) the best-fitting control samples for sample 2 are selected. Both test samples fitwithin the 99.7% confidence interval of their own best matching control group, but compared with the 99.7% confidence interval of the other control group, there are overrepresented and underrepresented regions.

3.2.4 CNV Prediction Score Calculation

After the control group selection, the selected control samples are used as a reference set. All samples are normalized to enable comparison between samples. Two types of analysis, the ratio score analysis and the distribution score analysis, are performed to determine determine the relative difference between the sample of interest and the selected control samples. Results of

both calculations are combined and, together with quality metrics, are used to predict the presence of a CNV. Normalization within the sample is done in two different ways. The first (type A normalization) is the normalization using all (autosomal) targets (Fig. 3.1B). The second (type B normalization) alternatively normalizes the read number of the targets by dividing the average depth of coverage of the target of interest by the mean average depth of coverage of all targets belonging to the same gene as the target (Fig. 3.1D).

Ratio score

The ratio score shows the ratio of the read depth of the sample to the expected read depth (Fig. 3.1E). This score is calculated for each target by dividing the type A normalized depth of coverage by the average type A normalized depth of coverage in the selected control samples. If no deletion or duplication is present, the sample of interest is expected to have the same normalized average depth of coverage as the selected control samples, a condition indicated by ratio scores close to 1.0. Deletions and duplications are expected to have a ratio of ~0.5 and ~1.5, respectively. Default cut-offs are set at a ratio below 0.65 for deletions and a ratio above 1.4 for duplications. Ratios below 0.10 or above 1.75 indicate homozygous deletions or amplifications, respectively. This is in concordancewith the cut-offs used in MLPA [141], with the exception of the duplication threshold, which we increased from 1.3 to a more stringent 1.4 to improve specificity. Targets with an average coverage of 0 are excluded from further analysis.

Distribution score

The distribution score calculates the number of standard deviations by which the read depth of a target in the sample analyzed differs from the mean read depth of the control samples (Fig. 3.1E). For both type-A- and type-B-normalized targets, a Z-score is calculated by subtracting the average normalized depth of coverage of the selected control samples fromthe normalized depth of coverage for the sample and dividing the result by the standard deviation of the normalized depth of coverage of the selected control samples. If the Z-score is higher than three (i.e., three standard deviations or more from the average), the distribution score is indicative of a duplication. If the Z-score is lower than minus three, the distribution score is indicative of a deletion. When 30 or more control samples are selected, the normalized average coverage of a target in the selected control samples is expected to have a normal distribution. The optimal number of best matching control samples to select is dependent on the number of possible control samples and the consistency of the coverage patterns.

3.2.5 Quality Control Metrics

CoNVaDING provides three different quality control (QC) metrics: Match QC shows how well the coverage pattern of the sample fits the selected control samples, Sample QC shows the variability between all targets within the sample, and Target QC shows the variability for each target within the control samples.

Match QC

To determine whether the selected control samples have a similar coverage pattern to that of the sample of interest, a Match QC score is calculated. This score is equal to the mean of the match scores of the selected control samples. Match QC is provided for troubleshooting purposes and can be used to determine how repre- sentative the selected control samples are for the sample analyzed. No thresholds are specified, but a higherMatch QC score indicates a less representative control group.

Sample QC

For the sample of interest, a QC metric is calculated that makes the variability in the sample explicit. First, the informative targets are selected by excluding the standard low-quality targets, because they would erroneously lower sample quality. Targets for which there is no coverage in all possible control samples and type A-normalized targets in which more control samples than allowed (default: over 20%) show a Z-score outside the confidence intervals (default 99.7%) are considered low quality. For each target of the sample of interest, a second normalization is done by dividing the type A-normalized depth of coverage of the target in the sample by the average type A-normalized depth of coverage of that target in all selected control samples. The double normalized informative targets are sorted from low-to-high normalized depth of coverage. Finally, the Sample QC metric is calculated by using the average and standard deviation of the center 95% of these targets to calculate a coefficient of variation.

Target QC

For each target, a QC metric is calculated. This metric specifies the variability of the specific target in the control samples and consists of the coefficient of variation of the type A-normalized depth of coverage for the selected control samples. Targets with a higher coefficient of variation thanallowed (default setting 0.10) are labeled as low quality.

3.2.6 CNV Calling

In short, the output of CoNVaDING consists of three lists: a high-sensitivity "longlist" containing all CNV calls regardless of quality, a high-specificity "shortlist," using Target QC values of the sample analyzed for filtering, and a high-specificity "final list" using Target QC information of all control samples to filter CNVs. CNV calling is performed based on the combined information from ratio and distribution scores (Fig. 3.1F). For a target to be labeled as a CNV, the type A ratio and distribution scores and the type B distribution score have tobe indicative of a deletion or a duplication. If two or more adjacent targets are labeled as a CNV, only one of the three scores has to be indicative for a deletion or a duplication. Rows of consecutive deleted or duplicated targets are considered as a single CNV. Because large deletions can disrupt the type B distribution score, a secondary calling strategy is applied to detect CNVs that comprise a half or more of a gene. If half or more of the targets of a specific gene are indicative of a deletion or a duplication for both the type A ratio and distribution score, those targets are labeled as a CNV. A CNV is labeled as a homozygous deletion or amplification only when this is indicated by all targets of the CNV. All the CNVs are added to the CNV longlist.

Filtered targets

Not all targets are suitable for reliable CNV detection. The high variability of low-quality targets decreases sensitivity and specificity. Therefore, CNV calls consisting only of low-quality targets are filtered fromthe longlist to create the shortlist. To further increase specificity, targets that are often of a low quality within the control group are filtered out from the shortlist to create the final list. For this, all possible control samples are analyzed with their own respective best matching control samples. When the TargetQC fails for too many samples (default >20%), the target is filtered. Samples or targets failing QC are not suitable for single exon CNV detection. However, CNVs spanning multiple exons that contain low-quality targets are still reliably detected as long as some of the targets pass Target QC.

3.2.7 Implementation of CoNVaDING

CoNVaDING is implemented in a Perl command line script that can be easily integrated into automated analysis pipelines (see Supplemental User Manual). The software depends only on standardPerl packages and SAMtools [113] for mean coverage calculations and duplicate marking. CoNVaDING software is

available under the GNU GPL open source license and can be freely downloaded from
https://github.com/molgenis/CoNVaDING

3.2.8 Validation of CoNVaDING

Patients/samples

Samples were included retrospectively from the population of patients with cardiomyopathy and pulmonary arterial hypertension[1] (CM) (N = 200) or familiar cancer (FC) (N = 120) referred to the genetics department of the University Medical Center Groningen. Targeted NGS had been performed previously for SNP analysis using a panel consisting of 73 genes associated with FC (Supplemental Table S1) and a panel containing of 61 genes associated with CM (Supplemental Table S2). Positive control samples (N = 10) with a known CNV were randomly included for retrospective analysis. These CNVs were previously identified using MLPA in BRCA1 (2x del 1 exon, 1x dup 2 exons, 1x del 3 exons, 1x del 5 exons), EPCAM (1x del 2 exons), MSH2 (1xdel 1exon, 1x del 10 exons MSH2, and 2 exons EPCAM), MLH1 (1x del 1 exon), or PMS2 (1x del 3 exons). Except for the positive control samples, no prior CNV detection using MLPA was performed for these samples. Laboratory procedures were performed as described in Sikkema-Raddatz et al. (2013) [190] using a biotinylated cRNA probe solution, manufactured byAgilent Technologies (Agilent Technologies, Santa Clara, CA). All samples were sequenced 151 bp paired-end on an IlluminaMiseq sequencer (Illumina, San Diego, CA).

Data analysis

For each sample, the sequence data were aligned to the human reference genome build b37, as released by the 1000 Genomes Project [55], using BWA [114]. Subsequently, duplicate readsweremarkedby Picard [161]. Using the Genome Analysis Toolkit (GATK) [134], realignment around insertions and deletions detected in the sequence data and in the 1000 Genomes Project pilot [55] was performed, followed by base quality score recalibration. During the full process, the quality of the data was assessed by performing Picard, GATK Coverage, and custom scripts. This production pipeline was implemented using the MOLGENIS compute [?] platform for job generation, execution, and monitoring. The resulting BAM files were used as input for CNV analysis. For CoNVaDING CNV detection, the 30 best matching samples were used

[1] In the original article wrongly the term 'artificial' was used instead of 'arterial'

as control samples. To assess the effect of coverage on the performance of CoNVaDING, the BAM file of each sample was randomly downsampled to an average coverage of autosomal targets of 100x and of 50x using SAMtools [113]. For both the 100x and the 50x average coverage samples, a CoNVaDING analysis was performed as described above.

3.2.9 Comparison to CoNIFER, XHMM, and CODEX

To assess theperformance of our tool,we compared CoNVaDING with two well-evaluated CNV analysis tools for targeted NGS data that do not require a paired normal control sample [82, 127, 10, 208]: CoNIFER [101] and XHMM [69]. In addition, CODEX [94], a more recent CNV analysis tool, was included in the comparison. We optimized the settings of these tools to obtain the highest possible sensitivity and specificity using the following changes to their default settings. For CoNIFER in the analyze step, targets were combined on a virtual chromosome to ensure that enough targets were present to make analysis possible. Optimal singular value decomposition (svd) values were determined at 4 for the FC panel and at 10 for the CM panel. Samples with a standard deviation of the SVD-ZRPKM values (produced with the --write_sd parameter during the analyze step [143] exceeding 0.5 were treated as samples failing Sample QC. This is in line with CoNIFER QC as describedin Krumm et al. (2012)[101]. CNV calls in samples that passed Sample QC were interpreted as positive results. XHMM analysis yielded the best results using a CNV rate of $1x10^{-6}$ and a mean number of targets in CNV of 2. Filter settings during the matrix step [125] were set to 1000 for maxMeanSampleRD and 1500 for maxMeanTargetRD. For all other parameters default settings were used. Samples excluded during analysiswith the --matrix --excludeSamples parameter [125] were interpreted as samples failing Sample QC, whereas targets excluded during analysis with the --matrix --excludeTargets parameter [125] were interpreted as failing Target QC. We tested CODEX using default settings. CODEX sample QC checks for samples with a low on-target read count and target QC filters exons in case of a low coverage (median <20x), exon length (<20 bp), low mappability (<0.9),or an extreme GC content (outside the 20–80% range). We ran CoNVaDING, CoNIFER, XHMM, and CODEX on all samples. For true positive (TP)/FP analysis, CNV calls detected by CoNIFER or XHMM and calls on the CoNVaDING final list in samples that passed Sample QC were also analyzed via MLPA. Due to a high number of CODEX calls, we did not perform MLPA on new calls and did not accurately determine specificity for CODEX. We also tested CONTRA [115], but did not detect any CNVs in our control samples, so we excluded CONTRA from further comparison. We have determined

sensitivity and specificity for CoNVaDING, CoNIFER, XHMM, and CODEX by calculating TP, FP, FN, and true-negative (TN) results. Calls analyzed with MLPA were considered TP when confirmed and FP when MLPA did not show a CNV and the sample and targets passed QC. If a CNV was detected using MLPA and no CNV was detected in the NGS data and the sample and targets passed QC, the call was considered FN. All targets in which none of the tools detected a CNV were considered as TN results, because only rare CNVs are expected in the genes analyzed and thus there is a low apriori risk of there being a CNV.

3.3 Results

3.3.1 Validation of CoNVaDING

The FC and CM panels consisted of 1,002 and 1,281 autosomal targets, respectively, for a total of 376,440 targets analyzed. The average coverage was 220x for FC samples and 487x for CM samples. Of the total number of samples, 93% of FC and 92% of CM samples passed CoNVaDING Sample QC. Of these, on average 916 (91%) and 1,118 (87%) targets passed Target QC for the FC and CM panel, respectively, resulting in 308,574 high-quality targets.

CoNVaDING identified 15 CNVs in samples that passed Sample QC, 10 of which were confirmed with MLPA and labeled TP (Fig. 3.3A). Five had a normal MLPA result and were labeled FP (Fig. 3.3B). The TP CNVs included the seven BRCA1, EPCAM, and PMS2 positive control aberrations, as well as one extra finding in the FC panel, a 16 exon ALK duplication, and two extra findings in the CM panel, a deletion of the DSP gene (24 exons), and a 2 exon deletion in CTNNA3 (Supplemental Table S3). In the 10 positive control samples, the two MSH2 deletions were detected in a sample failing Sample QC. The MLH1 deletion was filtered out from the final list after failing Target QC. Thus, CoNVaDING had 100% sensitivity and 99.998% specificity for targets passing QC. The analysis speed of CoNVaDING was tested on the 200 CM samples, using a BED file specifying the targets, on a desktop PC. From average count file to final list all samples can be analyzed in less than 90 minutes using maximum 1 GB RAM.

3.3.2 Comparison to CoNIFER, XHMM and CODEX

In the CoNIFER analysis, 42% of samples failed to pass Sample QC: 31 and 102 for the FC and CM panels, respectively. In the remaining samples only

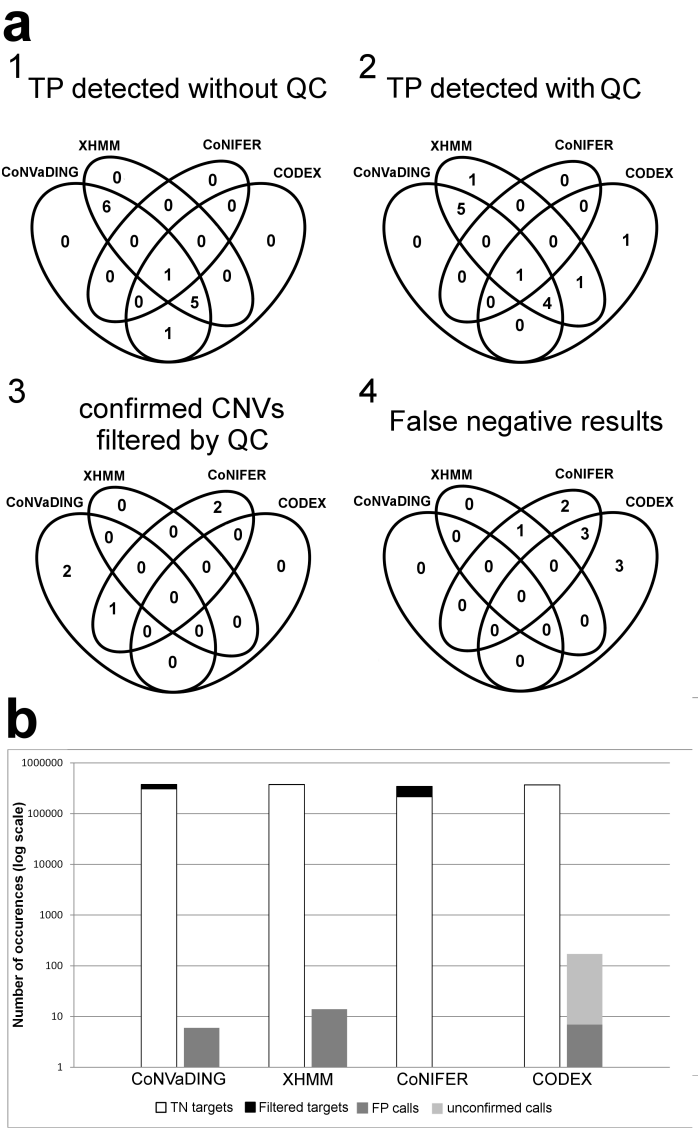

Figure 3.3: Caption next page.

Figure 3.3: (Previous page.)CNV detections made by CoNVaDING, XHMM, CoNIFER, and CODEX. A: Venn diagrams showing true- positive (TP) and false-negative (FN) calls (1) TP detected without quality control (QC), (2) TP detected with QC, (3) confirmed CNVs filtered by QC, and (4) FN results. B: Bar plot using a log 10 scale showing the true-negative (TN), filtered targets (FT), false-positive (FP) results, and unconfirmed calls.

one TP CNV (del 5 exons BRCA1) was identified and no additional CNVs were detected.

In the XHMM analysis, all samples passed Sample QC and only three targets in the FC panel and five in the CM panel failed Target QC. Twelve TP and thirteen FP CNVs were called. Only one of the FP results, a one exon PLN duplication, was also detected by CoNVaDING. XHMM produced one FN result, since it did not detect the 1 exon MSH2 deletion, even though that sample and target had passed QC. In the CODEX analysis, all samples passed Sample QC and fourteen targets in the FC panel and thirty in the CM panel failed Target QC. In total, seven TP CNVs were called among 165 other calls, 49 in the FC, and 116 in the CM panel, respectively (Supplemental Table S4). Of those other calls, 112 calls were found in samples that failed CoNVaDING sample QC, 36 and 76 for the FC and CM panels, respectively. Due to the high number of novel calls, we did not confirm CNVs that were called only by CODEX. However, six calls were confirmed FP, because these were either called by XHMM or were present on the CoNVaDING shortlist. CoNIFER, XHMM, and CODEX analysis resulted in sensitivities of 16.7%, 92.3%, and 53.8% and specificities of 100%, 99.997%, and 99.955%–99.998%, respectively, for targets passing all QC. Ten of the 13 FP findings by XHMM were located in samples or targets that failed CoNVaDING Sample QC or Target QC. Supplemental Table S3 shows all CNVs detected by one ormore of the tools. A comparison of FP and TN results is shown in Figure 3.1B.

3.3.3 Performance of CoNVaDING on Low-Coverage Data

Using default settings, 101 FC and eight CM samples passed sample QC at an average coverage of 100x and no sample passed sample QC at a coverage of 50x. To enable analysis, sample QC thresholds were increased to 0.11 and 0.13 for the 100x and 50x coverage samples, respectively. Using these settings, 117 FC and 179 CM samples passed sample QC at a coverage of 100x. These numberswere 112 and 31 for the FC and CM panels, respectively, at 50x coverage. At a coverage of 100x, only 60,663 (50%) and 38,749 (15%)

of the targets analyzed passed all QC for the FC and CM panel, respectively. At a coverage of 50x, these numbers were 2,825 (2.3%) and 1,014 (0.4%). At 100x coverage, eight of the 13 CNVs that were confirmed by MLPA were detected and one remained at a coverage of 50x (Supplemental Table S5). However, given a target passing both Target QC and Sample QC, the sensitivity stayed at 100%. Specificity was 99.993% (seven FP results) and 100% at a coverage of 100x and 50x, respectively.

3.4 Discussion

We have developed CoNVaDING, as a tool for detecting single exon CNVs in targeted NGS data. CNV detection in targeted NGS data is a challenge, because not every targeted region can be analyzed reliably. Therefore, for each target, CoNVaDING determines whether a high sensitivity and specificity can be obtained. This is especially important in a clinical diagnostic setting, where it is necessary to know exactly those targets for which a CNV could remain undetected.Adding information about failed targets indicates which targets should be tested using another method and for which targets a deletion or duplication can be detected or ruled out with high confidence. In our validation, we used high-coverage NGS data from targeted gene panels. By analyzing all potential CNVs using MLPA, we could validate calls as small as a single exon and accurately determine sensitivity and specificity. After MLPA, we determined a 100% sensitivity and a 99.998% specificity for CoNVaDING analysis in targets passing QC. Previous validations of XHMM and CoNIFER were based on concordance between SNP array calls and whole-exome sequencing data. The validation studies using this approach determined a sensitivity of 67% for XHMM [69] and 76%–84% for CoNIFER [101]. In contrast, we found a higher sensitivity for XHMM calls (92.3%) and much lower sensitivity (16.7%) for CoNIFER. It may be that CoNIFER CNV calling was hampered by the small CNV size in our positive control samples. In the previous CODEX validation study, sensitivity was determined using a simulation data set and approached 100% sensitivity for rare CNVs having a minimum length of five exons [94]. In our study, we called three out of four CNVs having five exons or more (75%) and four out of nine (44.4%) CNVs smaller than five exons.

Our data show that CoNVaDING outperforms CoNIFER, XHMM, and CODEX because of its QC metrics, making high-coverage NGS gene panel data suitable as first line CNV detection data, regardless of the CNV size. CoNVaDING flagged around 10% of the targets as low quality, indicating that these targets are not suitable for single exon variation detection due to a high variability of that target in the selected control samples. However, multiple

exon variations containing low-quality targets can still be detected, as long as part of the CNV region is of sufficient quality. The moderate numbers of samples and targets flagged as low quality by CoNVaDING, combined with FP XHMM results in these samples and targets, suggest that CoNVaDING quality metrics successfully filter out samples and targets with a higher likelihood of FP results. The high number of excluded CoNIFER samples and the absence of failed samples and near absence of failed targets in XHMM and CODEX analysis suggest suboptimal QC performance of these tools. Our results also suggest that specificity can be even further improved by combining CoNVaDING with the other algorithms, since there is only a small overlap between FP calls and a high concordance in TP calls (Supplemental Table S3). CoNVaDING is primarily designed for detection of rare germline CNVs by targeted sequencing and for use in both research and clinical settings. The presence of (common) CNVs in the set of possible control samples may lead CoNVaDING to consider the targets within the CNV region as low quality. We determined the effect of a lower coverage on the performance of CoNVaDING. Since variability between samples increases at a lower coverage,more targetswere labeled as low quality. The number of targets passing QC was considerably higher in the FC than in the CM panel, suggesting that the minimum coverage needed differs per capturing panel. Given the results of the analysis of downsampled targets, we expect CoNVaDING to be able to analyze 15%–50% of the targets in a 100x coverage exome at a single-exon resolution. At a lower resolution, we expect more targets to pass QC. We also tested CoNVaDING on low-coverage whole-genome sequencing data (30x average) using 10 kb bins as targets. Although the increased bin size lowered the resolution as comparedwith analysis in high coverage data, a high concordance with SNP array data was found for calls larger than 50 kb. The extent to which this can be used as a method to detect smaller CNVs is currently being investigated. In conclusion, CoNVaDING improves sensitivity and specificity as well as QC for CNV analysis of NGS data. Our tool shows not only which CNVs are detected, but also which specific targets are unreliable for CNV analysis. We consider CoNVaDING uniquely fit for detection of single exon CNVs in targeted NGS data, making it an indispensable addition to the CNV detection tool box in both research and clinical diagnostic settings.

3.5 Acknowledgments

We thank Jackie Senior and Kate Mc Intyre for editorial advice.

Disclosure Statement

The authors declare no conflict of interest.

Supplemental Material

Supplemental methods and tables:
https://onlinelibrary.wiley.com/doi/abs/10.1002/humu.22969

CoNVaDING source code and documentation:
https://github.com/molgenis/CoNVaDING

CoNVaDING video tutorial:
https://www.youtube.com/watch?v=-geFWkvKZzE&feature=youtu.be

Chapter 4

Genetic screening test to detect translocations in acute leukemia by use of targeted locus amplification

Clinical Chemistry 2018;64(7):1096-1103.
DOI: 10.1373/clinchem.2017.286047
PubMed ID: 29794109

M.Z. Alimohamed[1,*], L.F. Johansson[1,2,*], E.N. de Boer[1], E. Splinter[3], P. Klous[3], M. Yilmax[3], A. Bosga[1], M. van Min[3], A.B. Mulder[4], E. Vellenga[5], R.J. Sinke[1], R.H. Sijmons[1], E. van den Berg[1], B. Sikkema-Raddatz[1]

1. University of Groningen, University Medical Center Groningen, Department of Genetics, Groningen, The Netherlands
2. University of Groningen, University Medical Center Groningen, Genomics Coordination Center, Groningen, The Netherlands
3. Cergentis b.v., Utrecht, The Netherlands 4. University of Groningen, University Medical Center Groningen, Department of Laboratory Medicine, Groningen, The Netherlands
5. University of Groningen, University Medical Center Groningen, Department of Hematology, Groningen, The Netherlands

Received 2017 Dec 19; Accepted 2018 Apr 16; Published online May 2018.

* Contributed equally

Abstract

BACKGROUND: Over 500 translocations have been identified in acute leukemia. To detect them, most diagnostic laboratories use karyotyping, fluorescent in situ hybridization, and reverse transcription PCR. Targeted locus amplification (TLA), a technique using next-generation sequencing, now allows detection of the translocation partner of a specific gene, regardless of its chromosomal origin. We present a TLA multiplex assay as a potential first-tier screening test for detecting translocations in leukemia diagnostics. METHODS: The panel includes 17 genes involved in many translocations present in acute leukemias. Procedures were optimized by using a training set of cell line dilutions and 17 leukemia patient bone marrow samples and validated by using a test set of cell line dilutions and a further 19 patient bone marrow samples. Per gene, we determined if its region was involved in a translocation and, if so, the translocation partner. To balance sensitivity and specificity, we introduced a gray zone showing indeterminate translocation calls needing confirmation. We benchmarked our method against results from the 3 standard diagnostic tests. RESULTS: In patient samples passing QC, we achieved a concordance with benchmarking tests of 81% in the training set and 100% in the test set, after confirmation of 4 and nullification of 3gray zone calls (in total). In cell line dilutions, we detected translocations in 10% aberrant cells at several genetic loci. CONCLUSIONS: Multiplex TLA

shows promising results as an acute leukemia screening test. It can detect cryptic and other translocations in selected genes. Further optimization may make this assay suitable for diagnostic use.

4.1 Introduction

Molecular investigations of structural genomic aberrations and determination of the genotype have contributed to the understanding of the pathogenesis of leukemias and are essential for their diagnosis, treatment, and prognosis[189]. Currently, 500 translocations involving multiple genes have been described in hematologic malignancies, in particular, acute leukemias [59]. Routine diagnostic methods such as karyotyping, fluorescent in situ hybridization (FISH), and reverse transcription PCR (RT-PCR) are used to detect recurrent chromosomal aberrations but have limited genomic resolution or analytical sensitivity and are, at times, inadequate[178]. Translocation detection methods based on next-generation sequencing (NGS) offer several advantages over conventional clinical laboratory methods, such as the ability to detect cryptic rearrangements and unknown fusion partner genes at multiple locations simultaneously[136]. Whole-genome sequencing (WGS) can detect chromosomal translocations in acute leukemia patients[233]. However, owing to the possibly low load of leukemic cells, deep sequencing is required to reach a high sensitivity. Therefore, WGS is not yet the method of choice in a diagnostic setting. To overcome the limitations of WGS, targeted sequencing approaches can be used to analyze a specific set of genes or gene regions and detect translocation partners in cancer-related genes[53]. Despite the higher number of reads targeting genes of interest, the short length of the DNA fragments used in NGS means that only a small fraction of the reads will capture the translocation partner and be informative. One strategy to overcome this problem is to use outward orientated primers, as in the genomic inverse PCR for exploration of ligated breakpoints (GIPFEL) technique, which can detect chromosomal translocations in childhood leukemia[70]. However, targeted methods such as GIPFEL require prior knowledge of both the translocation partners and the genomic locations of breakpoints. The many possible breakpoints and gene fusion partners limit the applicability of such techniques and make these techniques less suitable as stand-alone techniques in a diagnostic setting. A more robust, comprehensive, and unbiased method for detection of translocations is therefore required. A recently reported technique, targeted locus amplification (TLA), enables translocations to be detected regardless of the identity of the chromosomal partner[47]. TLA uses the principles of proximity ligation of crosslinked DNA, followed by targeted amplification us-

ing outward-orientated primers and subsequent sequencing of any locus of interest, thereby capturing hundreds of kilobases of surrounding DNA[47]. TLA can thus detect translocations involving a gene of interest without prior knowledge of the fusion partner and allows the breakpoint to be located at some distance from the probe used, potentially capturing novel translocation partners. We aimed to develop a TLA assay as a first-tier screening test to detect translocations in acute leukemia. Here we present a comprehensive, multiplex gene panel designed to cover 17 common genes involved in acute leukemias and known to be associated with hundreds of fusion gene partners. In this proof-of-principle study, we compared the clinical utility of targeted translocation detection using our acute leukemia NGS gene panel with the results from current genetic diagnostic tests in a series of patient bone marrow samples.

4.2 Material and Methods

4.2.1 Patient bone marrow cells and cell lines

Bone marrow cells were obtained from 36 patients diagnosed with leukemia following informed consent. The study protocol was approved by the Ethics Committee of the University Medical Centre Groningen (METC 2014.051, 10–2-2014). The cells were washed with 1X red blood cell lysis buffer(Stem Cell Technologies). Mononuclear cells were isolated by centrifugation (10 min at 250g) and stored in complete RPMI 1640 culture medium (Lonza), supplemented with 10% v/v DMSO (Merck KGaA) at -140 °C. In addition, we used 5 different cell lines, carrying known translocations that included genes present in our panel: KOPN-8 [t(11;19)(q23;p13), t(8;13)(q24;q21.1); lysine methyltransferase 2A (*KMT2A*), MYC proto-oncogene, bHLH transcription factor (*MYC*)]; HAL-01 [t(17;19)(q22;p13); transcription factor 3 (*TCF3*)]; FKH-1 [t(6;9)(p23;q34); DEK proto-oncogene (*DEK*)]; REH [t(12;21)(p13;q22); ETS variant 6 (*ETV6*)/runt related transcription factor 1 (*RUNX1*)]; and MV4-11[t(4;11)(q21;q23); *KMT2A*; all from Leibniz Institute DSMZ (Deutsche Sammlung von Mikroorganismen und Zellkulturen); see Table 1 in the Data Supplement that accompanies the online version of this article at http://www.clinchem.org/content/vol64/ issue7]. Cell line GM12878 (Coriell institute) was used to test the multiplex primer quality (see Fig. 1 in the online Data Supplement). All cell lines used were cultured according to the instructions provided by their repository.

4.2.2 TLA acute leukemia gene panel

Seventeen genes involved in gene fusions associated with acute leukemia were selected [ABL proto-oncogene 1, non-receptortyrosinekinase(*ABL1*), baculoviral IAP repeat containing 3 (*BIRC3*), core-binding factor subunit beta (*CBFB*), *DEK*, *ETV6*, fibroblast growth factor receptor 1 (*FGFR1*), homeobox A9 (*HOXA9*), lysine acetyltransferase 6A (*KAT6A*), *KMT2A* (*MLL*), *MYC*, nucleophosmin1 (*NPM1*), phosphatidylinositol binding clathrin assembly protein (*PICALM*), retinoic acid receptor alpha (*RARA*), RNA binding motif protein 15 (*RBM15*), *RUNX1*, *TCF3*, and zinc finger MYM-type containing 2 (*ZMYM2*)]. Target regions within these genes are involved in numerous chromosomal translocations and were defined according to known breakpoints reported in the literature[189, 59, 136, 53, 21] (see Table 2 in the online Data Supplement). To enable comprehensive coverage of the target regions, we designed 43 inverse primer sets. After single primer testing, the primers were placed in optimal concentrations in 2 multiplex assays. Multiplex 1 consisted of 26 primer sets designed to cover known breakpoint regions, whereas multiplex 2 had 17 primer sets to boost the coverage around the target regions (see Table 3 and Fig.2 in the online Data Supplement).

4.2.3 Multiplex TLA sample preparation, sequencing, and data analysis

Before TLA was performed, cells were harvested (cell lines) or thawed (bone marrow cells) and washed with RPMI 1640 media, and the concentration was determined using the average of 3 cell counts (Sysmex KX21N; Sysmex Corporation). A total of 5 - 10 $\times$ 10^6 cells were used as starting material. Cell suspensions were homogenized and TLA was performed separately for multiplexes 1 and 2 according to the manufacturer's protocol[47]. Full protocols are described in the online Data Supplement. In short, purified circular DNA fragments were sheared, end-repaired, dA-tailed, and adapter-ligated. Fragments in the 300- to 320-bp range were equimolarly pooled per 24 samples and loaded at a concentration of 0.65 pmol/L on a NextSeq 500 platform (Illumina) using a high-output flow cell kit having paired end reads at 2 $\times$ 151-bp read length and v2 reagents. Using a set of training samples as described below, we set up the data analysis procedure. In short, duplicate reads were removed and digested in silico at CATG sites (the NlaIII restriction site used in the TLA procedure). Reads were aligned to the human genome (build 37) and split into 17 separate files, 1 for each region of interest. Then, for each region of interest, reads were counted in 10-kb bins and filtered. We determined the presence of peaks and represented them on genome-wide plots

and in a tabulated report. Data QC was assessed and standardized based on peak width and noise level, leading to a quality label for each sample and region of interest. Based on the quality of the sample and region, and on the size of the captured peak on the potential translocation partner, we made a definitive translocation call or a gray zone translocation call needing confirmation (see Methods—Translocation calling in the online Data Supplement). This was generalized for all targets.

4.2.4 Routine genetic and cytogenetic methods

Karyotyping and additional FISH were performed according to Dutch national guidelines[194]. We analyzed a total of 20 GPG-banded metaphase cells in all patient samples and cell lines with karyotyping. FISH was performed on BCR, RhoGEF, and GTPase activating protein (*BCR*)/*ABL1*, *ETV6*, *ETV6*/*RUNX1*, MDS1 and EVI1 complex locus (*MECOM*), *FGFR1*, *KMT2A*, *MYC*, promyelocytic leukemia (*PML*)/*RARA*, *RUNX1*/RUNX1 translocation partner 1 (*RUNX1T1*) or T cell leukemia homeobox 3 (*TLX3*)-*NPM1* or in samples having an inconclusive karyotype (see Table 4 in the online Data Supplement). The KOPN-8 cell line was also analyzed using an *MYC* breakapart probe (KBI-10611; Kreatech) to confirm the presence of a breakpoint in or near *MYC* (see Fig. 3 in the online Data Supplement). In addition, we isolated RNA from mononuclear cells in the bone marrow, and performed reverse transcription to prepare cDNA. RT-PCR using fusion-gene specific primers was performed according to the methods used by van Dongen et al.[217] to detect the most frequent chromosomal rearrangements of leukemia: *BCR-ABL*, *ETV6-RUNX1*, *PML-RARA*, *RUNX1-RUNX1T1*.

4.2.5 Validation of the multiplex TLA method

Samples were processed in 2 sets: (a) a training set used to optimize analysis and interpretation procedure and (b) a test set used to validate the procedures.

Training set. The training set consisted of 17 patient samples with a karyotype known to the researcher and the REH and FKH-1 cell lines, as well as a cell line dilution series using the KOPN-8 and HAL-01 cell lines (see Table 5.1 in the online Data Supplement). All samples were used to set filter thresholds for data analysis and interpretation. The dilution series were also used to determine the minimum percentage of aberrant cells detectable at our set thresholds.

Test set. To assess the performance of the multiplex TLA procedure, we selected, anonymized, and tested a set of 19 patient bone marrow samples,

as described above, using the optimum thresholds from the training set analysis. In the test set we repeated the dilution series using mixed cell lines of KOPN-8, HAL-01, FKH-1, and MV4–11 (see Table 5.2 in the online Data Supplement) to confirm the minimum percentage of aberrant cells detectable by our assay. Sensitivity was further assessed by random downsampling of aligned reads of the test set's cell line dilution series (see Table 6 in the online Data Supplement). The outcomes were benchmarked against the results obtained from routine genetic tests. A finding was considered true-positive if it was concordant in the TLA and routine diagnostic tests; it was considered true-negative if it was not detected by any of the tests. A sample finding was considered false-negative if the translocation involving genes present in the multiplex TLA panel was not detected by the TLA assay but was seen in routine tests. It was considered false-positive if the TLA assay indicated the presence of a translocation, but the routine tests could not detect it.

4.3 Results

4.3.1 Validation of the TLA multiplex panel - Training set

Optimized analysis and interpretation of patient bone marrow samples. We optimized translocation calling by the TLA multiplex pipeline by adding data filtering and defining data QC and data interpretation steps according to the location and size of the captured peaks (see Methods in the online Data Supplement). Using the analysis settings optimized for the 17 bone marrow samples, 16 samples, including 88% of targets, passed our QC. Sample #13 failed because of the absence of sequence reads (peaks) on target regions owing to a low cell count (see Table 7 in the online Data Supplement) and was eliminated from further analysis. In total, 9 definitive translocation calls were made (Table1). In sample #9 there were 2 separate events (see Table 8 in the online Data Supplement). The first involved captured peaks smaller than the threshold in the ABL1 and MYC targets, resulting in a translocation call in the gray zone that required confirmation. Procedure-wise, this call was followed up, which led to further evaluation using the karyotype information, after which the gray zone call was considered negative. A translocation known to be present in sample #9, t(8;21)(q22;q22), led to a false-negative result, because the expected peak on chromosome 8, from the RUNX1 viewpoint, was not detected. In a further 2 samples, a translocation was missed. These translocations were labeled as false negatives. In 1 of these samples [#10, t(11; 19)(q23;p13.1)], as well as the earlier mentioned sample #9 – t(8;21)(q22;q22), multiplex amplification on the targeted region was not able to generate a sufficient number of reads on the translocation partner to

pass our data filter threshold. In sample #5, t(11;17)(q23;q25) was missed. Here, there were no reads present on the translocation partner. Four other samples in which the multiplex TLA panel detected no translocations had normal karyotypes. No false-positive results were found. In total, 13 of the 16 samples passing the QC generated concordant results to routine genetic and cytogenetic results (see Table 9 and Fig. 5 in the online Data Supplement).

Sensitivity to detect translocations present in a low percentage of cells. Dilution series of the cell lines KOPN-8 and HAL-01 with 5% to 100% aberrant cells were prepared to determine the translocation detection sensitivity of the TLA panel. Optimized analysis settings using the filter and interpretation steps labeled all samples and 94% of targeted regions as passing QC. In the HAL-01 cell line, t(17;19)(q22;p13),including *TCF3*, was seen in samples having at least 10% aberrant cells. This also holds for t(11;19)(q23;p13) in the KOPN-8 cell line, including *KMT2A*. In the same cell line, t(8;13)(q24;q21.2) was seen in the presence of 25% aberrant cells. In total, above 10% aberrant cells, 20 translocation calls were made, of which 3 were labeled as gray-zone. All calls were positive after confirmation. MYC was not detected at 10% aberrant cells, leading to detection of 20 out of 21 translocations (see Table 8 in the online Data Supplement). No false-positive calls were made in the cell line training set. As additional positive controls for complex cryptic translocations, the cell lines REH and FKH-1 were tested on samples with 100% aberrant cells. Cell line REH was previously karyotyped (see Table 1 in the online Data Supplement) as carrying a 4-way translocation t(4;12;21;16)(q32;p13;q22;q24.3)[156]. TLA did not find partner chromosome 4 from the position of the chromosome 12 target region, although it successfully detected partner chromosome 21. TLA also detected chromosomal partners 12 and 16 captured from the target region on chromosome 21 (see Table 8 in the online Data Supplement). TLA results were confirmed by additional karyotyping, leading to recharacterization of the translocation to t(12;21;16)(p13;q22;q24.3). In cell line FKH-1, we detected t(6;9)(p23;q34), resulting in a DEK-nucleoporin 214 (*NUP214*) fusion gene. In addition, we identified a translocation t(9;12) (q34;p13), which was not present in the cytogenetic information of the cell line catalogue[155]. FISH using the *BCR/ABL1* and *ETV6* probes supports this finding (see Fig. 4 in the online Data Supplement).

4.3.2 Validation of the TLA multiplex panel - Test set

High concordance between TLA multiplex panel and routine tests for bone marrow samples. We assessed the clinical utility of the optimized and fixed data analysis and interpretation procedure on anonymized test set samples.

Results from the TLA procedure and routine genetic tests were compared. A total of 14 out of 19 samples, including 74% of targets, passed QC. All 5 samples that failed QC (#25, 26, 28, 29, and 33) were from nonhomogeneous cell suspensions, leading to the absence of sequence reads (peaks) on target regions. In the samples that passed QC, we made 3 definitive translocation calls and 6 gray zone calls needing confirmation. Four of the 6 gray zone calls, 3 t(12;21) and 1 t(3;12), were confirmed (Table 4.1) by other genetic tests. Two were considered negative after follow up with confirmatory tests and routine diagnostic data. We detected no translocations in 7 samples. All translocation calls were concordant with the benchmarking tests. No translocations involving genes present in the multiplex TLA panel were missed and no false-positive translocations were called (see Table 9 and Fig. 5 in the online Data Supplement).

Reproducibility of sensitivity to detect translocations in aberrant cell lines. We performed a second dilution series in a range of 1% to 50% aberrant cells, involving test cell lines (KOPN-8, HAL-01, FKH-1, and MV4-11) to confirm the translocation detection sensitivity of the TLA panel in repeated cell line samples. Translocations including *TCF3*, *DEK*, *ETV6*, *RUNX1*, and *KMT2A* were detected in samples with a minimum of 10% aberrant cells. Similar to the training set dilution series, all the test set samples, including 99% of targets, passed QC. The translocation involving MYC was detected in samples containing at least 25% aberrant cells. In total, above 10% aberrant cells, 18 translocation calls were made, of which 4 were labeled as gray zone. After confirmation, 2 of the gray zone calls were positive and 2 were nullified. *MYC* was not detected at 10% aberrant cells, leading to detection of 16 out of 17 translocations—including FKH-1 t(9;12)(q34;p13) (see Table 8 in the online Data Supplement). No false positive translocation calls were made.

Table 4.1: TLA and benchmarking of the results from the training and test sets

Sample	Referral reason	Translocation in ROI	Karyotype	FISH	RT-PCR	TLA
Training	set					
1	ALL	t(12;21)(p13;q22)	1[1]	n/a	+[2]	+
3	ALL	t(8;14)(q24;q32)	+	n/a	n/a	+
4	CML	t(9;22)(q34;q11.2)	+	n/a	+	+
5	AML	t(11;17)(q23;q25)	+	+*[3]	n/a	-
6	CML	t(9;22)(q34;q11.2)	+	n/a	+	+
9	AML	t(8;21)(q22;q22)	+	+	+	-
10	AML	t(11;19)(q23;p13.1)	+	+*	n/a	-
11	AML	t(9;22)(q34;q11.2)	+	+	+	+
12	ALL	t(1;19)(q23;p13.3)	+	n/a	n/a	+
13	AML	t(15;17)(q34;q11.2)	+	+	+	n/a
15	CML	t(9;22)(q34;q11.2)	+	+	+	+
16	AML	t(15;17)(q24;q21)	+	+	+	+
17	ALL	t(4;11)(q21;q23)	+	+*	n/a	+
2	ALL	None	-	-	-	-
7	AML	None	-	-	n/a	-
8	AML	None	-	n/a	-	-
14	AML	None	-	-	n/a	-
Test	set					
18	AML	t(9;22)(q34;q11.2)	+	+	+	+
19	AML	t(11;19)(q23;p13.1)	+	+*	n/a	+
20	AML	t(3;12)(q26;p12)	+	+*	n/a	+
24	ALL	t(12;21)(p13;q22)	-	n/a	+	+
26	AML	t(9;22)(q34;q11.2)	+	n/a	+	+
30	ALL	t(12;21)(p13;q22)	-	n/a	+	+
35	ALL	t(12;21)(p13;q22)	-	n/a	+	+
36	ALL	t(12;21)(p13;q22)	-	+	+	+
21	ALL	None	-	-	n/a	-
22	AML	None	-	n/a	n/a	-
23	AML	None	-	-	-	-
25	ALL	None	-	-	n/a	n/a
27	ALL	None	-	-	n/a	-
28	AML	None	-	-	-	n/a
29	ALL	None	-	-	n/a	n/a
31	ALL	None	-	-	-	-
32	ALL	None	-	-	-	-
33	ALL	None	-	-	-	n/a
34	ALL	None	-	-	-	-

[1] (-) Translocation absent
[2] (+) Translocation present
[3] (+*) Break seen on 1 translocation partner

4.4 Discussion

We have developed a genetic screening assay to detect translocations relevant to acute leukemia using a multiplex TLA panel in combination with NGS. The TLA assay allows screening of multiple genomic regions and numerous samples simultaneously on a single platform, including those with cryptic translocations such as t(12; 21). Up to now, karyotyping, in combination with FISH and/or RT-PCR, has been required to detect such translocations [178]. Using our assay, we were able to detect translocations in cell lines with at least 10% aberrant cells for the genes tested (*MYC* at 25%). This sensitivity is in the same range as that offered by karyotyping [162, 26], although karyotyping often fails in detecting cryptic translocations and complex aberrations, and it also needs cells to be cultured. RT-PCR and FISH have sensitivities of 0.01%–1% [25, 176] and 5%–10% [184, 8, 117], respectively, but these tests only work on specific targeted translocations or give no information on the translocation partner. Our TLA assay offers a competitive option for screening of unknown and cryptic translocation partners. For the patient samples that passed QC, we achieved a concordance with routine genetic testing of 81% in the training set and 100% in the test set for detecting translocations involving genes included in our TLA multiplex panel. In the training set, 2 translocations, t(8;21)(q22; q22) and t(11;19)(q23;p13), had too few reads to be distinguished from backgroundsignal. It is likely that the 5 million cells used in the assay were suboptimal in yielding sufficient quality for the detection of rearrangements. This was solved by doubling the number of cells used, which led to detection of all targeted translocations in test samples. We have observed that some targets are susceptible to suboptimal sample quality, resulting in inadequate enrichment. We also found that a nonhomogeneous cell suspension and clots in frozen samples yielded low-quality results. We therefore recommend starting with fresh material or assessing cell viability after thawing of frozen samples and starting the TLA procedure with 10 million viable cells. Primer concentrations for sensitive targets such as *BIRC3*, *CBFB*, and *KAT6A* need further optimization to improve the robustness of the panel. The third translocation we missed was t(11;17) (q23;q25). This translocation was present in around 70% of karyotyped metaphases of sample #5. However, no reads were present on chromosome 17 in the TLA multiplex panel, although FISH demonstrated the chromosome 11 breakpoint to be in the *KMT2A* gene. Often, seemingly balanced translocations are accompanied by deletions[136]. Both *KMT2A* probes used in our panel are located within 10 kb of the major breakpoint region between exons 7 and 13[25]. A possible explanation for the missed translocation would be a deletion of this region. This will result in the absence of *KMT2A* probe target locations on

the translocation chromosome and a subsequent false-negative result. Such known complexity around breakpoints should be taken into account when designing the panel and interpreting the results. Including an additional TLA primer set further from the expected breakpoint could avoid this problem in future experiments. In our sample cohort we obtained 100% specificity with no false-positive results. Another multiplex TLA panel, described earlier, targeting 19 BCP-ALL (B-cell precursor acute lymphoblastic leukemia) genes, identified all known rearrangements but did not mention the specificity of the panel[102]. Occasionally, owing to a low percentage of aberrant cells in a sample, a translocation can be missed when using strict analysis thresholds. To ensure optimal sensitivity and specificity, we introduced a gray zone. Captured chromosomal regions with few reads suggesting the presence of a translocation are considered as a gray zone translocation call. This enables a more explicit assessment of indeterminate translocation calls that have a moderate coverage to prevent false positive calls and missed translocations. In such cases, an additional confirmation test is required. In our small test cohort, starting with an optimal number of cells, 67% of the gray zone calls were confirmed. Using this strategy, a 100% sensitivity and specificity was obtained. Our multiplex TLA assay potentially captures all translocations involving 1 of the 17 targeted genes up to breakpoint distances of several hundreds of kilobases. It is illustrative that when TLA was applied to samples containing complex structural variation, it resulted in the recharacterization of the genotypes described earlier in cell lines REH and FKH-1. Our screening assay identified translocations in not only targeted genes, but also in genes not directly targeted, such as *NUP214*, located 200 kb from *ABL1*, which led to detecting the *DEK-NUP214* fusion in the FKH-1 cell line, even with only 10% aberrant cells present. Furthermore, we showed that the TLA panel can be applied in other hematological malignancies, because it can detect the t(9;22)(q34;q11) and t(8; 14)(q24;q32) translocations that are found in up to 95% of patients with chronic myeloid leukemia and in 80%of those with Burkitt lymphoma [60, 64]. Using the panel, we detected 3 different *KMT2A* translocations in our small cohort: 2, t(11;19)(q23; p13.3)[*KMT2A-ENL*] and t(4;11)(q21;q23) [*KMT2A-AF4*], in the cell lines, and 1, t(11;19)(q23;p13.1), in a test set sample, likely resulting in a *KMT2A-ELL* gene fusion (Table)4.1). The KMT2A gene alone has 80 known fusion partners [137, 237]. Likewise, the other 16 panel genes can, in principle, detect all known translocations as well as novel ones. In contrast, other methods such as translocation comparative genomic hybridization[80] and GIPFEL[70] detect only specific fusions and show lower sensitivity. Alternatively, RNA-based techniques could be considered for translocation detection [118, 211, 186, 110, 245] and are major competitors to the TLA assay. RNA-based platforms are instrumen-

tal in the detection of single-nucleotide variants, insertions, deletions, copy number changes, and fusions[245]. However, these techniques can detect only translocations with breakpoints in exonic or intronic regions and are dependent on the expression of the fusion gene, limiting their use for the detection of non-transcript altering translocations such as those involving MYC. We determined that our assay required a minimum of10% aberrant cells in a sampletodetecttranslocations involving targeted regions, with the exception of the *MYC* target region, where the detection limit was 25% for t(8;13)(q24;q21.1). A likely explanation for this lower sensitivity is that, for MYC, probes were designed solely in the 190-kb region associated with the most common breakpoint regions for translocations t(8;14),t(2;8), and t(8;22), whereas it is known that breakpoints around MYC can be present in a much larger area of 2 Mb [214]. However, we reduced the location of the breakpoint to the 740-kb region covered by the MYC break-apart probe, of which 620 kb is located distally from our targetedbreakpointregion. It is therefore possible that the breakpoint of the rare t(8;13) translocation is located outside our region of interest, making it harder to capture the translocation partner and thus lowering the sensitivity. In conclusion, in this proof-of-principle study, our multiplex TLA assay shows promising results that indicate it is suitable as a first-tier screening test in acute leukemia, chronic myeloid leukemia, and Burkitt lymphoma for detection of most common cryptic and other translocations, without prior knowledge of particular fusion partners. Further improvements in probe concentrations, input quality control, and automation of total workflow will enhance robustness and sensitivity and may make the assay suitable for diagnostic use.

4.5 Acknowledgments

We thank Jackie Senior and KateMc Intyre for editorial advice.

Authors' Disclosures or Potential Conflicts of Interest

Disclosures and/or potential conflicts of interest: Employment or Leadership: E. Splinter, Cergentis b.v.; P. Klous, Cergentis b.v.; M. Yilmaz, Cergentis b.v.; M. van Min, Cergentis b.v. Consultant or Advisory Role: None declared. Stock Ownership: M. van Min, Cergentis b.v. Honoraria: None declared. Research Funding: ZONMW, grant no 40-41200-98-9159. Expert Testimony: None declared. Patents: None declared. Role of Sponsor: The funding organizations played no role in the design of study, choice of enrolled patients, review and interpretation of data, or final approval of manuscript

4.6 Online data supplement

http://clinchem.aaccjnls.org/content/clinchem/suppl/2018/04/27/clinchem.2017.286047.DC1/clinchem.2017.286047-1.pdf

Chapter 5

Novel algorithms for improved sensitivity in Non-Invasive Prenatal Testing

Scientific Reports 2017;7(1):1838.
DOI: 10.1038/s41598-017-02031-5
PubMed ID: 28500333

L.F. Johansson[1,2,*], E.N. de Boer[1,*], H.A. de Weerd[1,2], F. van Dijk[1,2], M.G. Elferink[3], G.H. Schuring-Blom[3], R.F. Suijkerbuijk[1], R.J. Sinke[1], G.J. te Meerman[1], R.H. Sijmons[1], M.A. Swertz[1,2], B. Sikkema-Raddatz[1]

1. University of Groningen, University Medical Center Groningen, Department of Genetics, Groningen, The Netherlands
2. University of Groningen, University Medical Center Groningen, Genomics Coordination Center, Groningen, The Netherlands
3. University Medical Center Utrecht, Department of Genetics, Utrecht, The Netherlands

Received 2017 Jan 6; Revised 2017 Apr 4; Published online May 12.

* Contributed equally

Abstract

Non-invasive prenatal testing (NIPT) of cell-free DNA in maternal plasma, which is a mixture of maternal DNA and a low percentage of fetal DNA, can detect fetal aneuploidies using massively parallel sequencing. Because of the low percentage of fetal DNA, methods with high sensitivity and precision are required. However, sequencing variation lowers sensitivity and hampers detection of trisomy samples. Therefore, we have developed three algorithms to improve sensitivity and specificity: the chi-squared-based variation reduction (χ2VR), the regression-based Z-score (RBZ) and the Match QC score. The χ2VR reduces variability in sequence read counts per chromosome between samples, the RBZ allows for more precise trisomy prediction, and the Match QC score shows if the control group used is representative for a specific sample. We compared the performance of χ2VR to that of existing variation reduction algorithms (peak and GC correction) and that of RBZ to trisomy prediction algorithms (standard Z-score, normalized chromosome value and median-absolute-deviation-based Z-score). χ2VR and the RBZ both reduce variability more than existing methods, and thereby increase the sensitivity of the NIPT analysis. We found the optimal combination of algorithms was to use both GC correction and χ2VR for pre-processing and to use RBZ as the trisomy prediction method.

5.1 Introduction

The discovery of cell-free fetal DNA (cffDNA) fragments in the maternal bloodstream [122] in combination with the development of massively parallel sequencing has made it possible to perform non-invasive prenatal testing (NIPT). The traditional invasive procedures for prenatal aneuploidy testing, amniocentesis and chorionic villi biopsy, are associated with an elevated miscarriage risk [2]. This disadvantage can be overcome by NIPT, which can detect fetal aneuploidies in maternal blood as early as ten weeks into the pregnancy without the need for an invasive procedure [62]. NIPT makes use of cell-free DNA fragments isolated from blood plasma. Some of these fragments, the cffDNA, originate from the placenta and are informative of the fetus: when a chromosomal trisomy is present, the number of fragments originating from that chromosome will be higher than what is expected based upon statistical analysis using a set of non-trisomy control samples. Because NIPT is based upon analysis of very small amounts of DNA, measurements are very sensitive to the introduction of variability between samples and experiments. The statistical analysis in NIPT was first improved by the introduction of the Z-score calculation [35], which compares the individual sample with a set of non-trisomy controls. However, when applying the standard Z-score calculation without prior data correction, a high variability was found for chromosomes 13 and 18 [31]. This is undesirable because it lowers the sensitivity of the test. Thus, if a low fraction of cffDNA is present, there is a risk of false-negative results.

An important cause of variability is the guanine and cytosine (GC) content of the DNA fragments analyzed. There are various GC-bias correction methods, such as those based on locally weighted scatterplot smoothing regression (LOESS) [31, 107, 158, 116] or on the average coverage of genomic regions having a similar GC-content [63]. We used the latter method in combination with a peak correction that removes regions having significantly more reads than average [63].

Variability can also be reduced by adapting the Z-score calculation, for instance by using the normalized chromosome value (NCV) [107, 188] or the median absolute deviation (MAD) based Z-score [203].

Our aim here was to further decrease variability and thus increase the sensitivity of NIPT. We therefore developed three new algorithms: the chi-squared-based variation reduction (χ2VR), the regression-based Z-score (RBZ), and the Match QC score. The χ2VR reduces the weight of the number of reads in regions that have a higher variation than expected by chance, regardless of the origin of the bias. The RBZ uses a model based on forward regression for prediction. The Match QC score calculates whether the

non-trisomy control set is representative for the analyzed sample.

We compared the performance of our algorithms against and in combination with existing algorithms. Furthermore, we show that the Match QC score can indicate whether a sample fits within a control set.

5.2 Material and Methods

To assess the added value of the χ2VR, RBZ and the Match QC score to the sensitivity and quality control of trisomy prediction, the performance of the algorithms was compared to that of existing variation reduction methods (peak correction and bin or LOESS GC correction) and trisomy prediction methods (standard Z-score, NCV and MAD-based Z-score) (Figure:)6.1). We included all methods used, except peak correction and the MAD-based Z-score, in NIPTeR, an R package publicly available under the GNU GPL open source license on CRAN and at https://github.com/molgenis/NIPTeR.

We focused on whole genome sequencing analysis, in which the fraction of sequenced reads originating from the chromosome of interest in the sample is compared with that of a set of non-trisomy control samples. In all analyses, only data from autosomal chromosomes was used.

Each chromosome was partitioned into bins of 50,000 base pairs. This bin size is in line with previous methods [62, 31, 107, 158, 63]. In each bin, the number of reads aligned to the forward and reverse strands reads were counted. The bin counts were used as the basic components for all further processing.

5.2.1 Chi-squared-based variation reduction

The novel χ2VR reduces the weight of the number of reads in bins that have a higher variation than expected by chance and thus reduces the impact of these bins on the chromosomal fractions. No prior knowledge on the origin of the variation is needed. The χ2VR performs a sum of squares calculation: per bin, the sum of the chi-squared value is calculated over all the selected control samples. For this calculation, the observed read counts o are first normalized by multiplying them with a normalization factor. This factor is the mean number of observed total read counts for all autosomal bins i of all control samples j divided by the mean number of observed total read counts for all autosomal bins of the sample s. In short, the observed normalized read count for a specific bin (on_i) can be calculated as follows:

$$on_{is} = o_{is} \times \frac{(\sum_{ij=1}^{n} o_{ij}))/(n_i \times n_j)}{(\sum_{i=1}^{n} o_{is})/n_i}$$

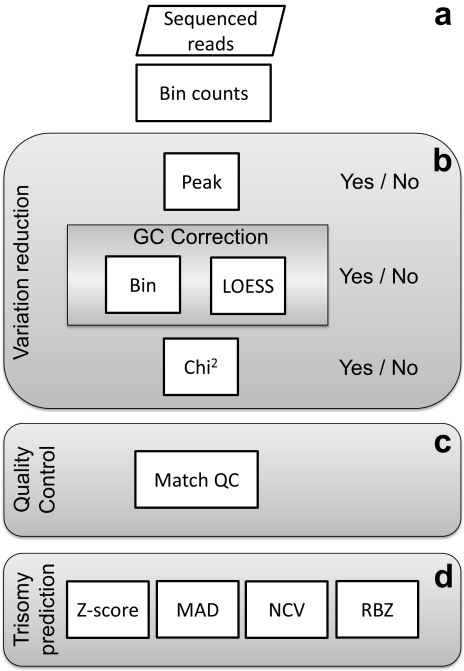

Figure 5.1: Flowchart showing the analysis steps. (a) First, sequenced reads are aligned, partitioned into 50,000 bp bins and counted. These bins are the units for further analysis and data quality can be improved using zero or more variation reduction methods. (b) Peak correction removes bins showing an unusually high coverage compared with the average coverage of bins on the same chromosome. GC correction corrects for coverage differences between bins having a different GC percentage, using one of two methods: 'bin' or 'LOESS' GC-correction. The chi-squared variation reduction corrects bins showing a higher variation in read counts between samples than expected by chance. Analysis is performed based on (corrected) read counts. (c) The Match QC indicates whether a control-group is informative for the analyzed sample. (d) Various algorithms (standard Z-score, MAD-based Z-score, Normalized Chromosome Value and Regression-based Z-score) are used for predicting trisomy.

where n_i is the number of bins and n_j is the number of control samples. Then, the chi-squared value for each bin i is calculated for each control sample j by dividing the squared difference between the expected and observed normalized read count by the expected normalized read count for that bin, where the expected normalized read count is the average normalized read count for a specific bin in all control samples (μ_{ij}). The sum chi-squared value is calculated by adding up the chi-squared values of all the control samples for the bin:

$$\sum_{j=1}^{n} \chi_{ij}^2 = \frac{(\mu_{ij} - on_{ij})^2}{\mu_{ij}}$$

The sum chi-squared value for each bin is transformed to a standard normal distribution N(0, 1) by subtracting the degrees of freedom df (number of control samples minus one) from the sum chi-squared value and dividing this by the square root of two times the degrees of freedom.

$$N(0,1) = \frac{(\sum_{j=1}^{n} \chi_{ij}^2) - df}{\sqrt{2df}}$$

This results in a Z-score, which shows the number of standard deviations (SD) an observation differs from the expectation. Reads in bins with a Z-score higher than 3.5 are divided by the sum chi-squared value divided by the degrees of freedom, thereby reducing the variability between the samples. Normalized read counts in bins with a Z-score lower than 3.5 are not corrected. The justification for this procedure is that probability plots show the expected chi-squared distribution up to a Z-value of about 3.5. Values above 3.5 are much more frequent than would be expected, so instead of ignoring those bins we chose to reduce the weights, assuming that there is still information present in the over-dispersed bin counts. An overview of the analysis steps and their effects is shown in Supplement 1[1].

5.2.2 Regression-based Z-score

The RBZ combines linear regression with a Z-score calculation. In the RBZ calculation the fraction of the chromosome of interest is predicted using stepwise regression with forward selection, in short forward regression. The reads aligned to the forward and reverse strands are used as separate predictors, because several chromosomes show a small, but consistent, over- or under-representation of reads aligned to the forward or reverse strand (Supplement

[1] added at the end of this chapter

2). However, all reads aligned to the chromosome of interest are taken together rather than separated, because the higher number of reads leads to a lower variability in the number of reads aligned to the chromosome of interest.

For each chromosome of interest, the four best predictor sets, which each consist of four predictors, are determined by forward regression, using the adjusted R squared of the model as a selection criterion. The predictors can have either a positive or a negative correlation with the chromosome of interest. Within each predictor set only one predictor can be selected from each chromosome, limiting the risk of introducing bias.

Using the models created for each control sample s the expected chromosomal fraction (ef) is calculated for the chromosome of interest. Subsequently, the observed chromosomal fraction of the total read count of the chromosome of interest (of) is divided by this expected fraction. In combination with the standard deviation of the prediction, a Z-score is calculated for each sample. Because the mean of the control group after regression is one, the coefficient of variation of the control group has the same value as the SD.

In short, the RBZ can be formulated as:

$$\frac{of_s/ef_s - 1}{\sqrt{\sum_{j=1}^{n}(of_j/ef_j - \overline{of/ef})^2/n - 1}}$$

where s is the sample of interest, j is an individual control sample and n is the total number of control samples.

The RBZ not only uses information from chromosomes having a positive correlation of read counts with the chromosome of interest, but also from chromosomes showing a negative correlation. An overview of an example RBZ calculation is shown in Supplement 3[2].

5.2.3 Match QC score

For the sample of interest, the novel Match QC score algorithm calculates how well the overall pattern of chromosomal fractions matches the pattern of the control samples. If the pattern of the sample differs too much from that of the controls, the sample does not fit within the control group, making the control set non-representative for the sample. Cut-offs are control-group-specific and can be set using the Match QC scores of the individual control group samples. The Match QC score uses the data used for trisomy prediction as input. Variation reduction, e.g. GC-correction or χ2VR, is applied before calculating the Match QC score.

[2]added at the end of this chapter

To obtain the Match QC score, first the chromosomal fractions (of) are calculated for the sample and all control samples. This is done by dividing the (weighted or corrected) total read count of each chromosome by the total read count of all autosomal chromosomes, excluding chromosomes 13, 18 and 21. Subsequently, for each control sample, the sum of squared differences of the chromosomal fractions between the sample and the control for all autosomal chromosomes, excluding chromosomes 13, 18 and 21, is calculated.

In short, the Match QC score between a sample of interest s and an individual control sample j can be formulated as:

$$\sum_{k=1}^{n} (of_{ks} - of_{kj})^2$$

where k is the chromosome and m is the total number of chromosomes, excluding chromosomes 13, 18 and 21.

Smaller differences indicate a better match. An overall Match QC score is calculated by taking the average of the results of all samples. The formula for the overall Match QC score is:

$$\frac{\sum_{j=1}^{n} \sum_{k=1}^{m} (of_{ks} - of_{kj})^2}{j}$$

where n is the number of control samples.

5.2.4 Validation of algorithms

Samples

To assess the effects of different variation reduction and trisomy prediction algorithms, we sequenced 128 non-trisomy and 43 trisomy samples using the SOLiD Wildfire platform (Life Technologies, Carlsbad, CA, USA) and 142 non-trisomy and 7 trisomy samples using the HiSeq 2500 platform (Illumina, San Diego, CA, USA). A further 34 non-trisomy samples had an alternative plasma-isolation and were sequenced on a HiSeq. The trisomy status of all samples was determined using karyotyping or quantitative fluorescence PCR following amniocentesis or chorionic villi biopsy.

Samples were selected in accordance with and as part of the trial by Dutch laboratories for evaluation of non-invasive prenatal testing (TRIDENT) program, supported by the Dutch Ministry of Health, Welfare and Sport (11016-118701-PG). The program was also approved by the Ethics Committee of the University Medical Center Groningen. All participants signed an informed consent form.

Plasma isolation, sample preparation and sequencing

Plasma was obtained from two different sources. The first source was fresh EDTA blood, either processed within 3 hours of blood collection or within 24 hours if stabilizing reagent was present in the tubes (Streck Inc., Omaha, NE, USA). For samples sequenced using the Illumina platform, blood was first centrifuged at 1200 rcf for 10 minutes, without using brakes to stop the rotor. The plasma was then transferred to another tube and centrifuged at 2400 rcf for 20 minutes. The plasma was transferred to a third tube and stored at -80 °C. For samples sequenced on the SOLiD platform, the centrifugal forces used were 1600 rcf and 16000 rcf, respectively. The second source of plasma was obtained using an alternative isolation method using only the first centrifugation step at 1200 rcf, after which the blood plasma was stored at -20 °C.

For samples sequenced on the HiSeq, we isolated cell-free DNA (cfDNA) from 1.5 ml plasma with the QIAamp MinElute Virus Spin kit (Qiagen, Valencia, CA, USA) (90 non-trisomy and 6 trisomic samples), the Qiagen circulating nucleic acid kit (Qiagen) (21 non-trisomy samples) and the Akonni TruTip kit (Akonni Biosystems, Frederick, MD, USA) (31 non-trisomy samples and 1 trisomic sample). After DNA isolation, sample preparation was performed with NEBNext Multiplex Oligos for Illumina (New England Biolabs Inc., Ipswich, MA, USA). Before the amplification step, we performed a two-step size selection using Agencourt AMPure xp beads (Beckman Coulter, Inc., Brea, CA, USA), using a beads/sample ratio of 0.6:1 in the first step and a ratio of 1.2:1 in the second step. Samples were sequenced with a 50 bp read length on a HiSeq 2500 sequencing platform (Illumina).

For samples sequenced on the SOLiD, cfDNA was extracted from 1 ml plasma using the QIAamplDSP DNA blood mini kit (Qiagen). Libraries were prepared according to factory protocol and sequenced with a 35 bp read length on the SOLiD 5500 Wildfire sequencing platform (Life Technologies).

Read alignment

For Illumina data, after an initial quality control of the fastq data using the program fastqc (v.0.7.0), the data were aligned to the human reference genome build b37 as released by the 1000 Genomes project [55] using BWA aln samse (0.5.8_patched) with default settings [114]. After alignment a Sam output file [113] was created for each sample. Using Picard tools 1.6.1, a set of tools designed by the Broad Institute (Cambridge, USA) (http://broadinstitute.github.io/picard/) for processing and analyzing next generation sequencing data, the Sam files were transformed into Bam files. These Bam files were sorted and Bam index files formed. The Bam index

files link the reads to the genome position. Quality metrics files were then created and the duplicate reads in the Bam files marked.

For SOLiD data, raw reads were mapped against the human reference genome (GRCh37/hg19) using BWA v0.5.913. Options used for mapping were -c, -l 25, -k 2, and -n 10. The Bam files were filtered using Sambamba v0.4.5 [209] to retain non-duplicate reads, uniquely mapped reads (XT:A:R), reads with no mismatches to the reference genome (CM:i:0), and reads with no second best hits in the reference genome (X1:i:0).

After filtering and removal of duplicate reads, the total autosomal read count was on average 20.2 million (SD 5.6 million) for SOLiD data and 12.5 million (SD 2.2 million) for Illumina data.

Variation reduction

Aligned reads were divided into 50,000 bp bins and variation between samples was reduced using all possible combinations of zero or more variation reduction methods: peak correction, GC-correction and χ2VR. When more than one method was used, they were performed in the order described above (Fig. 1). A maximum of one GC-correction method was used. Since the LOESS GC-correction has been described more often [31, 107, 158, 116] than the weighted bin GC-correction [63], we used LOESS GC-correction to evaluate the other variation reduction and prediction methods.

Peak correction

Peak correction was performed as described by Fan and Quake [63]. This method removes bins having a read count that significantly differs from the average using the information of all control samples. A bin was considered to deviate from normal if the total read count fell outside 1.96 SD compared with total read counts in the bins on the same chromosome for that sample. We interpreted bins to have a consistent pattern of region-specific variations if the variation deviated from normal in 95% or more of the control samples.

GC-correction

An important factor explaining the systematic uncontrolled variation between chromosomes is the guanine and cytosine (GC) content of the DNA fragments analyzed. When this GC-bias is corrected during preprocessing of the data, it results in a significantly lower variability [116]. GC-correction was performed based on total read counts using two different methods. The first GC-correction method is based on a LOESS curve fitted to the reads counts

in bins sorted on GC content [31, 107, 158, 116] and based on R v3.0.2 default settings (span 0.75; degree = 2). The second GC-correction method is based on the average coverage of bins having a similar GC-content [63]. The GC% of each bin is determined for both methods. Bins not containing any reads and bins with an unknown base composition are ignored. The weights of the correction factors were based on GC-content intervals of 0.1% and consisted of the average coverage of the bins within the GC-interval divided by the average coverage of all bins.

Trisomy prediction

We predicted trisomies using four different prediction methods: standard Z-score prediction [31], NCV, using only the most informative chromosomes [188], MAD-based Z-score [203] and RBZ. Depending on the variation reduction methods employed, we used corrected or uncorrected read counts for prediction. For all analyses chromosomes 13, 18 and 21 were not used as predictor chromosomes, since the prediction would be affected if a trisomy was present in one of the chromosomes used for prediction.

In short, the standard Z-score calculates the fraction of reads originating from the chromosome of interest compared with all reads originating from autosomal chromosomes, and then subtracts the mean fraction – which is the expected fraction – of the chromosome of interest in a set of control samples. The result is then divided by the SD of the fraction in the control set.

The NCV does not use all the autosomal chromosomes to calculate the fraction of the chromosome of interest, instead using the most informative chromosomes, which were selected using a training set [188]. All combinations of denominator chromosomes were tested for both the Illumina and SOLiD datasets, and the combinations yielding the lowest CVs were selected. The NCV is sometimes compared to using an internal reference6 because, during analysis, the selected reference chromosomes behave similarly to the chromosome of interest. This positive correlation results in less sample to sample variation, reduces the need for GC correction, and increases prediction precision.

The MAD-based Z-score replaces the SD by 1.4826 * MAD, making the calculation more tolerant of outliers in the control set [203]. The MAD was calculated in three steps. First, the median of the fractions of the chromosome of interest in the control set was calculated. Second, the absolute difference of the chromosomal fraction to the median was calculated for each control sample. Finally, the MAD was calculated by taking the median of these absolute differences.

Comparison of the algorithms

In comparing the algorithms we used the CV as a benchmark for performance. The CV is a standardized measure of dispersion of a probability distribution and is defined as the ratio of the SD to the mean. In this manner it enables comparison between normal distributions with a different mean. The height of the CV of the control group, together with the percentage cffDNA, determines the discriminative power between normal and trisomic samples. When the CV decreases, the sensitivity increases (Supplement 4). We determined the added value of each variation reduction or prediction algorithm to lowering the CV to determine the best combination of algorithms.

For our analysis, we used all the non-trisomy samples sequenced with the same platform that underwent the same plasma isolation procedure as control samples. This resulted in control group sizes of 142 for the Illumina and 128 for the SOLiD sequencer. For all algorithms, the control group is only used when it is normally distributed as determined using the Shapiro Wilk statistical test ($p > 0.05$).

Algorithm combinations tested

We evaluated the effects of both peak correction and χ2VR on the CV of the control samples, the effect of the two different GC correction methods in combination with all prediction methods on the CV, and the effect of the different prediction methods on CV and Z-scores in combination with all possible variation reduction methods, except peak correction and the bin GC correction. The consistency of the RBZ trisomy prediction was determined by estimating three additional trisomy prediction models for each analysis.

Match QC score

To provide a proof of principle for the Match QC score performance, we divided the Illumina control group into a training set of 85 and a test set of 57 samples. The 34 Illumina samples that underwent a different plasma isolation protocol were used as an example of samples having undergone an alternative procedure.

We then calculated the Match QC score for all samples, using uncorrected, χ2VR, LOESS GC, and combined LOESS GC and χ2VR-corrected data. Cut-offs for the Match QC score were set on the average Match QC of the training set plus three SD. For all samples Z-scores were calculated for chromosomes 13, 18 and 21 to determine whether the scores fall within three SD of the average of the control set.

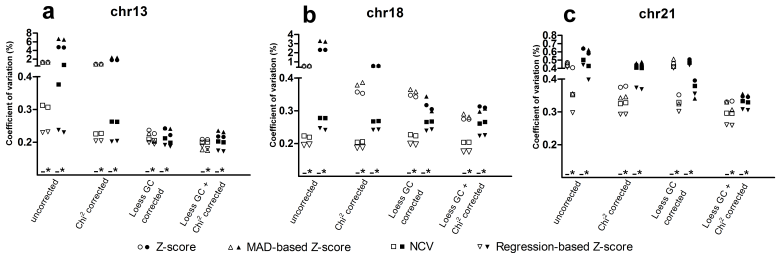

Figure 5.2: Effect of peak correction on the CV of control samples. The effect is shown for SOLiD (white) and Illumina data (black) with no other correction, for data that also had a chi-squared correction, or LOESS GC correction, or both LOESS GC and chi-squared correction. For each type of correction the CV of four prediction algorithms (standard Z-score, MAD-based Z-score, Normalized Chromosome Value and regression-based Z-score) are shown for (a) chromosome 13, (b) chromosome 18 and (c) chromosome 21. –not peak corrected; *peak corrected.

5.3 Results

For both the SOLiD and Illumina control groups, the CV of chromosomes 13, 18 and 21 was determined for all combinations of variation reduction and trisomy prediction methods and their theoretical effect on sensitivity and specificity was calculated (Supplement 5). The estimated percentages of cffDNA in the tested trisomy samples are shown in Supplement 6.

5.3.1 Effect of peak correction

To examine the effect of correcting bins with a coverage that deviates significantly from the average, we compared the CV of the peak-corrected data with that on which no peak correction was performed. Peak correction reduced the CV in most analysis strategies (Fig. 5.2). The largest relative effect for all chromosomes was observed when a GC-correction was also performed. The effect was largest in chromosome 21, which was the chromosome showing the lowest GC-bias when no correction was applied, suggesting that the influence of coverage peaks on variability only comes to light when GC-bias is limited. In data that was also χ2VR corrected, the variation did not further decrease but it did sometimes increase after use of a peak correction. This suggests that the peak correction and the χ2VR are partly correcting the same sources of bias.

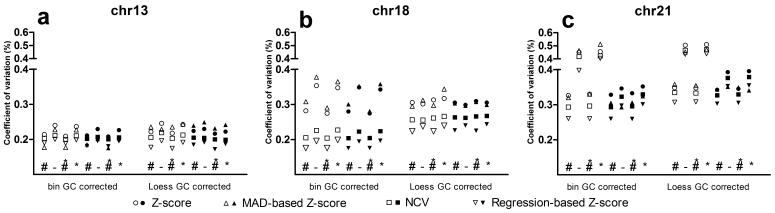

Figure 5.3: Comparison of the effect of two GC correction methods (bin GC correction and LOESS GC correction) on the CV of the control samples. SOLiD data (white) and Illumina data (black). For each type of correction the CVs of four prediction algorithms (standard Z-score, MAD-based Z-score, Normalized Chromosome Value and regression-based Z-score) are shown for (a) chromosome 13, (b) chromosome 18 and (c) chromosome 21. #Chi-squared corrected; -not corrected; *peak corrected.

5.3.2 Effects of the two GC correction methods

To examine the performance of the weighted bin GC correction and the LOESS GC-correction, we compared the performance of both methods in combination with all other variation reduction and prediction methods for chromosomes 13, 18 and 21 (Fig. 5.3) . For chromosome 13, both GC correction methods performed equally well regardless of the other variation reduction and prediction methods used. For chromosome 18, the weighted bin GC correction had a better performance for the NCV and RBZ compared to LOESS GC correction. However, the Z-score and MAD-based Z-score predictions performed better using the LOESS GC-correction. For chromosome 21, the weighted bin GC correction performed best, regardless of the other methods used. The data sets used made no difference to the performance of either GC-correction method.

5.3.3 Effect of chi-squared-based variation reduction

To examine the performance of the χ2VR, we compared the control group CV using all other variation and prediction methods, with and without the χ2VR (Fig. 5.4). The χ2VR resulted in a lower CV in most analysis strategies for all chromosomes. The effect was most striking in chromosome 21, regardless of the other methods used.

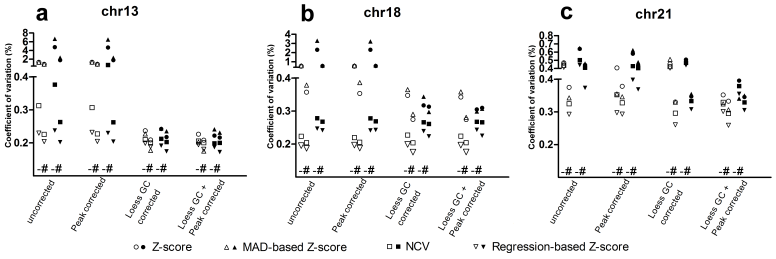

Figure 5.4: Effect of chi-squared-based variation reduction on the CV of control samples. SOLiD (white) and Illumina data (black) with no other correction, or with a peak correction, or LOESS GC correction or both LOESS GC and peak correction. For each type of correction the CVs of four prediction algorithms (standard Z-score, MAD-based Z-score, Normalized Chromosome Value and regression-based Z-score) are shown for (a) chromosome 13, (b) chromosome 18 and (c) chromosome 21. –not chi-squared corrected; #chi-squared corrected.

5.3.4 Effect of trisomy prediction algorithms

To examine the effect of the prediction algorithms (standard Z-score, MAD-based Z-score, NCV and RBZ), we compared the CV using uncorrected, χ2VR, LOESS GC, and combined χ2VR and LOESS GC corrected data. Since the peak correction provides no added value to the χ2VR, it was not used for comparison. The RBZ produced the lowest CV for all variation reduction methods except the SOLiD combined LOESS GC and χ2VR corrected data, in which the MAD-based Z-score for chromosome 13 produced an even lower CV (Fig. 5.5). The variation using the NCV is higher than that using the RBZ, but the CV is still much lower than the CVs of the methods that used all autosomal chromosomes. The standard Z-score had the highest coefficient of variation in all models.

A lower CV yields a more extreme Z-score, which means that in the case of a trisomy, the Z-score is more likely to be higher than the threshold, resulting in a higher sensitivity. The Z-scores of the trisomy samples of the four prediction algorithms for the uncorrected, χ2VR, LOESS GC, and combined χ2VR and LOESS GC corrected data are listed in Supplement 7. False-negative and false-positive results were determined for all the above combinations of variation reduction algorithms and prediction algorithms, based on a 99.7% confidence interval (Z-score threshold of three) (Supplement 8).

Of the 50 trisomic samples, a false-negative result was found in two trisomy 13 and three trisomy 18 samples for the Z-score or the MAD-based Z-score when no variation reduction was done. One confirmed trisomy 18

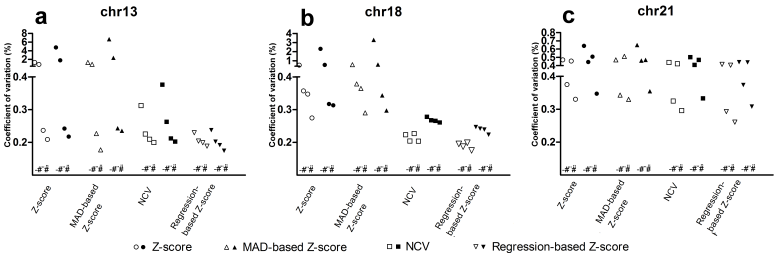

Figure 5.5: Effect of the different prediction algorithms on the CV of control samples. SOLiD data (white) and Illumina data (black). Results from the four different prediction algorithms (standard Z-score, MAD-based Z-score, Normalized Chromosome Value and regression-based Z-score) are shown for (a) chromosome 13, (b) chromosome 18 and (c) chromosome 21. –Variation was not reduced, #chi-squared corrected, " LOESS GC corrected, #" both LOESS GC and chi-squared corrected before prediction.

sample did not give a positive result with any combination of algorithms, possibly due to a low fetal percentage. No false-negatives were found for chromosome 21. For all true-positive results, all four RBZ models showed a Z-score higher than three.

To better show the effect of the different variation reduction and prediction algorithms on the Z-score, we selected three samples, sequenced on the SOLiD platform, each having a trisomy 13, 18 or 21 (Fig. 5.6). Based on the Z-scores and CVs, each sample had an estimated fetal percentage of 5–6%. The NCV and RBZ consistently yielded higher Z-scores than the standard Z-score and the MAD-based Z-score. The effect of the GC-correction is reflected in the results of the standard Z-score and the MAD-based Z-score for chromosome 13 and the effect of the χ2VR shows in the chromosome 21 results.

Of the 270 non-trisomy samples, four samples showed a false-positive result for more than one prediction algorithm. For one sample, all four prediction methods showed a result higher than three. The more sensitive NCV and RBZ prediction methods resulted in more false-positive results than the standard Z-score or MAD-based Z-score because more parameters are estimated, which leads to some overfitting and therefore underestimation of the prediction accuracy for new samples. This effect will be reduced when larger control groups are used. Three other false-positive results were only seen in one of the variation reduction methods, one for NCV and three for RBZ. In all these cases, Z-scores were just above three. In all cases adding or removing

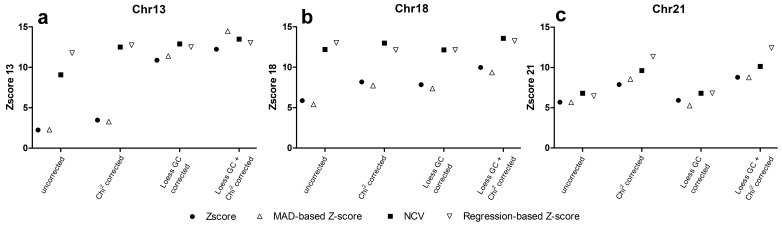

Figure 5.6: Z-scores for three trisomies using different combinations of variation reduction and prediction algorithms. All three examples are based on SOLiD data. Results from the four different prediction algorithms (standard Z-score, MAD-based Z-score, Normalized Chromosome Value, and regression-based Z-score), in combination with uncorrected, chi-squared corrected, LOESS GC corrected, and both LOESS GC and chi-squared corrected are shown for (a) chromosome 13, (b) chromosome 18 and (c) chromosome 21.

a variation reduction step, resulted in a negative call. For samples having a false-positive RBZ result, at least one of the additional RBZ predictions resulted in a negative prediction, except for the sample having a Z-score higher than three in all prediction methods.

5.3.5 Match QC score

To examine whether the Match QC score could accurately predict whether a sample fits within a control group, we calculated the Match QC scores and all the Z-scores for a training set, a test set of samples that had been prepared in the same manner as the training set, and a third set of samples originating from single centrifuged plasma. For all three sets, we used uncorrected, χ2VR, LOESS GC and combined χ2VR- and LOESS GC-corrected data (Fig. 5.7). Test set samples had Match QC scores in the same range as the training set samples and Z-scores that fell within three SD of the mean for all types of corrected data. Single centrifuged samples, however, showed Match QC scores in the same range as the control group samples for uncorrected and χ2VR corrected data, but above the three-SD threshold for LOESS GC corrected data and combined LOESS GC- and χ2VR-corrected data.

Z-score distributions for the training set samples and the test set samples were indistinguishable for all correction methods, but Z-scores based on uncorrected or χ2VR corrected data were not normally distributed for chromosomes 13 and 18. For the single centrifuged samples, Z-scores did not deviate from the normal distribution for the uncorrected data of chromosome 21. Match QC scores for all the samples analyzed, thresholds and Z-score

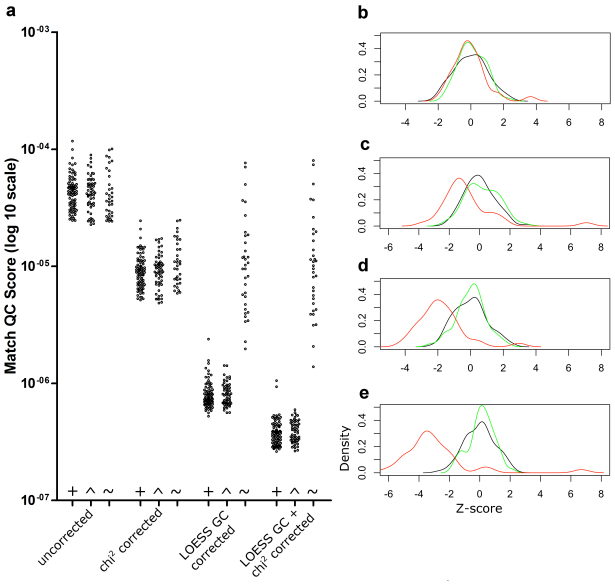

Figure 5.7: Match QC scores and Z-scores for matching and non-matching samples. (a) Match QC scores per sample for uncorrected, chi-squared corrected, LOESS GC corrected and both LOESS GC and chi-squared corrected data for the control group, matching samples, and non-matching samples. Chromosome 21 Z-scores for (b) uncorrected data, (c) chi-squared corrected data, (d) LOESS GC corrected data and (e) both LOESS GC and chi-squared corrected data. + and black line, control group samples; ând green line, samples that underwent the same sample preparation procedure; ãnd red line, single centrifugation plasma samples.

distributions for chromosomes 13, 18 and 21 are shown in Supplement 9.

5.4 Discussion

We show that both the χ2VR and the RBZ reduced the variability of the NIPT result and thus increased its sensitivity in both Illumina and SOLiD data. Furthermore, we show that a Match QC exceeding a three-SD threshold, determined using control samples, identified those samples for which the controls were not representative. Although the algorithms described in this study are designed to improve analysis of NIPT data, they may also be of use in similar types of analyses that need high sensitivity such as copy number variation detection in liquid biopsy data [29, 108].

The lower variability between samples decreases the percentage of fetal DNA needed for NIPT. A low percentage of fetal DNA is an important contributor to false negative or inconclusive results [126]. Moreover, the average percentage of fetal DNA is lower in trisomy 13 and trisomy 18 pregnancies than in non-trisomy pregnancies [230][6]. A low variability is therefore even more important for these pregnancies for the test to have a high sensitivity. Moreover, our novel algorithms produce a lower variability for a given number of reads, resulting in the need for fewer reads and lowering sequencing costs. Alternatively, only DNA-fragments originating from regions of interest could be selected [199, 5, 246]. However, such a selection requires additional amplification during sample preparation, which could also create additional variation due to increased over-dispersion [142, 50]. We therefore chose to reduce variation by correcting for bias in read counts before analysis, leading to a more comparable distribution of reads over the chromosomes between samples. Other studies have shown that variability can be introduced by bias present in the data, such as GC-bias [62, 31, 107, 158, 116, 63], or peaks of extreme coverage, probably caused by repeats [63]. However, due to a higher number of available reads, better results were obtained using a non-repeat-masked reference genome [31, 158]. For this reason, we did not mask any regions based on mappability tracks or blacklisted regions in our comparison.

In our comparison the lowest CVs for chromosomes 13, 18 and 21 were produced using the combination of the weighted-bin-based GC-correction method and the χ2VR with the RBZ. However, each variation reduction algorithm we tested reduced the variability when used alone. The effect of the peak variation reduction was small when combined with the χ2VR. This shows that the χ2VR corrects bias caused by regions of extreme coverage. Moreover, since the χ2VR focuses on variation present in each specific bin, and not on chromosomal averages, it can correct for variation that is too sub-

tle for peak correction. And since no assumptions are made about the origin of the bias, no prior knowledge is needed for correction. However, when using the χ2VR on the X-chromosome, variability should be determined using only data from pregnancies of a female fetus to prevent variability in the fetal percentage adding to the total variability on that chromosome. After application of GC-correction, χ2VR reduced variation even further, suggesting that χ2VR corrects for sources of bias other than that from GC. Since up to 50% of the human genome is repetitive [192], we suggest that part of the extra corrected bias is due to repeat structures. It has also been suggested that biological factors play a role in bias in NIPT [215, 30], so part of the corrected bias might have a biological origin.

Where peak correction and χ2VR only remove reads to reduce variation, GC-correction removes reads in bins having a GC-percentage containing more reads than average, but it adds virtual reads in bins with a GC-percentage containing fewer reads than average. Although, after GC correction, more reads seem to be present for several chromosomes, dispersion is still based on the original number of reads aligned to those chromosomes.

We demonstrated that the prediction method used can also reduce variability and increase sensitivity. The RBZ resulted in the lowest variability and decreased the need for GC-correction because this method takes this kind of systematic bias into account. However, there may be some pitfalls. Similar to the NCV, prediction is based on a limited number of predictor chromosomes. The effect of an aberration in one of the predictor chromosomes on the prediction is larger for the RBZ and NCV than for the standard Z-score, which uses all autosomes for prediction. To limit the effect of possible aberrations, we recommend comparing four independent predictor sets for the RBZ. Conflicting results of different models are a warning of possible false-positive results. In our data, all 49 trisomies detected were predicted independently by the four RBZ prediction sets. Only one false-positive call was made by all four sets. This call was also made by all the other prediction methods, suggesting that there may indeed be a higher fraction of reads of the called chromosome present in the data. Since the NCV can be based on only one denominator chromosome, we suggest multiple predictions using different denominators should also be used for NCV.

Our results show that a Match QC score below the three-SD threshold does not guarantee that the control group is representative for a sample, but a score exceeding the threshold does indicate that the analysis is not accurate. The main assumption in NIPT analysis is that the control set is representative of the sample analyzed. A non-representative control set leads to an inaccurate prediction and possibly to false-positive or false-negative results. It is therefore important that all samples undergo the same prepara-

tion, sequencing procedure and bioinformatics analysis. However, even when standard procedures are used, bias can vary between sequencing runs [1]. Prediction methods with a higher sensitivity are more vulnerable to the effects of unaccounted biological variation because deviations in the expected chromosomal fractions will more rapidly lead to false-positive results. Sample quality metrics are therefore essential for reliable analysis.

Our study shows that both the χ2VR and the RBZ increase the sensitivity of NIPT compared to previously published methods. Furthermore, we show that the Match QC score identifies samples for which the non-trisomy control set was not informative. Moreover, these algorithms may have a broader applicability than NIPT analysis, for instance in analysis of copy number variations in liquid biopsy data. We recommend our novel algorithms, as included in the NIPTeR package, as a useful addition to the NIPT analysis toolbox, resulting in a higher sensitivity, in theory making it possible to detect trisomies in blood with a fetal DNA amount as low as 2%.

Acknowledgments

We thank Jackie Senior and Kate Mc Intyre for editorial advice.

5.5 Supplementary material

Supplements 1 and 3 are added as an addendum to this chapter. The other supplements can be accessed online: https://www.nature.com/articles/s41598-017-02031-5#Sec24

5.6 Supplement 1: Example of chi-squared based variation reduction for chromosome 21

This supplement contains a series of graphs to visualize the effect of the chi-squared based variation reduction (χ2VR).

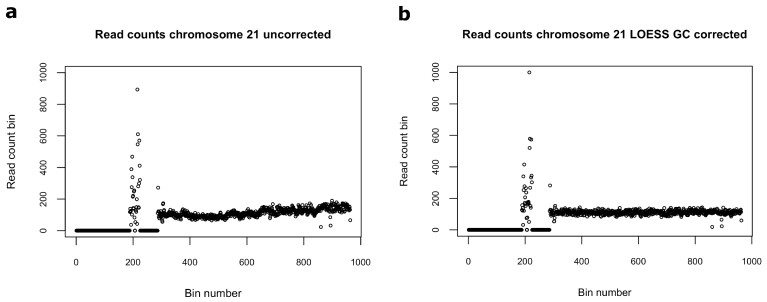

Figure 5.8: Read counts bins chromosome 21 without χ2VR of one of the Illumina control group samples (a) uncorrected data. (b)LOESS GC corrected data.

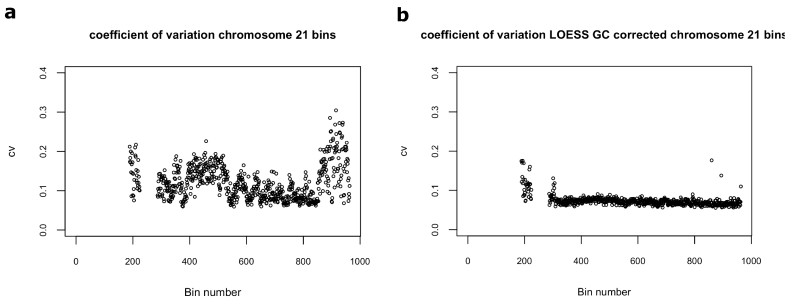

Figure 5.9: Coefficient of variation bins chromosome 21 without χ2VR of the Illumina control group samples (a) uncorrected data. (b)LOESS GC corrected data.

The input of the χ2VR are sample and control group, bin-counts of uncorrected data or data corrected using different variation reduction methods, such as GC correction (Figure 5.8). The examples are based upon the 142 Illumina control samples. In some images read counts of a single sample are

shown. For these images a random sample was selected from the control group.

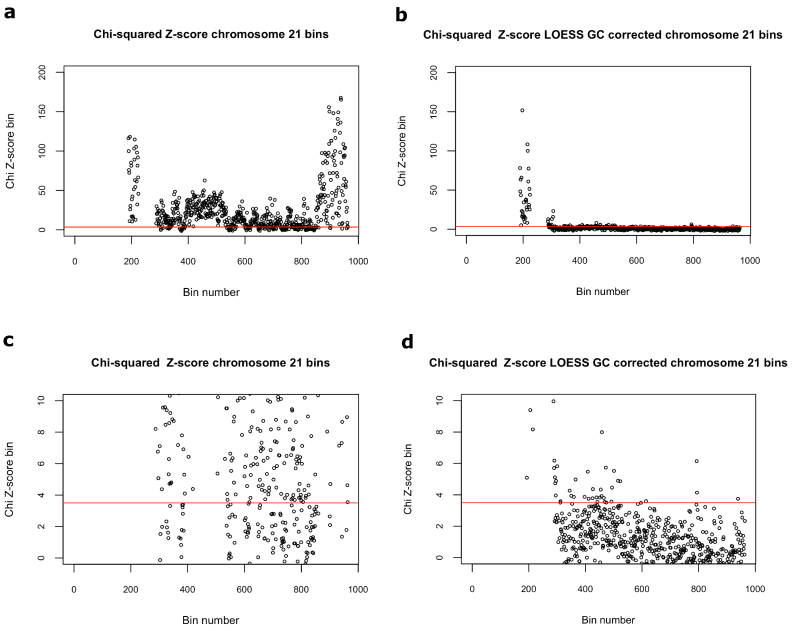

Figure 5.10: Z-score sum chi-squared value after transformation to normal distribution for all bins chromosome 21 based upon the Illumina control group samples (a) uncorrected data, total range. (b)LOESS GC corrected data, total range. (c) uncorrected data, plotted until a maximum Z-score of 10. (d) LOESS GC corrected data, pltoted until a maximum Z-score of 10.

First the data is normalized by dividing the mean read count of the bin by the mean read count of all autosomal bins. After this normalization sample read counts can be compared. In some of the bins the normalized read count is consistent between samples, resulting in a low coefficient of variation (CV). Other bins have a higher variability between samples, resulting in a higher CV (Figure 5.9). A GC correction can correct part of the variation. However, even after GC correction some bins still show a high variation. After normalization for each bin the sum chi-squared value is calculated, using the control samples, and transformed to a standard normal distribution, resulting in a Z-score for each bin (Figure 5.10).

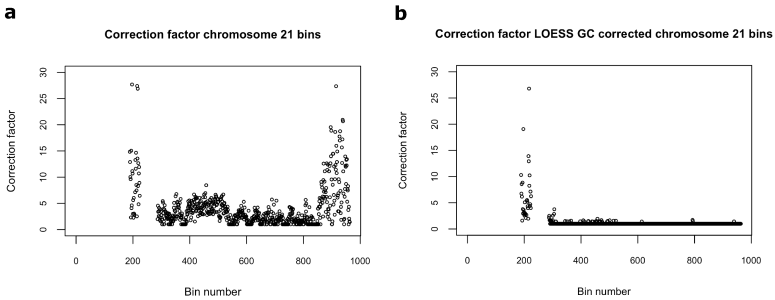

Figure 5.11: χ2VR correction factor bins chromosome 21 based upon Illumina control group (a) uncorrected data. (b)LOESS GC corrected data.

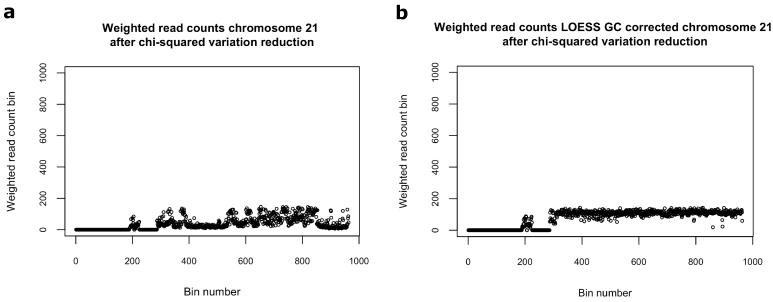

Figure 5.12: Weighted read counts bins chromosome 21 for one of the Illumina control group samples (a) uncorrected data. (b)LOESS GC corrected data.

A threshold was set at a Z-score of 3.5. In the case all the variation was introduced by chance 99.9998% of the bins show a Z-score below 3.5. The variation in bins having a Z-score greater than 3.5 (overdispersed bins) is thus very unlikely to result from random variation and these bins have a higher variability than expected. The χ2VR is based upon the assumption that there is still information present in the overdispersed bins. Instead of ignoring those bins, those exceeding the threshold will be weighted by dividing them by a correction factor (Figure 5.11, Figure 5.12). The correction factor consists of the sum chi-squared value divided by the degrees of freedom.

Note that weighting read counts of overdispersed bins does not change the CV of those bins. Variability between samples is not affected at bin

level. However, variability between chromosomal fractions is decreased after χ2VR (Figure 5.13). The chromosomal fractions are defined as the number of (weighted) read counts on chromosome 21 divided by the (weighted) read count of all autosomes. In figure 5.13 the fractions of chromosome 21 are normalized by dividing the fraction of each sample by the mean fraction of its control group.

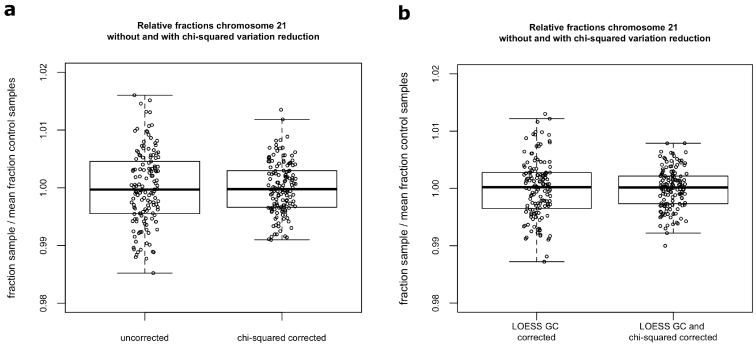

Figure 5.13: Relative fractions chromosome 21 before and after χ2VR of Illumina control group samples (a) uncorrected data. (b)LOESS GC corrected data.

5.7 Supplement 3: Regression model for chromosome 13

This supplement contains a series of graphs to visualize an example of a model upon which the RBZ is based. The input of the RBZ model are the chromosomal fractions of the control group samples. Chromosomal fractions of reads aligned to the forward strand and reads aligned to the reverse strand are considered as separate predictors, since there are consistent differences between those fractions (Supplement S2). However, reads aligned to the forward or reverse strand are considered together for the chromosome of interest, because this yields the lowest CV. Table 5.1 and 5.14 show a regression model using four predictors to predict the expected chromosomal fraction of chromosome 13 based upon the 142 Illumina control samples, without any variation correction.

Table 5.1: Coefficients of regression model chromosome 13 Illumina

Coefficients

	Estimate	Std. Error	t	value	Pr (<|t|)
Intercept	0.018236	0.004737	3.85	0.00018	[1]
4F	0.527854	0.056882	9.28	3.36E-16	[1]
6F	0.391124	0.086029	4.546	1.19E-05	[1]
16F	-0.20697	0.04596	-4.503	1.42E-05	[1]
1F	-0.25465	0.067397	-3.778	0.000235	[1]

[1] significance <0.001

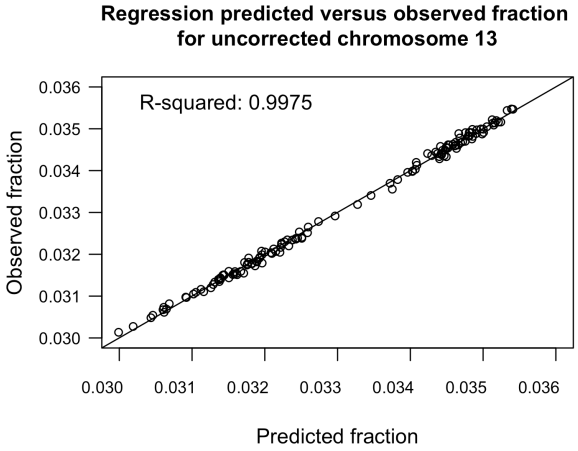

Figure 5.14: Regression model for prediction of expected read count for chromosome 13 based upon uncorrected Illumina control group samples

The four predictors in the regression model are selected using stepwise regression with forward selection. Which predictors are selected depends on the control group. For the 142 Illumina control samples, the best predictors were reads aligned to the forward strands of chromosomes 1, 4, 6 and 16. The reads aligned to chromosomes 4 and 6 showed a positive correlation with the number of reads on chromosome 13, while the reads aligned to chromosomes 1 and 16 showed a negative correlation (Figure 5.15). The read counts in the graphs are normalized by dividing them by the mean read count of the sample and multiplying them by the average mean read count of all control samples.

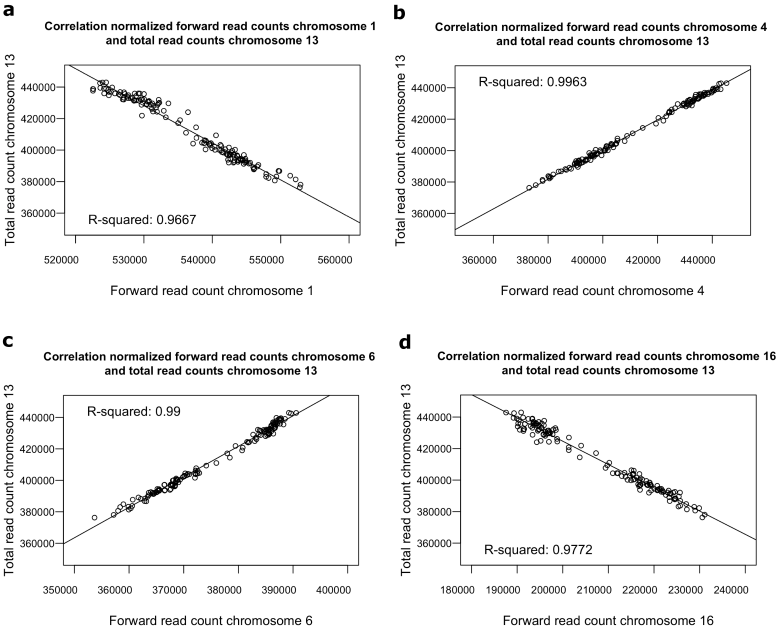

Figure 5.15: Correlation betweeen normalized read counts of predictor chromosomes and normalized read counts on chromosome 13 for 142 Illumina control samples (a) Chromosome 1 (b) chromosome 4 (c) chromosome 6 and (d) chromosome 16.

The predicted chromosomal fraction is equal to the expected chromosomal fraction in a nontrisomy situation (ef). For each sample a ratio between predicted and observed chromosomal fraction is calculated, resulting in a ratio observed/predicted fraction (of/ef) (Figure **??**). Using these values a Z-score can be calculated for each sample (Figure **??**). The general structure of the formula is equal to the standard Z-score formula:

$$\frac{x - \mu}{\sigma}$$

Because the mean of the control group after regression is one, the coefficient of variation of the control group has the same value as the SD. Using the same structure, the RBZ can be formulated as:

$$\frac{of_s/ef_s - 1}{\sqrt{\sum_{j=1}^{n}(of_j/ef_j - \overline{of/ef})^2/n - 1}}$$

Where s is the sample of interest, j is an individual control sample and n is the total number of control samples. The regression model for trisomy prediction for chromosome 13 in uncorrected Illumina data, described in table **??**, resulted in a mean fraction of 1.0000 and a CV of 0.0024 (0.24%).

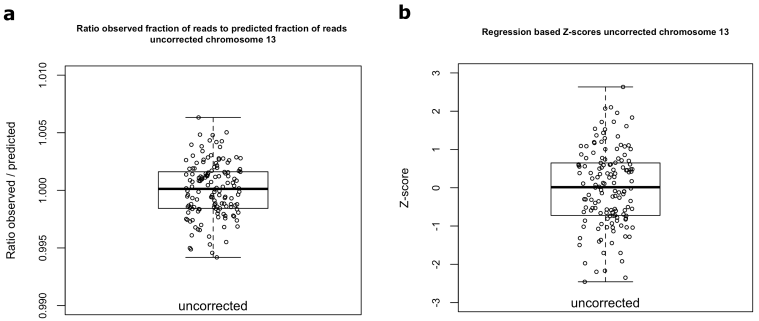

Figure 5.16: Ratios observed / predicted and Z-scores for chromosome 13 for 142 uncorrected Illumina control samples (a) ratios observed / predicted (b)Z-scores.

The number of predictors used in the RBZ can be as low as one or as high as all autosomes. However, we advise using a minimum of four predictor chromosomes, since an aberration in one of the other chromosomes (in mother or child) could influence the prediction. The effect of such an aberration is larger when fewer predictors are used. For the same reason we advise not using both the reads aligned to the forward strand and reads aligned to the reverse strand of the same chromosome in the same model. Different independent RBZ models can be created for each analysis. We advise creating four different models, because reads originating from the same chromosome can be included in a maximum of two different models. Results affected by an aberration in one of the predictor chromosomes can be identified using the additional models.

Chapter 6

NIPTeR: an R package for fast and accurate trisomy prediction in non-invasive prenatal testing

BMC Bioinformatics 2018;19:531.
DOI: 10.1186/s12859-018-2557-8
PubMed ID: 30558531

L.F. Johansson[1,2], H.A. de Weerd[1,2,3], E.N. de Boer[1], F. van Dijk[1,2], G.J. te Meerman[1], R.H. Sijmons[1], B. Sikkema-Raddatz[1], M.A. Swertz[1,2]

1. University of Groningen, University Medical Center Groningen, Department of Genetics, Groningen, The Netherlands
2. University of Groningen, University Medical Center Groningen, Genomics Coordination Center, Groningen, The Netherlands
3. School of Bioscience, Systems biology research center, University of Skövde, Skövde, Sweden

Received 2018 Oct 2; Accepted 2018 Dec 4; Published online 2018 Dec 17.

Abstract

Background Various algorithms have been developed to predict fetal trisomies using cell-free DNA in non-invasive prenatal testing (NIPT). As basis for prediction, a control group of non-trisomy samples is needed. Prediction accuracy is dependent on the characteristics of this group and can be improved by reducing variability between samples and by ensuring the control group is representative for the sample analyzed.

Results NIPTeR is an open-source R Package that enables fast NIPT analysis and simple but flexible workflow creation, including variation reduction, trisomy prediction algorithms and quality control. This broad range of functions allows users to account for variability in NIPT data, calculate control group statistics and predict the presence of trisomies.

Conclusion NIPTeR supports laboratories processing next-generation sequencing data for NIPT in assessing data quality and determining whether a fetal trisomy is present. NIPTeR is available under the GNU LGPL v3 license and can be freely downloaded from https://github.com/molgenis/NIPTeR or CRAN.

6.1 Background

Non-invasive prenatal testing (NIPT) is rapidly becoming the new standard in prenatal screening for fetal aneuploidy [3]. In NIPT, cell-free DNA from the pregnant woman's blood plasma, which consists of both maternal and fetal DNA fragments, is analysed. Next to SNP-based methods [84], low-coverage whole genome next-generation sequencing (NGS) is often used [35, 188],

and various algorithms, software programs and packages have been developed to analyse this type of data [32, 202, 239, 181, 160]. In literature, many methods have been described that depend on a statistical comparison between a sample of interest and a reference set of non-trisomy control samples [35, 188, 63, 95]. The RAPIDR and DASAF R packages, for instance, have been described [121, 119] and they made several of these algorithms available, including GC-correction, the standard Z-score and the Normalized Chromosome Value (NCV), to create an analysis workflow in R. However, those packages lack features like chi-squared-based variation reduction (χ2VR), regression-based Z-score (RBZ) and Match QC. These are all algorithms that we have extensively discussed before [95]. In short, χ2VR detects chromosomal regions that have a higher variability than expected by chance and reduces their weight so that, after correction, they have less impact on the fraction of reads mapped to the different chromosomes. The RBZ is an alternative Z-score calculation based on stepwise regression with forward selection. In the RBZ positive or negative correlation between chromosomal fractions is used to predict the number of reads to map onto the chromosome of interest if no trisomy is present. The Match QC score is a sum-of-squares-based approach to compare chromosomal fractions between the test sample and controls, and it provides a measure by which to determine whether a control group is representative for a specific sample. Here we report NIPTeR, an R package that provides fast NIPT analysis for research and diagnostics and provides users with multiple methods for variation reduction, prediction and quality control based upon comparison of a sample with a set of negative control samples.

6.2 Implementation

NIPTeR users can create different workflows for variation reduction and aneuploidy prediction using thirteen functions as building blocks (Fig. **??**). A stepwise practical example for using these building blocks is presented as a case report in Additional file 1.

NIPTeR analysis uses two core objects. The first object is NIPTSample, which contains the counts of aligned sequence reads in 50,000 bp bins for a specific sample. The second object is NIPTControlGroup, which contains a series of NIPTSamples for comparison. Users generate NIPTSample using the function bin_bam_sample, which needs a BAM file [113] as input. The user can optionally select to count reads mapped to the forward and reverse strands separately, so that they can each be used as a separate predictor. The as_control_group function converts a series of NIPTSample objects into a

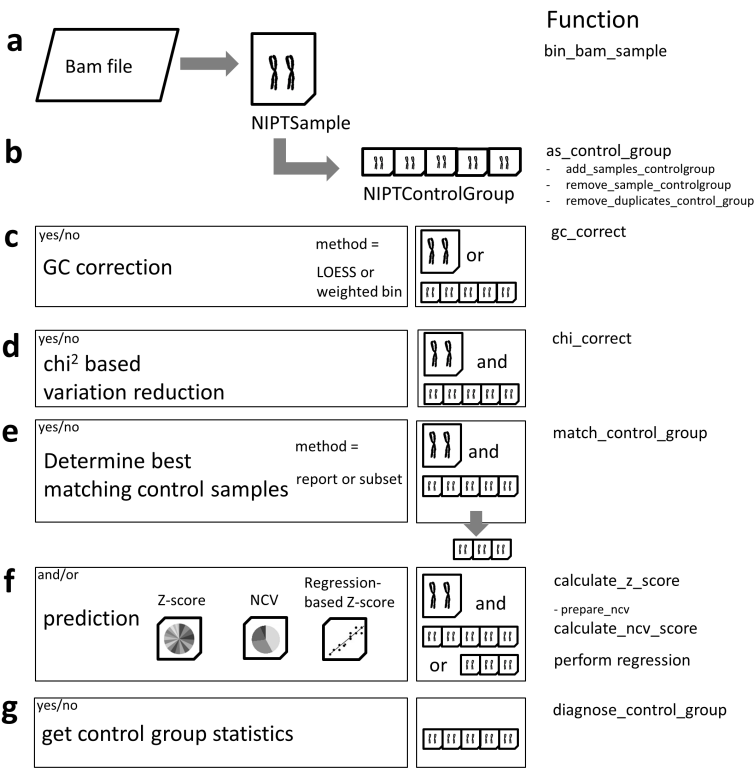

Figure 6.1: Workflow and functions of NIPTeR. **a** A BAM file is transformed into an NIPTSample object; **b** a series of NIPTSample objects can then be transformed into an NIPTControlGroup object; **c** optional LOESS or weighted bin GC correction; **d** optional chi-squared-based variation reduction; **e** optional comparison of NIPTSample and NIPTControlGroup and possible selection of a subset that best-matches the control group samples; **f** three different prediction methods: Z-score, normalized chromosome value or regression-based Z-score; **g** optional check of control group statistics

NIPTControlGroup. Within NIPTeR, users can manage an existing NIPTControlGroup using the add_samples_controlgroup, remove_sample_controlgroup and remove_duplicates_controlgroup functions.

Both NIPTSample and NIPTControlGroup can undergo one or more variation reduction steps to adjust the bin read counts, either using the gc_correct function for weighted bin GC correction [63] or LOESS GC correction [31] or the chi_correct function for χ2VR. Each NIPTSample object shows the correction status for the autosomes and the sex chromosomes separately and indicates which variation reduction methods have been performed (or that they are 'uncorrected'). χ2VR can be applied to uncorrected or GC-corrected samples, and makes use of a NIPTSample and a NIPTControlGroup having an identical correction status.

Using the fractions of reads mapped to the different chromosomes, trisomy prediction can be generated for a given NIPTSample based on the NIPTControlGroup using three different prediction algorithms: (1) calculate_z_score, which uses a standard Z-score [35]; (2) calculate_ncv_score, which uses an NCV [188]; and (3) perform_regression, which uses RBZ. All three trisomy prediction functions use NIPTControlGroup to calculate the expected fraction of reads on the chromosome of interest. For NCV, this calculation is done in a separate function, prepare_ncv, because the calculation is time-intensive and only has to be performed once for each NIPTControlGroup. The prediction functions then compare the observed fraction of reads of the chromosome of interest in the NIPTSample with the expected fraction. In NCV and RBZ calculations, users have the option of excluding selected chromosomes as predictors. Since chromosomes 13, 18 and 21 are the most likely candidates for a trisomy, these are excluded by default, but users do have the option of including them. The functions prepare_ncv and perform_regression provide users the option of using a train and test set to prevent over-fitting the models they create.

In addition to providing Z-scores, the functions also produce control group statistics. The function match_control_group provides a Match QC score, a calculation that shows how well the sample fits within the control group based on the fraction of reads mapped to the different chromosomes, a measure that can be shown in a report. Alternately, users can select a subset of best-matching control samples as a sample-specific control group using the arguments mode = "report" or "subset". When a sample has an anomalously high Match QC score, the control samples being used are not suitable as a control group for the sample being analyzed. A second quality control function, diagnose_control_group, calculates Z-scores for all samples and chromosomes in a NIPTControlGroup as well as the mean, standard deviation and Shapiro-Wilk test of those Z-scores. This information can be used

to curate the control group as explained in detail in Additional file 1.

6.3 Results

6.3.1 Workflow

All these NIPTeR building blocks can be combined into an analysis workflow. For example, the NIPTeR workflow for the Fan & Quake analysis [63], using a weighted bin GC correction and a standard Z-score prediction for trisomy 21, and given a GC-corrected control group is:

```
> NIPTsample <- bin_bam_sample(bam_filepath =
   "/Path/to/bam/sample.bam")
> NIPTsample_gc <- gc_correct(nipt_object = NIPTsample, method =
"bin")
> Zscore21_NIPTsample <- calculate_z_score(nipt_sample =
   NIPTsample_gc, nipt_control_group = NIPTControlGroup_gc,
   chromo_focus = 21)
```

In addition, control group statistics and the match control of the sample to the control group can be performed:

```
> NIPTcontrol_diagnose - diagnose_control_group(nipt_control_group
   = NIPT_control_group_gc)
> MatchQC <- match_control_group(nipt_sample = NIPTsample_gc,
   nipt_control_group = NIPT_control_group_gc, mode = "report")
```

6.3.2 Prediction and control group statistics

The output formats of the calculate_z_score and calculate_ncv_score functions are similar. An example result of the main output reads:

```
Zscore21_NIPTsample$sample_Zscore
[1] 0.4575612

Zscore21_NIPTsample$control_group_statistics
mean                SD                  Shapiro_P_value
1.380646e-02        7.184378e-05        9.498096e-01
```

Here, the Z-score is 0.45, which falls within the -3 to 3 range and leads to the conclusion that this sample does not have a trisomy 21. The control_group_statistics show the mean fraction of sequence reads mapping to chromosome 21 and the standard deviation (SD) of the fractions between the control samples. The Shapiro_P_value tests for control group normality, and control groups with a value above 0.05 can be considered to be normally distributed.

The output of perform_regression is slightly different and gives four predictions based on different models when set to the default setting:

	Prediction_set_1	Prediction_set_2	Prediction_set_3	Prediction_set_4
Z_score_sample	0.695389767405796	0.436463271170429	0.437555582217223	-0.268842730284741
CV	0.00536568258297721	0.00502335300817695	0.00483989627449594	0.00486660271957713
cv_types	Practical_CV	Practical_CV	Practical_CV	Practical_CV
P_value_shapiro	0.430190936876808	0.844844184734285	0.478810106756347	0.606229054979589
Pred_chrom[1]	3F 1F 2R 7F	3R 22F 1R 5R	6R 10F 8R 17F	20F 12F 19R 14F
Mean_test_set	0.998406705791639	0.997692920712523	0.998044728541847	0.997802000172399
CV_train_set	0.00441576466562767	0.004609720864648	0.00479265227193279	0.00492160650642337

Here, in addition to the RBZ, the coefficient of variation (CV) of the test set is given as a measure of control group variability. The type of CV is given as well, in which "Practical CV" is the true CV. If there is a risk of over-fitting the model on the control set, a theoretical CV is used. In addition to the Shapiro P value, perform_regression reports the mean of the test set (which should be close to one) and the CV of the training set (based on which the chromosomes used to create the prediction model are selected), where reads mapped to the forward and reverse strands are used as separate entities.

6.3.3 Quality control

Using the diagnose_control_group function, control samples that have outliers that could hamper prediction can be detected.

```
> NIPTcontrol_diagnose$abberant_scores

   Chromosome  Sample_name  Z_score
1   17F         sample21     3.13281485801102
2   1R          sample21     3.1290608434065
3   17R         sample21     3.33995848430216
4   22R         sample24     3.08496372975161
...
19  8F          sample21     -3.85723794269498
20  5R          sample21     -3.16594249087773
21  16R         sample21     -3.5467264109158
```

[1] In practice Pred_chrom is written in full as: Predictor_chromosomes. For layout purposes a shorthand is used here.

This example shows that, for many chromosomes in sample 21 one or both of the strands have a Z-score higher than 3. This means that there is more variability in this sample than expected, pointing to a low quality sample. As explained in more detail in Additional file 1, we recommend that users remove samples that have more than one aberrant score (Z-score outside the -3 to 3 range) from the control group.

When looking at the individual Match QC scores of the GC corrected NIPTSample compared to the GC corrected NIPTControlGroup, the list of sum of squares of differences in chromosomal fractions of the test sample compared to each control sample is shown:

```
           Sum_of_squares
sample86   1.919715e-07
sample74   2.155461e-07
...
sample40   1.089867e-06
sample21   2.028651e-06
```

In general, the lower the sum of squares, the more representative a control sample is for the test sample. The average of all sum of squares for an NIPTSample is the Match QC score. A Match QC score for a specific sample that falls outside 3 SD of the control group Match QC, indicates that the control group is not suitable for analysis of the sample.

Further examples and results can be found in the NIPTeR package vignette [112] and the case report provided in Additional file 1. A demonstration of the NIPTeR GC-correction methods is given in Additional file 2 and a comparison of NIPTeR results with manual calculations is available for the χ2VR in Additional file 3 and for the prediction methods and Match QC score in Additional file 4.

The NIPTeR package requires R 3.1.0 or higher, the stats and sets packages as available on CRAN, and the RSamtools and S4Vectors Bioconductor packages.

6.3.4 Performance

NIPTeR performance was tested on three different machines and operating systems (Additional file 5). Given a pre-processed control group of 100 samples, one sample was processed in 3 to 4 min (on average), including both GC correction and χ2VR and using the Z-score and RBZ as prediction algorithms for chromosomes 13, 18 and 21. NCV analysis was performed in an additional 1 to 6 min using a maximum number of 6 to

9 chromosomes as denominator.

6.4 Conclusion

NIPTeR allows for fast NIPT analysis and flexible workflow creation and includes variation correction and prediction algorithms as well as QC control. Algorithms used in NIPTeR are validated as described in Johansson and de Boer et al. (2017) [95]. NIPTeR is available under the GNU GPL open source license and can be freely downloaded from https://github.com/molgenis/NIPTeR or CRAN.

6.5 Availability and requirements

Project name: NIPTeR. Project home page: https://CRAN.R-project.org/package=NIPTeR Source page: https://github.com/molgenis/NIPTeR Operating system(s): Linux, MacOS, Windows. Programming language: R. Other requirements: R (3.1.0 or higher), RSamtools, sets, stats, S4Vectors. Licence: GNU Lesser General Public License v3.0. Any restrictions to use by non-academics: none

Acknowledgments

We thank Kate Mc Intyre for editorial advice.

Authors' contributions

LJ is the main author. LJ and HdW conceived and designed the NIPTeR package. Together with FvD they developed and implemented the application. LJ, HdW, EdB and GtM designed and validated algorithms and implementation. RS, BS and MS were responsible for project administration and supervision. All authors read and approved the final version of this manuscript.

Ethics approval and consent to participate

Not applicable.

Consent for publication

Not applicable.

Competing interests

The authors declare that they have no competing interests.

6.6 Additional files

Additional files can be accessed online:
https://bmcbioinformatics.biomedcentral.com/articles/10.1186/s12859-018-2557-8

Chapter 7

NIPTRIC: an online tool for clinical interpretation of non-invasive prenatal testing (NIPT) results

Scientific Reports 2016;6:38359.
DOI: 10.1038/srep38359
PubMed ID: 27917919

B. Sikkema-Raddatz[1], L.F. Johansson[1,2,*], E.N. de Boer[1,*], Elles M.J. Boon[3], R.F. Suijkerbuijk[1], K. Bouman[1], C.M. Bilardo[4], M.A. Swertz[2], M. Dijkstra[2], I.M. van Langen[1], R.J. Sinke[1], G.J. te Meerman[1]

1. University of Groningen, University Medical Center Groningen, Department of Genetics, Groningen, The Netherlands
2. University of Groningen, University Medical Center Groningen, Genomics Coordination Center, Groningen, The Netherlands
3. Leiden University Medical Center, Department of Clinical Genetics, Laboratory for Diagnostic Genome Analysis, Leiden The Netherlands
4. University of Groningen, University Medical Center Groningen, Department of Obstetrics and Gynaecology, Groningen, The Netherlands

Received 2016 May 17; Accepted 2016 Nov 9; Published online 2017 Dec 5.

Abstract

To properly interpret the result of a pregnant woman's non-invasive prenatal test (NIPT), her a priori risk must be taken into account in order to obtain her personalised a posteriori risk (PPR), which more accurately expresses her true likelihood of carrying a foetus with trisomy. Our aim was to develop a tool for laboratories and clinicians to calculate easily the PPR for genome-wide NIPT results, using diploid samples as a control group. The tool takes the a priori risk and Z-score into account. Foetal DNA percentage and coefficient of variation can be given default settings, but actual values should be used if known. We tested the tool on 209 samples from pregnant women undergoing NIPT. For Z-scores <5, the PPR is considerably higher at a high a priori risk than at a low a priori risk, for NIPT results with the same Z-score, foetal DNA percentage and coefficient of variation. However, the PPR is effectively independent under all conditions for Z-scores above 6. A high PPR for low a priori risks can only be reached at Z-scores >5. Our online tool can assist clinicians in understanding NIPT results and conveying their true clinical implication to pregnant women, because the PPR is crucial for individual counselling and decision-making.

7.1 Introduction

Non-invasive prenatal testing (NIPT) for foetal aneuploidies, by analysing cell-free DNA in maternal blood, has been offered to pregnant women increasingly since 2011 [reviews refs [13, 58, 73]]. Large clinical studies including about 150,000 pregnancies have reported a sensitivity and specificity for NIPT of more than 99% for foetal trisomy 13 or 21, and of 98% for trisomy 18 [refs [242] and [150], reviews refs [13] and [58]]. This performance of NIPT in the general population of pregnant women [73, 242, 150, 44, 148, 61, 106, 19] appears to be similar for both low-risk and high-risk pregnancies [242, 150, 19, 45]1.

NIPT can identify pregnancies at risk for a trisomy and is therefore a screening tool, not a diagnostic test. For an individual woman, a positive NIPT result with a sensitivity and specificity of more than 99% does not mean that she actually has more than a 99% chance of carrying a foetus with a trisomy. Her true likelihood depends not only on her NIPT result, but also on the prevalence of the anomaly in the population she belongs to [138], which is expressed as an a priori risk. Thus, her individual a priori risk for a specific foetal trisomy is based on her age, the gestational age at which NIPT is performed, and the results of other screening tests such as the first trimester combined test (FCT). The result of a NIPT for an individual woman in most of the genome-wide methods is calculated as a Z-score, where the individual sample is compared with a control group of normal (diploid) samples. However, presenting NIPT results to clinicians and pregnant women as "normal or abnormal" or as a Z-score makes it difficult for clinicians to interpret and use the result to correctly inform a pregnant woman of her true likelihood of carrying a foetus with a trisomy. In order to properly counsel women about a positive result from a cell-free foetal DNA screening, it can be useful to express the result as a personalised a posteriori risk (PPR), which takes the woman's a priori risk into account.

Although not all cell-free foetal DNA screening providers calculate a Z-score or need a priori risks, it is important for women to know their true chance of carrying a Down syndrome foetus after a positive test. This chance might be far lower than that concluded from the Z-score percentile (e.g. 99%) that might otherwise be a reason for them to undergo a confirmatory amniocentesis. Knowing the true risk could help avoid a hasty and sometimes unnecessary termination of pregnancy [236, 33], or a pregnant woman being wrongly reassured by being given a negative NIPT result. Thus, in clinical counselling and decision-making following a (positive) NIPT result, the PPR is the most important factor for the

parents.

NIPT is currently dominated by commercial testing providers. However, only a few of them provide the PPR with the NIPT result, nor is the calculation of the PPR published or straightforward for the clinician to understand [14].

We have therefore developed a web-based tool to calculate the PPR according to the a priori risk (for trisomy 13, 18, 21) of the mother in combination with the outcome of her NIPT test, expressed as a Z-score. Our tool can easily be used by cell-free foetal DNA screening providers and healthcare professionals.

7.2 Results

Our tool is freely available online (www.niptric.eu). To test the tool's validity we calculated a PPR for a range of extreme values: for a specific a priori risk, given the observed Z-score but unknown percentage of foetal DNA and coefficient of variation (see also Supplementary Table 1). The PPR based on the observed Z-score and the known percentage of foetal DNA, at an assumed coefficient of variation of 0.5 and an a priori risk of 1:1000, 1:100, and 1:10 are given in Supplementary Tables 2, 3, and 4. However, in the online tool, the PPR can be calculated for every combination of the four parameters (a priori risk, observed Z-score, percentage of foetal DNA and coefficient of variation).

The use of the PPR calculator and its interpretation is illustrated here by three examples. We show how the PPR is calculated from the woman's NIPT result to yield the likelihood of her carrying a foetus with Down syndrome: if she is at low risk (a priori risk of 1:1000), at high risk (a priori risk of 1:100), or at very high risk (a priori risk of 1:10). Here, the more general trends are shown for the impact of the four parameters.

Figure 7.1 shows the impact of variable a priori risk values and observed Z-scores on the PPR. The PPR increases when the Z-score increases and the woman has a higher a priori risk. Thus, the increase of PPR at a Z-score between 3 and 4 is more striking in high-risk pregnancies than in low-risk pregnancies. For a Z-score of 6 or higher, the PPR is approximately 100%, and is therefore effectively independent of the a priori risk (see Supplementary Table 1) for a given coefficient of variation and foetal DNA percentage value.

Figure **??** illustrates the impact of different percentages of foetal DNA on the PPR for different a priori risks and according to the Z-scores. At a Z-score of 3, the percentage of false-positive results is much higher for a

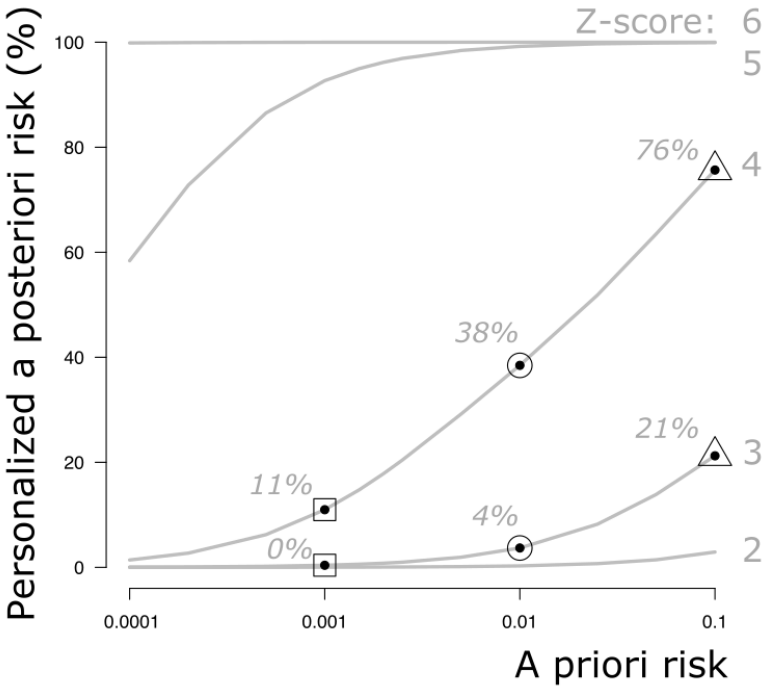

Figure 7.1: The PPR for the woman at low risk (1:1000 (0.001)) is <1% at a Z-score of 3, increasing to 11% for a Z-score of 4. This means that with a positive NIPT result, with a Z-score of 3 or 4, the actual chance of the woman carrying a foetus with Down syndrome is <1% or 11%, respectively. The woman at high risk (1:100 (0.01)) has a chance of 4% with a Z-score of 3, but a chance of 38% with a Z-score of 4. For the woman at very high risk (1:10 (0.1)), the PPR is 21% for a Z-score of 3 and 76% for a Z-score of 4.

woman who is at low a priori risk (1:1000) than for one at higher risk (1:100 or 1:10). Figure 2 also shows that, with the given foetal DNA percentages, the chance of carrying a foetus with Down syndrome is >99% for both low-risk (1:1000) and high-risk (1:100 and 1:10) women if the Z-score is above 6 (see also Supplementary Tables 2, 3, and 4).

7.2.1 Performance of the PPR calculator

The performance of our PPR calculator was tested in 209 samples. Of these 14 showed a Z-score $>$ 3 (Table 7.1). In ten samples, the Z-score was $>$ 6, resulting in a PPR of $>99\%$. In four samples, a Z-score of between 4 and 6 was calculated, resulting in PPRs between 4–40%. In one of these samples, a mosaic trisomy 21 was confirmed in chorionic villi and amniotic fluid, while two samples had a normal diploid outcome in amniotic fluid. In the fourth sample, the parents refused invasive follow-up because of a PPR of 4% for trisomy 13. No abnormalities were seen on ultrasound at 16 weeks' gestation and a healthy child was born.

7.3 Discussion

We present an easy-to-use online tool to assist cell-free foetal DNA screening providers and healthcare professionals in calculating a woman's PPR after a positive NIPT result. Our tool takes into account both test and patient characteristics. The online program can be used to estimate the PPR of any NIPT result according to a woman's personal a priori risk and Z-score.

Some screening services offering NIPT use dedicated proprietary algorithms to calculate an individual risk figure [177] or to discriminate between pregnancies with a low ($<1\%$) or high risk ($>1\%$) for a trisomy [198]; they take into account the combination of the Z- or likelihood score, a priori risk, and the percentage of foetal DNA in the NIPT test. However, most of these algorithms are not freely available and other services do not provide this essential information. Existing PPR calculators give only general information, such as sensitivity, specificity, positive predictive value, and a priori risk [79, 154]. These numbers do not relate to the individual situation of a pregnant woman.

To satisfy the need for a woman's personalised a posteriori risk figure, our PPR calculator can be applied to the results of genome-wide NIPT methods using diploid control samples. Different NIPT methods have been developed based on whole genome sequencing [62, 35] or on selected

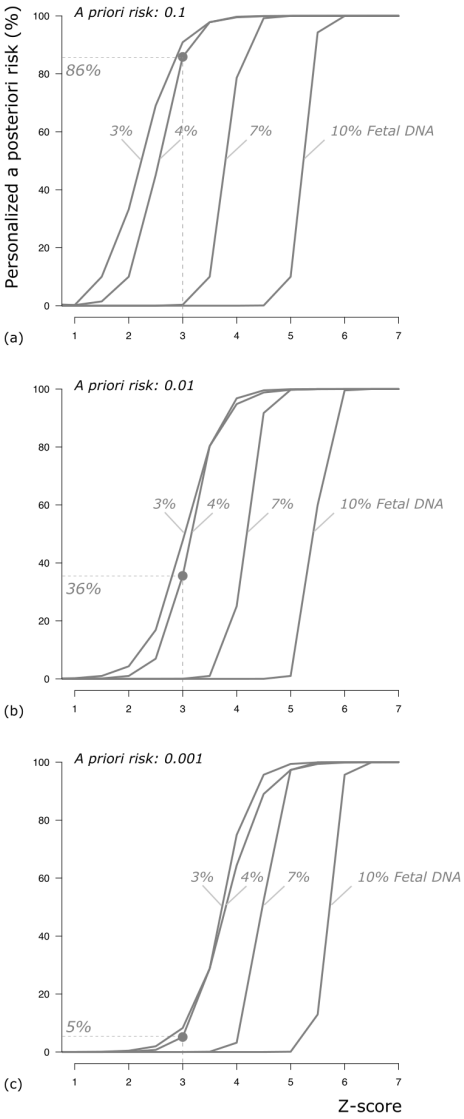
A priori risk: 0.1
Personalized a posteriori risk (%)
86%
3%
4%
7%
10% Fetal DNA
(a)
A priori risk: 0.01
3%
4%
7%
10% Fetal DNA
36%
(b)
A priori risk: 0.001
3%
4%
7%
10% Fetal DNA
5%
(c)
Z-score

Sample	First trimester combined test risk for Trisomy 21	Coefficient of variation #21	Z-score #21	Posterior Risk (%)	Confirmation by karyotyping in amniotic fluid
1	1/4	0.40	13.7	99.9	47#,+21
2	1/2	0.29	27.2	99.9	47#,+21
3	1/79	0.31	12.4	99.9	47#,+21
4	1/118	0.40	11.6	99.9	47#,+21
5	1/141	0.33	14.4	99.9	47#,+21
6	1/119	0.47	11.9	99.9	47#,+21
7	1/13	0.32	19.7	99.9	47#,+21
8	1/20	0.36	16.9	99.9	47#,+21
9	1/115	0.29	26.2	99.9	47#,+21
10	1/25	0.33	28.8	99.0	47#,+21
11	1 43	0.33	4.9	40.0	Mos 46#/47#,+21 also seen in chorionic villi
12	1/147	0.34	4.4	36.0	46#, no T21
13	1/80	0.32	4.2	33.0	46#, no T21
14*	#13 1:5000	#13 0.18	#13 4.4	4.0	No confirmation done, healthy baby born

Table 7.1: Summary of all samples with a Z-score >3 for chromosomes 12, 18 or 21 in 209 samples on which NIPT was performed. *A Z-score of 4.4 for chromosome 13 was detected, while the a priori risk for trisomy 21 was 1/121; no elevated risk was found for trisomy 13 after the first trimester combined test.

Figure 7.2: (a) a priori risk of 0.1 (1:10); (b) a priori risk of 0.01(1:100); and (c) a priori risk of 0.01(1:1000). x-axis: Z-score range 1–7. y-axis: Personalised a posteriori risk (%). After a positive NIPT result at a Z-score of 3 and at 4% foetal DNA, the low-risk woman has a 5% chance of carrying a foetus with Down syndrome and thus a 95% chance of the result being false-positive. In contrast, the higher-risk women have a 36% (1:100) and an 86% (1:10) chance of carrying a foetus with Down syndrome. Thus, the chance of a false-positive result at a risk of 1:100 and 1:10 is 64% and 14%, respectively.

chromosome targeted-sequencing [246, 199]. Most of these methods compare the individual sample with a population of normal (diploid) control samples, with the outcome usually presented as a Z-score. This can be based either on the difference of a number of single nucleotide polymorphisms [246], or on a fraction of reads from whole genome sequencing [62, 35] or from targeted-sequencing [199]. Using this Z-score, the PPR can then be calculated in combination with the a priori risk in our calculator. If providers do not calculate an a posteriori risk they can easily add the PPR calculation using our tool as part of their service. Those healthcare professionals who only receive a Z-score as the outcome from a NIPT test can then use our tool together with the individual woman's a priori risk to gain a more accurate a posteriori risk for counselling the individual woman or parents.

The outcome is still, of course, a risk estimation, not an exact number. Moreover, our PPR calculator may be applied to detect any aneuploidy provided that the a priori risk for the particular aneuploidy is known for the gestation period in which the NIPT is performed. However, a negative NIPT result may be falsely reassuring for women at high risk who also have nuchal translucency or ultrasound findings that cause concern if only chromosomes 13, 18 and 21 have been tested [193].

For each woman, the PPR of a diagnostic or screening test depends on the prevalence of the disease in her population [104]. Accordingly, we have shown that, after a positive NIPT result, the PPR is also influenced by the individual's risk profile. For Z-scores <5, the PPR is considerably higher at a high a priori risk than at a low risk for a NIPT result with the same Z-score, coefficient of variation and foetal DNA percentage, while the PPR becomes effectively independent of these parameters for Z-scores >6. A high PPR for a low a priori risk can only be reached at Z-scores >5. In line with our calculations, Bianchi et al. [19] demonstrated that even at a high sensitivity and specificity for NIPT, the positive predictive values for trisomy 21 and trisomy 18 in low- or average risk pregnancies

were only 45% and 40%, respectively, which means that the PPR for an individual woman is, on average, also equal to this percentage. This was confirmed in a routine screening of a prenatal population (N = 15,841) with a positive predictive value of 80%5, while Wang et al. [**?**] estimated values for the less common trisomy 18 and trisomy 13 at 64% and 44%, respectively, compared to 94% for trisomy 21. As Borrell and Stergiotou (2015) stated, some referring physicians may think that NIPT is a diagnostic test and they may not realise they also need take into account that the positive predictive value may vary strongly for individual women [22]. Some authors [138, 198] suggest that, at minimum, the a priori risk should be incorporated in assessing a NIPT result. Our calculations strongly support this suggestion.

Our PPR calculator can even be used when the coefficient of variation and the percentage of cell-free foetal DNA in the maternal plasma are unknown or not given. We included this option in our tool because some laboratories do not provide a foetal DNA percentage due to the difficulties in measuring samples in a pregnancy with a female foetus. At minimum, a Z-score and the a priori risk are needed as input for our tool, whereas default settings for the percentage of DNA and coefficient of variation can be used. However, several studies have shown that low percentages of foetal DNA in maternal plasma are related to test failures and false-negative results [28, 18]. Thus, a lower limit of 4% foetal DNA was proposed as the cut-off for a reliable result [61, 151]. Our online tool gives extra weight to the extreme values of the DNA foetal percentage in the population compared to a normal distribution to yield a higher PPR prediction in the presence of low percentages of foetal DNA. This is advantageous because the percentage of foetal DNA in maternal plasma might, in general, be lower for trisomy 13 and 18 [61, 84, 231, 157]. Nonetheless, in the ideal situation, the healthcare provider should also be given the coefficient of variation and percentage of foetal DNA, since these are important indicators for the sensitivity of NIPT. Use of the actual percentage of foetal DNA and coefficient of variation further improve the accuracy of the PPR calculation. Even when the percentage of foetal DNA is measured, a small range for the upper and lower limit is advisable because the measurement is not always precise. Without an estimation of the percentage of foetal DNA, we advise using 1% as the lower limit and 23% as the upper, which our tool has as default settings.

Computations using our PPR calculator with relatively low percentages of foetal DNA in maternal blood have shown two trends. First, a low percentage reduces the PPR far more in low-risk pregnancies than in high-risk ones, which could lead to more false-positive results. Second, in

high-risk pregnancies, negative results are more likely to be false for Z-scores between 2 and 3 in combination with low percentages (<7%) (e.g. PPR of 45% at Z = 2.5, coefficient of variation 0.5, a priori risk 1:10, foetal percentage 4%). This is partly in line with Bianchi et al.[20], who considered a Z-score between 2.5 and 4 as a borderline value.

Thus, false-negative results might be obtained if the actual percentage of foetal DNA is low and the coefficient of variation is higher than our default settings due to a lower sensitivity of the NIPT test. Measuring (and reporting) the percentage of foetal DNA28, and knowing the coefficient of variation, are therefore important prerequisites for the accurate interpretation of NIPT results [35, 107] now that easy-to-use methods are available [201].

False-positive results can also be obtained, because the NIPT result might only reflect the genetic status of the placenta and not that of the foetus due to confined placenta mosaicism [36, 228, 130]. This is relevant in trisomy 21, which results in a larger standard variation for trisomic samples. To avoid this problem, we recommend using a larger range for the lower and upper values of the foetal DNA percentage. Our tool calculates the risk of a non-mosaic trisomy. Thus, a Z-score that is lower than expected for a specific foetal percentage, but higher than expected for an euploid sample, might indicate the presence of mosaicism. In general, a positive NIPT result, even with a posterior risk of >99%, should always be confirmed with amniocentesis.

In conclusion, our PPR calculator can be easily used by cell-free foetal DNA screening providers and healthcare professionals to interpret NIPT results obtained by genome-wide methods. We urge them to use our tool in making further clinical decisions. The calculation of the PPR stresses the importance of confirming a positive NIPT result by invasive prenatal diagnosis, because not every pregnant woman with a positive result has the same likelihood of carrying a foetus with an aneuploidy. Our online software tool, figures and tables will help professionals and patients to better understand NIPT results and their implications in clinical practice.

7.4 Material and Methods

7.4.1 The PPR calculator

The PPR for a foetal trisomy (13, 18, or 21) for an individual pregnancy is estimated using four input parameters. By combining the a priori risk (calculated based on the mother's age and gestation, or based on other screening tests) with the individual NIPT result (computed as a Z-score),

the percentage of foetal DNA and the coefficient of variation of the control group, our tool can be used to calculate a meaningful personalised posterior risk (PPR) to aid interpretation of an individual NIPT result.

7.4.2 A priori risk

There are generally accepted risk tables for the population-based prevalence of trisomy 21 [195], trisomy 18, and trisomy 13 [196]. These tables are used in the PPR calculator, if necessary, using bivariate linear interpolation, to calculate the a priori risk from the maternal age in combination with the gestational age at which the NIPT was performed. If the risk has been determined based on a first trimester combined test (FCT) or a previous child with a trisomy, this risk should be used because it reflects the individual a priori risk more precisely.

7.4.3 Z-score

The result of a NIPT for an individual woman is expressed as a Z-score, where the individual sample is compared with a control group of normal (diploid) samples. In the case of an aneuploidy of a chromosome, a relative excess or deficit for that chromosome is present compared to the normal diploid situation. A Z-score represents the number of standard deviations that the sample fraction of that chromosome deviates from the mean measured in normal (diploid) pregnancies assessed by a Gaussian distribution. The distinction is based on the statistical assumption that 99.7% of the plasma samples derived from pregnant women with a diploid foetus give a Z-score between -3 and +3. Thus, the more the Z-score deviates from zero, the more the individual sample deviates from the control group and thus points towards an aneuploidy.

The higher value of the Z-score for aneuploid samples, and thus the reliability of NIPT, however, depends on the assay precision which, in turn, depends on a number of factors such as the number of reads, the reference samples chosen, the method of sample preparation, and sequencing method. All these factors are encompassed in the coefficient of variation of control samples and, together with the percentage of foetal DNA in the maternal plasma [7], they influence the Z-score.

7.4.4 Percentage of foetal DNA

The percentage of foetal DNA is essential to understanding the strengths and limitations of NIPT [61, 15] and it is a key factor in the NIPT procedure. For low percentages of foetal DNA, the distribution curves of the

diploid and aneuploid fractions will overlap, as demonstrated by Benn and Cuckle [15]. In principle, a low percentage of foetal DNA will result in a low Z-score for a trisomic sample. The percentage of foetal DNA at a gestational age between 12 and 23 weeks (a median of 16 weeks) shows roughly a normal distribution between 1–23%, with outliers between 23–30% [6, 159]. The mean measured foetal fraction for all samples is 12%. The rationale behind our default setting, which can be used when the percentage of foetal DNA is unknown, is to mimic a normal distribution with extra weight for the extreme values. We therefore chose a combination of two uniform distributions, one between 1–23% and another between 6–18% foetal DNA, with respective weights of 0.4 and 0.6. A few samples will have such extreme values (<6% or >18%). A low percentage of foetal DNA is the most critical parameter for calculating a low Z-score in aneuploidy samples and, if the percentage has been measured, it is known to only approximate score accuracy. A more precise prediction can be obtained by filling in the lower and upper limits of the measured foetal percentage in our tool.

Due to the extra weight given to low foetal percentages, the PPR will be higher than that calculated for actual percentages of foetal DNA lying between 1–6% compared to a normal distribution.

7.4.5 Coefficient of variation

The random variability of the test is measured as the coefficient of variation of the control group. The coefficient will increase as the assay precision decreases, depending on the quality of the laboratory procedure, i.e. sample preparation or number of reads. Increasing the number of reads can improve the assay precision and thus reduce the coefficient of variation of the control group. Different algorithms have been developed to increase precision, by reducing the variation in the control group, e.g. GC correction [63], or by using an adapted Z-score calculation, such as the normalised chromosome value [107, 188]. The coefficient of variation is used in combination with the percentage of foetal DNA to compute the expected distance between the two Gaussian distributions for diploid pregnancies and trisomic pregnancies. The calculation is made as follows[1]:

$$\mathrm{CV} = \frac{\text{standard deviation of fraction of chromosome control group}}{\text{mean of fraction of chromosome control group}}$$

[1] In the original paper CV was written out in full as coefficient of variation. For lay-out purposes terms were shortened here.

As the coefficient of variation increases, the distance between the diploid and aneuploid distribution will decrease, resulting in a decrease of sensitivity for detecting a trisomy. For example, a coefficient of variation of 0.5% for chromosome 21 would result in 99.87% sensitivity at a foetal DNA percentage of 6%, while the sensitivity would drop to 84.13% at a foetal DNA percentage of 4%. A 99.87% sensitivity at 4% foetal DNA can only be obtained with a coefficient of variation of 0.33%. Thus, a higher coefficient of variation will decrease the sensitivity, especially at low percentages of foetal DNA. A coefficient of variation of 0.5% (chromosome 21) is used as the default setting in our program because this is close to empirically measured values. For chromosomes 13 and 18, we recommend 0.4% as a default setting. The number of reads is higher for these chromosomes, leading to the expectation of a lower coefficient of variation than for chromosome 21. However, if the coefficient of variation is measured and lower than our default setting, this value should be used for a more accurate PPR calculation.

The PPR calculation is made as follows. First, the expected Z-score, if a trisomy is present, is calculated using the coefficient of variation of the control group and the percentage of foetal DNA:

$$\text{Z-expected} = \frac{\text{percentage of foetal DNA} \times 0.5}{100 \times \text{coefficient of variation}}$$

The actual Z-score in the case of a trisomy is a random variable with the "Z expected" value and standard deviation both equal to 1.0. Because the percentage of foetal DNA cannot be exactly measured, the empirical distribution of Z-scores will be a weighted sum of distributions over all possible values for the foetal DNA percentage. Technically, this percentage is a nuisance parameter that is integrated out to compute the probability that the observed Z-score originates from a trisomic pregnancy. In our computational model, we allow the range for the foetal DNA percentage to be known and input exactly. The actual integration of the nuisance parameter of foetal percentage is done by converting the foetal DNA percentage to a lower and upper value for the expected Z- score.

The post-test probability or personalised a posteriori risk (PPR) is calculated as[2]:

[2]In the original paper 'Upp', 'Low' and 'Papr' were written out in full as 'Upper', 'Lower' and 'Pa priori', respectively. For lay-out purposes terms were shortened here.

PPR range =

$$\frac{\int_{LowZexp}^{UppZexp} \frac{e^{\frac{-(Zexp-Zobs)^2}{2}}}{UppZexp-LowZexp} Zexp \times Papr}{(\int_{LowZexp}^{UppZexp} \frac{e^{\frac{-(Zexp-Zobs)^2}{2}}}{UppZexp-LowZexp} Zexp \times Papr) + (1 - Papr) \times e^{\frac{-(Zobs)^2}{2}}}$$

PPR range A:

$$\text{full range lower to upper Zexp}$$

PPR range B:

$$\text{lower Zexp} = \text{lower Zexp} + \frac{5}{22}(\text{upper Zexp - lower Zexp})$$

$$\text{lower Zexp} = \text{lower Zexp} + \frac{17}{22}(\text{upper Zexp - lower Zexp})$$

$$\text{Post-test probability} = 0.4 \times \text{PPR range A} + 0.6 \times \text{PPR range B}$$

7.4.6 Examples of the use of the PPR calculator

To demonstrate the use of the calculator and the effects of varying a priori risk values and observed Z-scores on the PPR, we have generated tables and concomitant figures. In order to clarify the calculations, we fixed the coefficient of variation at 0.5 and used a range of 1–23% of cell-free foetal DNA. The PPR was calculated as a percentage for a priori risks of 0.0001, 0.0002, 0.0005, 0.0010, 0.0015, 0.0020, 0.0025, 0.0050, 0.0100, 0.0250, 0.0500 and 0.1000, for observed Z-scores of 2, 2.5, 3, 3.5, 4, 4.5, 5, 5.5 and 6.

To demonstrate the additional effect on the PPR of variable foetal DNA percentages in maternal blood, the PPR was calculated for an a priori risk of 0.001, 0.01 and 0.1, for Z-scores varying from 0 to 7 and foetal DNA varying from 3% to 10%.

7.4.7 Performance of the PPR calculator

To test the performance of our PPR calculator, we analysed 209 maternal blood samples obtained from pregnant women with an elevated risk for trisomy 13, 18 or 21 due to an FTC $>$ 1:200 between 10 and 16 weeks of gestation. This was part of the trial by Dutch laboratories for evaluation of non-invasive prenatal testing (TRIDENT) program, and supported by

the Dutch Ministry of Health, Welfare and Sport (11016-118701-PG). The trial was conducted according prescribed laboratory protocols. Our study was approved by the Ethics Committee of the University Medical Centre Groningen. All participants signed an informed consent form.

Data were obtained from massively parallel, shotgun sequencing of cell-free DNA from maternal plasma with a Solid Wildfire sequencing system (Life Technologies Ltd., Paisley, UK). The sequencing data were used to calculate a Z-score. For the calculation of the PPR, we used as input the a priori risk as determined at FTC, the Z-score, the actual coefficient of variation, and the default setting for the percentage of foetal DNA. The outcome of the NIPT was either confirmed in amniotic fluid by karyotyping or by follow-up after birth.

Bibliography

[1] Daniel Aird, Michael G Ross, Wei-Sheng Chen, Maxwell Danielsson, Timothy Fennell, Carsten Russ, David B Jaffe, Chad Nusbaum, and Andreas Gnirke. Analyzing and minimizing pcr amplification bias in illumina sequencing libraries. Genome Biology, 12(2):R18, 2011.

[2] Zarko Alfirevic, Faris Mujezinovic, and Karin Sundberg. Amniocentesis and chorionic villus sampling for prenatal diagnosis. Cochrane Database of Systematic Reviews, Jul 2003.

[3] Megan Allyse, Mollie Minear, Margaret Rote, Anthony Hung, Subhashini Chandrasekharan, Elisa Berson, and Shilpa Sridhar. Non-invasive prenatal testing: a review of international implementation and challenges. International Journal of Women's Health, page 113, Jan 2015.

[4] R. Altmann. Elementärorganismen und ihre beziehungen zu den zellen. Metzger & Wittig, Leipzig, 1890 zweite auglage 1894.

[5] G. Ashoor, A. Syngelaki, E. Wang, C. Struble, A. Oliphant, K. Song, and K. H. Nicolaides. Trisomy 13 detection in the first trimester of pregnancy using a chromosome-selective cell-free dna analysis method. Ultrasound in Obstetrics and Gynecology, 41(1):21–25, Nov 2012.

[6] Ghalia Ashoor, Leona Poon, Argyro Syngelaki, Beatrice Mosimann, and Kypros H. Nicolaides. Fetal fraction in maternal plasma cell-free dna at 11–13 weeks' gestation: Effect of maternal and fetal factors. Fetal Diagnosis and Therapy, 31(4):237–243, 2012.

[7] Ghalia Ashoor, Argyro Syngelaki, Marion Wagner, Cahit Birdir, and Kypros H. Nicolaides. Chromosome-selective sequencing of maternal plasma cell–free dna for first-trimester detection of trisomy 21 and trisomy 18. American Journal of Obstetrics and Gynecology, 206(4):322.e1–322.e5, Apr 2012.

[8] Umut Aypar, Ryan A. Knudson, Kathryn E. Pearce, Anne E. Wiktor, and Rhett P. Ketterling. Development of an npm1/mlf1 d-fish probe set for

the detection of t(3;5)(q25;q35) identified in patients with acute myeloid leukemia. The Journal of Molecular Diagnostics, 16(5):527–532, Sep 2014.

[9] Sikkema-Raddatz B., S. Castedo, and G.J. te Meerman. Probability tables for exclusion of mosaicism in prenatal diagnosis. Prenat. Diagn., 17(2):860–866, 2009.

[10] Daniel Backenroth, Jason Homsy, Laura R. Murillo, Joe Glessner, Edwin Lin, Martina Brueckner, Richard Lifton, Elizabeth Goldmuntz, Wendy K. Chung, and Yufeng Shen. Canoes: detecting rare copy number variants from whole exome sequencing data. Nucleic Acids Research, 42(12):e97–e97, Apr 2014.

[11] J.G.J. Bauman, J. Wiegant, P. Borst, and P. van Duijn. A new method for fluorescence microscopical localization of specific dna sequences by in situ hybridization of fluorochrome-labelled rna. Exp. Cell Res., 128(2):485–490, 1980.

[12] C. Benda. Ueber die spermatogenese der vertebraten und höheren evertebraten. ii. theil. die histiogenese der spermien. Arch. Anal. Physiol., pages 393–398, 1898.

[13] P. Benn, H. Cuckle, and E. Pergament. Non-invasive prenatal testing for aneuploidy: current status and future prospects. Ultrasound in Obstetrics and Gynecology, 42(1):15–33, Jun 2013.

[14] Peter Benn. Posttest risk calculation following positive noninvasive prenatal screening using cell-free dna in maternal plasma. American Journal of Obstetrics and Gynecology, 214(6):676.e1–676.e7, Jun 2016.

[15] Peter Benn and Howard Cuckle. Theoretical performance of non-invasive prenatal testing for chromosome imbalances using counting of cell-free dna fragments in maternal plasma. Prenatal Diagnosis, 34(8):778–783, Apr 2014.

[16] David R. Bentley, Shankar Balasubramanian, Harold P. Swerdlow, Geoffrey P. Smith, John Milton, Clive G. Brown, Kevin P. Hall, Dirk J. Evers, Colin L. Barnes, Helen R. Bignell, and et al. Accurate whole human genome sequencing using reversible terminator chemistry. Nature, 456(7218):53–59, Nov 2008.

[17] L. Beulen, B. H. W. Faas, I. Feenstra, J. M. G. van Vugt, and M. N. Bekker. Clinical utility of non-invasive prenatal testing in pregnancies with ultrasound anomalies. Ultrasound in Obstetrics & Gynecology, 49(6):721–728, Jun 2017.

[18] D. W. Bianchi and L. Wilkins-Haug. Integration of noninvasive dna testing for aneuploidy into prenatal care: What has happened since the rubber met the road? Clinical Chemistry, 60(1):78–87, Nov 2013.

[19] Diana W. Bianchi, R. Lamar Parker, Jeffrey Wentworth, Rajeevi Madankumar, Craig Saffer, Anita F. Das, Joseph A. Craig, Darya I. Chudova, Patricia L. Devers, Keith W. Jones, and et al. Dna sequencing versus standard prenatal aneuploidy screening. New England Journal of Medicine, 370(9):799–808, Feb 2014.

[20] Diana W. Bianchi, Lawrence D. Platt, James D. Goldberg, Alfred Z. Abuhamad, Amy J. Sehnert, and Richard P. Rava. Genome-wide fetal

aneuploidy detection by maternal plasma dna sequencing. Obstetrics and Gynecology, 119(5):890–901, May 2012.

[21] S.K. Bohlander. Fusion genes in leukemia: an emerging network. Cytogenetic and Genome Research, 91(1-4):52–56, 2000.

[22] A. Borrell and I. Stergiotou. Cell-free dna testing: inadequate implementation of an outstanding technique. Ultrasound in Obstetrics and Gynecology, 45(5):508–511, Apr 2015.

[23] T. Boveri. Ergebnisse über die Konstitution der chromatischen Substanz des Zellkerns. Gustav Fischer, Jena, 1904.

[24] T. Boveri. Die blastomerenkerne von ascaris megalocephala und die theorie der chromosomenindividualität. Arch Zellforsch, 3:181–268, 1909.

[25] Thomas Burmeister, Claus Meyer, Daniela Gröger, Julia Hofmann, and Rolf Marschalek. Evidence-based rt-pcr methods for the detection of the 8 most common mll aberrations in acute leukemias. Leukemia Research, 39(2):242–247, Feb 2015.

[26] Jeremy J Buzzard, Nicholas M Gough, Jeremy M Crook, and Alan Colman. Karyotype of human es cells during extended culture. Nature Biotechnology, 22(4):381–382, Apr 2004.

[27] Cancer.net. Lynch syndrome: www.cancer.net/cancer-types/lynch-syndrome, 2005-2018.

[28] Jacob A. Canick, Edward M. Kloza, Geralyn M. Lambert-Messerlian, James E. Haddow, Mathias Ehrich, Dirk Boom, Allan T. Bombard, Cosmin Deciu, and Glenn E. Palomaki. Dna sequencing of maternal plasma to identify down syndrome and other trisomies in multiple gestations. Prenatal Diagnosis, 32(8):730–734, May 2012.

[29] K. C. A. Chan, P. Jiang, Y. W. L. Zheng, G. J. W. Liao, H. Sun, J. Wong, S. S. N. Siu, W. C. Chan, S. L. Chan, A. T. C. Chan, and et al. Cancer genome scanning in plasma: Detection of tumor-associated copy number aberrations, single-nucleotide variants, and tumoral heterogeneity by massively parallel sequencing. Clinical Chemistry, 59(1):211–224, Oct 2012.

[30] Dineika Chandrananda, Natalie P. Thorne, Devika Ganesamoorthy, Damien L. Bruno, Yuval Benjamini, Terence P. Speed, Howard R. Slater, and Melanie Bahlo. Investigating and correcting plasma dna sequencing coverage bias to enhance aneuploidy discovery. PLoS ONE, 9(1):e86993, Jan 2014.

[31] Eric Z. Chen, Rossa W. K. Chiu, Hao Sun, Ranjit Akolekar, K. C. Allen Chan, Tak Y. Leung, Peiyong Jiang, Yama W. L. Zheng, Fiona M. F. Lun, Lisa Y. S. Chan, and et al. Noninvasive prenatal diagnosis of fetal trisomy 18 and trisomy 13 by maternal plasma dna sequencing. PLoS ONE, 6(7):e21791, Jul 2011.

[32] Z. Chen. Development of Bioinformatics Algorithms for Trisomy 13 and 18 Detection by Next Generation Sequencing of Maternal Plasma DNA. The Chinese University of Hong Kong, 2011.

[33] Sau W. Cheung, Ankita Patel, and Tak Y. Leung. Accurate description of dna-based noninvasive prenatal screening. New England Journal of Medicine, 372(17):1675–1677, Apr 2015.

[34] Patrick F. Chinnery and Aurora Gomez-Duran. Oldies but goldies mtdna population variants and neurodegenerative diseases. Frontiers in Neuroscience, 12, Oct 2018.

[35] R. W. K. Chiu, K. C. A. Chan, Y. Gao, V. Y. M. Lau, W. Zheng, T. Y. Leung, C. H. F. Foo, B. Xie, N. B. Y. Tsui, F. M. F. Lun, and et al. Noninvasive prenatal diagnosis of fetal chromosomal aneuploidy by massively parallel genomic sequencing of dna in maternal plasma. Proceedings of the National Academy of Sciences, 105(51):20458–20463, Dec 2008.

[36] H. Choi, T. K. Lau, F. M. Jiang, M. K. Chan, H. Y. Zhang, P. S. S. Lo, F. Chen, L. Zhang, and W. Wang. Fetal aneuploidy screening by maternal plasma dna sequencing: "false positive" due to confined placental mosaicism. Prenatal Diagnosis, 33(2):198–200, Nov 2012.

[37] James Clarke, Hai-Chen Wu, Lakmal Jayasinghe, Alpesh Patel, Stuart Reid, and Hagan Bayley. Continuous base identification for single-molecule nanopore dna sequencing. Nature Nanotechnology, 4(4):265–270, Feb 2009.

[38] NIPT Consortium. Meerovernipt: Online: http://www.meerovernipt.nl/content/de-studies-trident-1-en-trident-2 (visited on march 9th 2018), 2018.

[39] Emily M. Coonrod, Rebecca L. Margraf, and Karl V. Voelkerding. Translating exome sequencing from research to clinical diagnostics. Clinical Chemistry and Laboratory Medicine, 50(7), Jan 2012.

[40] Cremer and Cremer. Rise, fall and resurrection of chromosome territories: A historical perspective. part i. the rise of chromosome territories. Eur. J. Histochem, 50(3):161–176, 2006.

[41] F. H. C. Crick, L. Barnett, S. Brenner, and R. J. Watts-Tobin. General nature of the genetic code for proteins. Nature, 192(4809):1227–1232, Dec 1961.

[42] E.W. Crow and Crow J.F. 100 years ago: Walter sutton and the chromosome theory of heredity. Genetics, 160:1–4, 2002.

[43] Chenghua Cui, Wei Shu, and Peining Li. Fluorescence in situ hybridization: Cell-based genetic diagnostic and research applications. Frontiers in Cell and Developmental Biology, 4, Sep 2016.

[44] Shan Dan, Wei Wang, Jinghui Ren, Yali Li, Hua Hu, Zhengfeng Xu, Tze Kin Lau, Jianhong Xie, Weihua Zhao, Hefeng Huang, and et al. Clinical application of massively parallel sequencing-based prenatal noninvasive fetal trisomy test for trisomies 21 and 18 in 11,105 pregnancies with mixed risk factors. Prenatal Diagnosis, 32(13):1225–1232, Nov 2012.

[45] Pe'er Dar, Kirsten J. Curnow, Susan J. Gross, Megan P. Hall, Melissa Stosic, Zachary Demko, Bernhard Zimmermann, Matthew Hill, Styrmir Sigurjonsson, Allison Ryan, and et al. Clinical experience and follow-up with large scale single-nucleotide polymorphism–based noninvasive prenatal aneuploidy testing. American Journal of Obstetrics and Gynecology, 211(5):527.e1–527.e17, Nov 2014.

[46] Joep de Ligt, Marjolein H. Willemsen, Bregje W.M. van Bon, Tjitske Kleefstra, Helger G. Yntema, Thessa Kroes, Anneke T. Vulto-van Silfhout, David A. Koolen, Petra de Vries, Christian Gilissen, and et al.

Diagnostic exome sequencing in persons with severe intellectual disability. New England Journal of Medicine, 367(20):1921–1929, Nov 2012.

[47] Paula J P de Vree, Elzo de Wit, Mehmet Yilmaz, Monique van de Heijning, Petra Klous, Marjon J A M Verstegen, Yi Wan, Hans Teunissen, Peter H L Krijger, Geert Geeven, and et al. Targeted sequencing by proximity ligation for comprehensive variant detection and local haplotyping. Nature e Biotechnology, 32(10):1019–1025, Aug 2014.

[48] Johan T. den Dunnen, Raymond Dalgleish, Donna R. Maglott, Reece K. Hart, Marc S. Greenblatt, Jean McGowan-Jordan, Anne-Francoise Roux, Timothy Smith, Stylianos E. Antonarakis, Peter E.M. Taschner, and et al. Hgvs recommendations for the description of sequence variants: 2016 update. Human Mutation, 37(6):564–569, Mar 2016.

[49] L. Devlin and P.J. Morrison. Accuracy of the clinical diagnosis of down syndrome. Ulster Med. J., 73:4–12, 2004.

[50] J. C. Dohm, C. Lottaz, T. Borodina, and H. Himmelbauer. Substantial biases in ultra-short read data sets from high-throughput dna sequencing. Nucleic Acids Research, 36(16):e105–e105, Aug 2008.

[51] D. Dominguez-Sola and J. Gautier. Myc and the control of dna replication. Cold Spring Harbor Perspectives in Medicine, 4(6):a014423–a014423, Jun 2014.

[52] Claudia E Dumitrescu and Michael T Collins. Mccune-albright syndrome. Orphanet Journal of Rare Diseases, 3(1), May 2008.

[53] Eric J Duncavage, Haley J Abel, Philippe Szankasi, Todd W Kelley, and John D Pfeifer. Targeted next generation sequencing of clinically significant gene mutations and translocations in leukemia. Modern Pathology, 25(6):795–804, Mar 2012.

[54] Richard M. Durbin, David L. Altshuler, Richard M. Durbin, Gonçalo R. Abecasis, David R. Bentley, Aravinda Chakravarti, Andrew G. Clark, Francis S. Collins, Francisco M. De La Vega, Peter Donnelly, and et al. A map of human genome variation from population-scale sequencing. Nature, 467(7319):1061–1073, Oct 2010.

[55] Richard M. Durbin, David L. Altshuler, Richard M. Durbin, Gonçalo R. Abecasis, David R. Bentley, Aravinda Chakravarti, Andrew G. Clark, Francis S. Collins, Francisco M. De La Vega, Peter Donnelly, and et al. A map of human genome variation from population-scale sequencing. Nature, 467(7319):1061–1073, Oct 2010.

[56] Andrew Ebenazer, Simon Rajaratnam, and Rekha Pai. Detection of large deletions in the vhl gene using a real-time pcr with sybr green. Familial Cancer, 12(3):519–524, Feb 2013.

[57] J. Eid, A. Fehr, J. Gray, K. Luong, J. Lyle, G. Otto, P. Peluso, D. Rank, P. Baybayan, B. Bettman, and et al. Real-time dna sequencing from single polymerase molecules. Science, 323(5910):133–138, Jan 2009.

[58] Norwitz E.R. and B. Levy. Noninvasive prenatal testing: The future is now. Rev Obstet Gynecol., 6(2):48–62, 2013.

[59] Mitelman F., Johansson B., and Mertens F (Eds.). Mitelman database of chromosome aberrations and gene fusions in cancer 2017, 2017.

[60] Stefan Faderl, Moshe Talpaz, Zeev Estrov, Susan O'Brien, Razelle Kurzrock, and Hagop M. Kantarjian. The biology of chronic myeloid leukemia. New England Journal of Medicine, 341(3):164–172, Jul 1999.

[61] Genevieve Fairbrother, Shayla Johnson, Thomas J. Musci, and Ken Song. Clinical experience of noninvasive prenatal testing with cell-free dna for fetal trisomies 21, 18, and 13, in a general screening population. Prenatal Diagnosis, 33(6):580–583, Mar 2013.

[62] H. C. Fan, Y. J. Blumenfeld, U. Chitkara, L. Hudgins, and S. R. Quake. Noninvasive diagnosis of fetal aneuploidy by shotgun sequencing dna from maternal blood. Proceedings of the National Academy of Sciences, 105(42):16266–16271, Oct 2008.

[63] H. Christina Fan and Stephen R. Quake. Sensitivity of noninvasive prenatal detection of fetal aneuploidy from maternal plasma using shotgun sequencing is limited only by counting statistics. PLoS ONE, 5(5):e10439, May 2010.

[64] J. A. Ferry. Burkitt's lymphoma: Clinicopathologic features and differential diagnosis. The Oncologist, 11(4):375–383, Apr 2006.

[65] W. Flemming. Zellsubstanz, Kern und Zelltheilung. F.C.W. Vogel, Leipzig, 1882.

[66] Laurent C Francioli, Androniki Menelaou, Sara L Pulit, Freerk van Dijk, Pier Francesco Palamara, Clara C Elbers, Pieter B T Neerincx, Kai Ye, Victor Guryev, and et al. Whole-genome sequence variation, population structure and demographic history of the dutch population. Nature Genetics, 46(8):818–825, Jun 2014.

[67] Steven A. Frank. Somatic mosaicism and disease. Current Biology, 24(12):R577–R581, Jun 2014.

[68] Rosalind E. Franklin and R. G. Gosling. Molecular configuration in sodium thymonucleate. Nature, 171(4356):740–741, Apr 1953.

[69] Menachem Fromer, Jennifer L. Moran, Kimberly Chambert, Eric Banks, Sarah E. Bergen, Douglas M. Ruderfer, Robert E. Handsaker, Steven A. McCarroll, Michael C. O'Donovan, Michael J. Owen, and et al. Discovery and statistical genotyping of copy-number variation from whole-exome sequencing depth. The American Journal of Human Genetics, 91(4):597–607, Oct 2012.

[70] Elisa Fueller, Daniel Schaefer, Ute Fischer, Pina F. I. Krell, Martin Stanulla, Arndt Borkhardt, and Robert K. Slany. Genomic inverse pcr for exploration of ligated breakpoints (gipfel), a new method to detect translocations in leukemia. PLoS ONE, 9(8):e104419, Aug 2014.

[71] J.G. Gall and Pardue M.L. Formation and detection of rna-dna hybrid molecules in cytological preparations. Proc Natl Acad Sci U S A, 63(2):378–83, 1969.

[72] Amy S Gargis, Lisa Kalman, Meredith W Berry, David P Bick, David P Dimmock, Tina Hambuch, Fei Lu, Elaine Lyon, Karl V Voelkerding, Barbara A Zehnbauer, and et al. Assuring the quality of next-generation sequencing in clinical laboratory practice. Nature Biotechnology, 30(11):1033–1036, Nov 2012.

[73] M. M. Gil, M. S. Quezada, B. Bregant, M. Ferraro, and K. H. Nicolaides. Implementation of maternal blood cell-free dna testing in early screening for aneuploidies. Ultrasound in Obstetrics and Gynecology, 42(1):34–40, Jun 2013.

[74] Christian Gilissen, Heleen H. Arts, Alexander Hoischen, Liesbeth Spruijt, Dorus A. Mans, Peer Arts, Bart van Lier, Marloes Steehouwer, Jeroen van Reeuwijk, Sarina G. Kant, and et al. Exome sequencing identifies wdr35 variants involved in sensenbrenner syndrome. The American Journal of Human Genetics, 87(3):418–423, Sep 2010.

[75] Christian Gilissen, Jayne Y. Hehir-Kwa, Djie Tjwan Thung, Maartje van de Vorst, Bregje W. M. van Bon, Marjolein H. Willemsen, Michael Kwint, Irene M. Janssen, Alexander Hoischen, Annette Schenck, and et al. Genome sequencing identifies major causes of severe intellectual disability. Nature, 511(7509):344–347, Jun 2014.

[76] Christian Gilissen, Alexander Hoischen, Han G Brunner, and Joris A Veltman. Disease gene identification strategies for exome sequencing. European Journal of Human Genetics, 20(5):490–497, Jan 2012.

[77] Sara Goodwin, John D. McPherson, and W. Richard McCombie. Coming of age: ten years of next-generation sequencing technologies. Nature Reviews Genetics, 17(6):333–351, Jun 2016.

[78] Sivakumar Gowrisankar, Jordan P. Lerner-Ellis, Stephanie Cox, Emily T. White, Megan Manion, Kevin LeVan, Jonathan Liu, Lisa M. Farwell, Oleg Iartchouk, Heidi L. Rehm, and et al. Evaluation of second-generation sequencing of 19 dilated cardiomyopathy genes for clinical applications. The Journal of Molecular Diagnostics, 12(6):818–827, Nov 2010.

[79] Matthew R. Grace, Emily Hardisty, Noah S. Green, Emily Davidson, Alison M. Stuebe, and Neeta L. Vora. Cell free dna testing–interpretation of results using an online calculator. American Journal of Obstetrics and Gynecology, 213(1):30.e1–30.e4, Jul 2015.

[80] Harvey A. Greisman, Noah G. Hoffman, and Hye Son Yi. Rapid high-resolution mapping of balanced chromosomal rearrangements on tiling cgh arrays. The Journal of Molecular Diagnostics, 13(6):621–633, Nov 2011.

[81] A.J.F. Griffiths, J.H. Miller, D.T. Suzuki, and et al. An Introduction to Genetic Analysis, 7th edition. W.H.Freeman, New York, 2000.

[82] Yan Guo, Quanghu Sheng, David C. Samuels, Brian Lehmann, Joshua A. Bauer, Jennifer Pietenpol, and Yu Shyr. Comparative study of exome copy number variation estimation tools using array comparative genomic hybridization as control. BioMed Research International, 2013:1–7, 2013.

[83] J.F. Gusella, N.S. Wexler, P.M. Conneally, S.L. Naylor, M.A. Anderson, R.E. Tanzi, P.C. Watkins, K. Ottina, M.R. Wallace, A.Y. Sakaguchi, and et al. A polymorphic dna marker genetically linked to huntington's disease. Nature, 306(5940):234–238, Nov 1983.

[84] Megan P. Hall, Matthew Hill, Bernhard Zimmermann, Styrmir Sigurjonsson, Margaret Westemeyer, Jennifer Saucier, Zachary Demko, and Matthew Rabinowitz. Non-invasive prenatal detection of trisomy 13 using a single nucleotide polymorphism- and informatics-based approach. PLoS ONE, 9(5):e96677, May 2014.

[85] J.L. Hamerton and P.A. Jacobs. Paris conference (1971): Standardization in human cytogenetics. Cytogenetics, 11:313–362, 1972.

[86] Nicolien M Hanemaaijer, Birgit Sikkema-Raddatz, Gerben van der Vries, Trijnie Dijkhuizen, Roel Hordijk, Anthonie J van Essen, Hermine E Veenstra-Knol, Wilhelmina S Kerstjens-Frederikse, Johanna C Herkert, Erica H Gerkes, and et al. Practical guidelines for interpreting copy number gains detected by high-resolution array in routine diagnostics. European Journal of Human Genetics, 20(2):161–165, Sep 2012.

[87] C.A. Heid, Stevens J., Livak K.J., and Williams P.M. Real time quantitative pcr. PCR Methods Appl., 6(10):986–994, 1996.

[88] Daniel S. Herman, Lien Lam, Matthew R.G. Taylor, Libin Wang, Polakit Teekakirikul, Danos Christodoulou, Lauren Conner, Steven R. DePalma, Barbara McDonough, Elizabeth Sparks, and et al. Truncations of titin causing dilated cardiomyopathy. New England Journal of Medicine, 366(7):619–628, Feb 2012.

[89] Benjamin J. Hindson, Kevin D. Ness, Donald A. Masquelier, Phillip Belgrader, Nicholas J. Heredia, Anthony J. Makarewicz, Isaac J. Bright, Michael Y. Lucero, Amy L. Hiddessen, Tina C. Legler, and et al. High-throughput droplet digital pcr system for absolute quantitation of dna copy number. Analytical Chemistry, 83(22):8604–8610, Nov 2011.

[90] Alexander Hoischen, Bregje W M van Bon, Christian Gilissen, Peer Arts, Bart van Lier, Marloes Steehouwer, Petra de Vries, Rick de Reuver, Nienke Wieskamp, Geert Mortier, and et al. De novo mutations of setbp1 cause schinzel-giedion syndrome. Nature Genetics, 42(6):483–485, May 2010.

[91] E.B. Hook. "exclusion of chromosomal mosaicism: tables of 90%, 95% and 99% confidence limits and comments on use. Am. J. Hum. Genet., 29:94–97, 1977.

[92] Ernest B. Hook and Dorothy Warburton. Turner syndrome revisited: review of new data supports the hypothesis that all viable 45,x cases are cryptic mosaics with a rescue cell line, implying an origin by mitotic loss. Human Genetics, 133(4):417–424, Jan 2014.

[93] Shan Jiang and Ali Mortazavi. Integrating chip-seq with other functional genomics data. Briefings in Functional Genomics, 17(2):104–115, Mar 2018.

[94] Yuchao Jiang, Derek A. Oldridge, Sharon J. Diskin, and Nancy R. Zhang. Codex: a normalization and copy number variation detection method for whole exome sequencing. Nucleic Acids Research, 43(6):e39–e39, Jan 2015.

[95] L. F. Johansson, E. N. de Boer, H. A. de Weerd, F. van Dijk, M. G. Elferink, G. H. Schuring-Blom, R. F. Suijkerbuijk, R. J. Sinke, G. J. te Meerman, R. H. Sijmons, and et al. Novel algorithms for improved sensitivity in non-invasive prenatal testing. Scientific Reports, 7(1), May 2017.

[96] A. Kallioniemi, O-P Kallioniemi, D. Sudar, D. Rutovitz, J.W. Gray, F. Waldman, and D. Pinkel. Comparative genomic hybridization for molecular cytogenetic analysis of solid tumors. Science, 258(5083):818–821, 1992.

[97] Sung-Hae L. Kang, Chad Shaw, Zhishuo Ou, Patricia A. Eng, M. Lance Cooper, Amber N. Pursley, Trilochan Sahoo, Carlos A. Bacino, A. Craig Chinault, Pawel Stankiewicz, and et al. Insertional translocation detected using fish confirmation of array-comparative genomic hybridization (acgh) results. American Journal of Medical Genetics Part A, 152A(5):1111–1126, May 2010.

[98] Zhi-Jie Kang, Yu-Fei Liu, Ling-Zhi Xu, Zi-Jie Long, Dan Huang, Ya Yang, Bing Liu, Jiu-Xing Feng, Yu-Jia Pan, Jin-Song Yan, and et al. The philadelphia chromosome in leukemogenesis. Chinese Journal of Cancer, 35(1), May 2016.

[99] I. Kant. Kritik der Reinen Vernunft. Felix Meiner Verlag, Hamburg, 1781/1787 Herausgabe 1956.

[100] Milo Keynes and TM Cox. William bateson, the rediscoverer of mendel. Journal of the Royal Society of Medicine, 101(3):104–104, Mar 2008.

[101] N. Krumm, P. H. Sudmant, A. Ko, B. J. O'Roak, M. Malig, B. P. Coe, A. R. Quinlan, D. A. Nickerson, and E. E. Eichler. Copy number variation detection and genotyping from exome sequence data. Genome Research, 22(8):1525–1532, May 2012.

[102] R.P. Kuiper, S.V. van Reijmersdal, M. Simonis, J. Yu, E. Sonneveld, B. Scheijen, and et al. Targeted locus amplification and next generation sequencing for the detection of recurrent and novel gene fusions for improved treatment decisions in pediatric acute lymphoblastic leukemia. Blood, 126(23):696, 2015.

[103] James LA. Comparative genomic hybridization as a tool in tumour cytogenetics. The Journal of Pathology, 187(4):385–395, 1999.

[104] Abdul Ghaaliq Lalkhen and Anthony McCluskey. Clinical tests: sensitivity and specificity. Continuing Education in Anaesthesia Critical Care and Pain, 8(6):221–223, Dec 2008.

[105] Eric S. Lander, Lauren M. Linton, Bruce Birren, Chad Nusbaum, Michael C. Zody, Jennifer Baldwin, Keri Devon, Ken Dewar, Michael Doyle, William FitzHugh, and et al. Initial sequencing and analysis of the human genome. Nature, 409(6822):860–921, Feb 2001.

[106] T. K. Lau, S. W. Cheung, P. S. S. Lo, A. N. Pursley, M. K. Chan, F. Jiang, H. Zhang, W. Wang, L. F. J. Jong, O. K. C. Yuen, and et al. Non-invasive prenatal testing for fetal chromosomal abnormalities by low-coverage whole-genome sequencing of maternal plasma dna: review of 1982 consecutive cases in a single center. Ultrasound in Obstetrics and Gynecology, 43(3):254–264, Feb 2014.

[107] Tze Kin Lau, Fang Chen, Xiaoyu Pan, Ritsuko K. Pooh, Fuman Jiang, Yihan Li, Hui Jiang, Xuchao Li, Shengpei Chen, and Xiuqing Zhang. Noninvasive prenatal diagnosis of common fetal chromosomal aneuploidies by maternal plasma dna sequencing. The Journal of Maternal-Fetal and Neonatal Medicine, 25(8):1370–1374, Feb 2012.

[108] R. J. Leary, M. Sausen, I. Kinde, N. Papadopoulos, J. D. Carpten, D. Craig, J. O'Shaughnessy, K. W. Kinzler, G. Parmigiani, B. Vogelstein, and et al. Detection of chromosomal alterations in the circulation of cancer patients with whole-genome sequencing. Science Translational Medicine, 4(162):162ra154–162ra154, Nov 2012.

[109] J. Lejeune, M. Gauthier, and R. Turpin. Les chromosomes humains en culture de tissus. C. R. Acad. Sci, 248:602–903, 1959.

[110] Joshua Z Levin, Michael F Berger, Xian Adiconis, Peter Rogov, Alexandre Melnikov, Timothy Fennell, Chad Nusbaum, Levi A Garraway, and Andreas Gnirke. Targeted next-generation sequencing of a cancer transcriptome enhances detection of sequence variants and novel fusion transcripts. Genome Biology, 10(10):R115, 2009.

[111] J. M. Levsky. Fluorescence in situ hybridization: past, present and future. Journal of Cell Science, 116(14):2833–2838, Jul 2003.

[112] Johansson LF and de Weerd HA. Nipter vignette, 2016.

[113] H. Li, B. Handsaker, A. Wysoker, T. Fennell, J. Ruan, N. Homer, G. Marth, G. Abecasis, and R. Durbin. The sequence alignment/map format and samtools. Bioinformatics, 25(16):2078–2079, Jun 2009.

[114] Heng Li and Richard Durbin. Fast and accurate long-read alignment with burrows–wheeler transform. Bioinformatics, 26(5):589–595, Jan 2010.

[115] Jason Li, Richard Lupat, Kaushalya C. Amarasinghe, Ella R. Thompson, Maria A. Doyle, Georgina L. Ryland, Richard W. Tothill, Saman K. Halgamuge, Ian G. Campbell, and Kylie L. Gorringe. Contra: copy number analysis for targeted resequencing. Bioinformatics, 28(10):1307–1313, Apr 2012.

[116] Desheng Liang, Weigang Lv, Hua Wang, Liangpu Xu, Jing Liu, Haoxian Li, Liang Hu, Ying Peng, and Lingqian Wu. Non-invasive prenatal testing of fetal whole chromosome aneuploidy by massively parallel sequencing. Prenatal Diagnosis, 33(5):409–415, Jan 2013.

[117] Michael Liew, Leslie Rowe, ParkerW Clement, RodneyR Miles, and MohamedE Salama. Validation of break-apart and fusion myc probes using a digital fluorescence in situ hybridization capture and imaging system. Journal of Pathology Informatics, 7(1):20, 2016.

[118] H Lilljebjörn, H Ågerstam, C Orsmark-Pietras, M Rissler, H Ehrencrona, L Nilsson, J Richter, and T Fioretos. Rna-seq identifies clinically relevant fusion genes in leukemia including a novel mef2d/csf1r fusion responsive to imatinib. Leukemia, 28(4):977–979, Nov 2013.

[119] Baohong Liu, Xiaoyan Tang, Feng Qiu, Chunmei Tao, Junhui Gao, Mengmeng Ma, Tingyan Zhong, JianPing Cai, Yixue Li, and Guohui Ding. Dasaf: An r package for deep sequencing-based detection of fetal autosomal abnormalities from maternal cell-free dna. BioMed Research International, 2016:1–7, 2016.

[120] S. Liu, L. Song, D. S. Cram, L. Xiong, K. Wang, R. Wu, J. Liu, K. Deng, B. Jia, M. Zhong, and et al. Traditional karyotypingvscopy number variation sequencing for detection of chromosomal abnormalities associated with spontaneous miscarriage. Ultrasound in Obstetrics & Gynecology, 46(4):472–477, Oct 2015.

[121] Kitty K. Lo, Christopher Bous tred, Lyn S. Chitty, and Vincent Plagnol. Rapidr: an analysis package for non-invasive prenatal testing of aneuploidy. Bioinformatics, 30(20):2965–2967, Jul 2014.

[122] Y.M.D. Lo, N. Corbetta, Chamberlain P.F., Rai V., Sargent I.L., Redman C.W.G., and Wainscoat J.S. Early report.presence of fetal dna in maternal plasma and serum. Lancet, 350:485–487, 1997.

[123] I. Lobo and K. Shaw. Discovery and types of genetic linkage. Nature Education, 1(1):139, 2008.

[124] Nicholas J Loman, Raju V Misra, Timothy J Dallman, Chrystala Constantinidou, Saheer E Gharbia, John Wain, and Mark J Pallen. Performance comparison of benchtop high-throughput sequencing platforms. Nature Biotechnology, 30(5):434–439, Apr 2012.

[125] Fromer M. and Purcell S. Xhmm, 2012.

[126] FL Mackie, K Hemming, S Allen, RK Morris, and MD Kilby. The accuracy of cell-free fetal dna-based non-invasive prenatal testing in singleton pregnancies: a systematic review and bivariate meta-analysis. BJOG: An International Journal of Obstetrics and Gynaecology, 124(1):32–46, May 2016.

[127] Alberto Magi, Lorenzo Tattini, Ingrid Cifola, Romina D'Aurizio, Matteo Benelli, Eleonora Mangano, Cristina Battaglia, Elena Bonora, Ants Kurg, Marco Seri, and et al. Excavator: detecting copy number variants from whole-exome sequencing data. Genome Biology, 14(10):R120, 2013.

[128] Savanie Maithripala, Ursula Durland, Jon Havelock, Sonya Kashyap, Jason Hitkari, Justin Tan, Mahmoud Iews, Sarka Lisonkova, and Mohamed A. Bedaiwy. Prevalence and treatment choices for couples with recurrent pregnancy loss due to structural chromosomal anomalies. Journal of Obstetrics and Gynaecology Canada, Dec 2017.

[129] Diana Mandelker, Ryan J. Schmidt, Arunkanth Ankala, Kristin McDonald Gibson, Mark Bowser, Himanshu Sharma, Elizabeth Duffy, Madhuri Hegde, Avni Santani, Matthew Lebo, and et al. Navigating highly homologous genes in a molecular diagnostic setting: a resource for clinical next-generation sequencing. Genetics in Medicine, 18(12):1282–1289, May 2016.

[130] Jun Mao, Ting Wang, Ben-Jing Wang, Ying-Hua Liu, Hong Li, Jianguang Zhang, David Cram, and Ying Chen. Confined placental origin of the circulating cell free fetal dna revealed by a discordant non-invasive prenatal test result in a trisomy 18 pregnancy. Clinica Chimica Acta, 433:190–193, Jun 2014.

[131] Elaine R. Mardis. Next-generation sequencing platforms. Annual Review of Analytical Chemistry, 6(1):287–303, Jun 2013.

[132] Marcel Margulies, Michael Egholm, William E. Altman, Said Attiya, Joel S. Bader, Lisa A. Bemben, Jan Berka, Michael S. Braverman, Yi-Ju Chen, Zhoutao Chen, and et al. Genome sequencing in microfabricated high-density picolitre reactors. Nature, 437(7057):376–380, Jul 2005.

[133] Nicholas McGranahan and Charles Swanton. Clonal heterogeneity and tumor evolution: Past, present, and the future. Cell, 168(4):613–628, Feb 2017.

[134] A. McKenna, M. Hanna, E. Banks, A. Sivachenko, K. Cibulskis, A. Kernytsky, K. Garimella, D. Altshuler, S. Gabriel, M. Daly, and et al.

The genome analysis toolkit: A mapreduce framework for analyzing next-generation dna sequencing data. Genome Research, 20(9):1297–1303, Jul 2010.

[135] G. Mendel. Versuche über pflanzen-hybriden. Verh. Naturforsch. Ver. Brünn, 4:3–47, 1866.

[136] Fredrik Mertens, Bertil Johansson, Thoas Fioretos, and Felix Mitelman. The emerging complexity of gene fusions in cancer. Nature Reviews Cancer, 15(6):371–381, Jun 2015.

[137] C Meyer, J Hofmann, T Burmeister, D Gröger, T S Park, M Emerenciano, M Pombo de Oliveira, A Renneville, P Villarese, E Macintyre, and et al. The mll recombinome of acute leukemias in 2013. Leukemia, 27(11):2165–2176, Apr 2013.

[138] Stephanie Morain, Michael F. Greene, and Michelle M. Mello. A new era in noninvasive prenatal testing. New England Journal of Medicine, 369(6):499–501, Aug 2013.

[139] H. J. Muller Morgan, Thomas Hunt; Alfred H. Sturtevant and C. B. Bridges. The mechanism of mendelian heredity. Henry Holt, New York, 1915.

[140] T. H. Morgan. Random segregation versus coupling in mendelian inheritance. Science, 34(873):384–384, Sep 1911.

[141] MRC Holland. MLPA DNA Protocol version MDP-005; last revised on September 22 2014, 2014.

[142] G.L. Mutter and K.A. Boynton. Pcr bias in amplification of androgen receptor alleles, a trinucleotide repeat marker used in clonality studies. Nucleic Acids Res, 1995:1411–1418, 1995.

[143] Krumm N. Conifer tutorial, n.d.

[144] Kensuke Nakamura, Taku Oshima, Takuya Morimoto, Shun Ikeda, Hirofumi Yoshikawa, Yuh Shiwa, Shu Ishikawa, Margaret C. Linak, Aki Hirai, Hiroki Takahashi, and et al. Sequence-specific error profile of illumina sequencers. Nucleic Acids Research, 39(13):e90–e90, May 2011.

[145] M.M.K. Nass and S. Nass. Intramitochondrial fibers with dna characteristics: I. fixation and electronic staining reactions. J. Cell Biol., 19:593–611, 1963.

[146] Christopher T Naugler. Population genetics of cancer cell clones: possible implications of cancer stem cells. Theoretical Biology and Medical Modelling, 7(1), Nov 2010.

[147] Sarah B Ng, Kati J Buckingham, Choli Lee, Abigail W Bigham, Holly K Tabor, Karin M Dent, Chad D Huff, Paul T Shannon, Ethylin Wang Jabs, Deborah A Nickerson, and et al. Exome sequencing identifies the cause of a mendelian disorder. Nature Genetics, 42(1):30–35, Nov 2009.

[148] Kypros H. Nicolaides, Argyro Syngelaki, Ghalia Ashoor, Cahit Birdir, and Gisele Touzet. Noninvasive prenatal testing for fetal trisomies in a routinely screened first-trimester population. American Journal of Obstetrics and Gynecology, 207(5):374.e1–374.e6, Nov 2012.

[149] Rasmus Nielsen, Joshua S. Paul, Anders Albrechtsen, and Yun S. Song. Genotype and snp calling from next-generation sequencing data. Nature Reviews Genetics, 12(6):443–451, Jun 2011.

[150] Mary E. Norton, Bo Jacobsson, Geeta K. Swamy, Louise C. Laurent, Angela C. Ranzini, Herb Brar, Mark W. Tomlinson, Leonardo Pereira, Jean L. Spitz, Desiree Hollemon, and et al. Cell-free dna analysis for noninvasive examination of trisomy. New England Journal of Medicine, 372(17):1589–1597, Apr 2015.

[151] Nadine Norton, Duanxiang Li, and Ray E. Hershberger. Next-generation sequencing to identify genetic causes of cardiomyopathies. Current Opinion in Cardiology, 27(3):214–220, May 2012.

[152] P.C. Nowell. Clonal evolution of tumor cell populations. Science, 194:23–38, 1976.

[153] P.C. Nowell and D.A. Hungerford. A minute chromosome in human chronic granulocytic leukemia. Science, 142:1497, 1960.

[154] National Society of Genetic Counselors. Nipt/cell free dna screening predicitve value calculator.

[155] Leibniz Institut DSMZ-German Collection of Microorganisms and Cell Cultures. Fkh1:dsmz no acc 614, 2017.

[156] Leibniz Institut DSMZ-German Collection of Microorganisms and Cell Cultures. Reh:dsmz no acc22, 2017.

[157] G. E. Palomaki, E. M. Kloza, G. M. Lambert-Messerlian, D. van den Boom, M. Ehrich, C. Deciu, A. T. Bombard, and J. E. Haddow. Circulating cell free dna testing: are some test failures informative? Prenatal Diagnosis, 35(3):289–293, Jan 2015.

[158] Glenn E. Palomaki, Cosmin Deciu, Edward M. Kloza, Geralyn M. Lambert-Messerlian, James E. Haddow, Louis M. Neveux, Mathias Ehrich, Dirk van den Boom, Allan T. Bombard, Wayne W. Grody, and et al. Dna sequencing of maternal plasma reliably identifies trisomy 18 and trisomy 13 as well as down syndrome: an international collaborative study. Genetics in Medicine, 14(3):296–305, Feb 2012.

[159] Eugene Pergament, Howard Cuckle, Bernhard Zimmermann, Milena Banjevic, Styrmir Sigurjonsson, Allison Ryan, Megan P. Hall, Michael Dodd, Phil Lacroute, Melissa Stosic, and et al. Single-nucleotide polymorphism–based noninvasive prenatal screening in a high-risk and low-risk cohort. Obstetrics and Gynecology, 124(2, PART 1):210–218, Aug 2014.

[160] Minh-Duy Phan, Thong V. Nguyen, Huong N. T. Trinh, Binh T. Vo, Truc M. Nguyen, Nguyen H. Nguyen, Tho T. Q. Nguyen, Thuy T. T. Do, Tuyet T. D. Hoang, Kiet D. Truong, and et al. Establishing and validating noninvasive prenatal testing procedure for fetal aneuploidies in vietnam. The Journal of Maternal-Fetal & Neonatal Medicine, page 1–7, Jul 2018.

[161] Picard. Picard, n.d.

[162] D. Pinkel, T. Straume, and J.W. Gray. Cytogenetic analysis using quantitative, high-sensitivity, fluorescence hybridization. Proc Natl Acad Sci USA, 83:2934–8, 1986.

[163] Daniel Pinkel, Richard Segraves, Damir Sudar, Steven Clark, Ian Poole, David Kowbel, Colin Collins, Wen-Lin Kuo, Chira Chen, Ye Zhai, and et al. High resolution analysis of dna copy number variation using comparative genomic hybridization to microarrays. Nature Genetics, 20(2):207–211, Oct 1998.

[164] Boone PM, Bacino CA, Shaw CA, Eng PA, and Hixson PM et al. Detection of clinically relevant exonic copy-number changes by array cgh. Human Mutation, 31(12):1326–1342, Nov 2010.

[165] Anna Posafalvi, Johanna C Herkert, Richard J Sinke, Maarten P van den Berg, Jens Mogensen, Jan D H Jongbloed, and J Peter van Tintelen. Clinical utility gene card for: Dilated cardiomyopathy (cmd). European Journal of Human Genetics, 21(10), Dec 2012.

[166] A.K. Raap, R.J. Florijn, L.A.J. Blonden, J. Wiegant, J.W. Vaandrager, H. Vrolijk, J. den Dunnen, H.J. Tanke, and G.J. van Ommen. Fiber fish as a dna mapping tool. Methods, 9(1):67–73, 1996.

[167] Richard Redon, Shumpei Ishikawa, Karen R. Fitch, Lars Feuk, George H. Perry, T. Daniel Andrews, Heike Fiegler, Michael H. Shapero, Andrew R. Carson, Wenwei Chen, and et al. Global variation in copy number in the human genome. Nature, 444(7118):444–454, Nov 2006.

[168] Genetics Home Reference. Color vision deficiency. online: https:ghr.nlm.nih.gov/condition/color-vision-deficiency, 2019.

[169] Wm. Rees B. Robertson. Chromosome studies. i. taxonomic relationships shown in the chromosomes of tettigidae and acrididae: V-shaped chromosomes and their significance in acrididae, locustidae, and gryllidae: Chromosomes and variation. Journal of Morphology, 27(2):179–331, Jun 1916.

[170] Simone Roeh, Peter Weber, Monika Rex-Haffner, Jan M. Deussing, Elisabeth B. Binder, and Mira Jakovcevski. Sequencing on the solid 5500xl system – in-depth characterization of the gc bias. Nucleus, 8(4):370–380, Jun 2017.

[171] Jonathan M. Rothberg, Wolfgang Hinz, Todd M. Rearick, Jonathan Schultz, William Mileski, Mel Davey, John H. Leamon, Kim Johnson, Mark J. Milgrew, Matthew Edwards, and et al. An integrated semiconductor device enabling non-optical genome sequencing. Nature, 475(7356):348–352, Jul 2011.

[172] J.D. Rowley. . letter: A new consistent chromosomal abnormality in chronic myelogenous leukaemia identified by quinacrine fluorescence and giemsa staining. Nature, 243:290–293, 1973.

[173] D.C. Rubinsztein, J. Leggo, R. Coles, E. Almqvist, V. Biancalana, J.J. Cassiman, K. Chotai, M. Connarty, D. Crauford, A. Curtis, D. Curtis, M.J. Davidson, A.M. Differ, C. Dode, A. Dodge, M. Frontali, N.G. Ranen, O.C. Stine, M. Sherr, M.H. Abbott, M.L. Franz, C.A. Graham, P.S. Harper, J.C. Hedreen, and M. R. Hayden. Phenotypic characterization of individuals with 30-40 cag repeats in the huntington disease (hd) gene reveals hd cases with 36 repeats and apparently normal elderly individuals with 36-39 repeats. Am. J. Hum. Genet., 59:16–22, 1996.

[174] R. Saiki, D. Gelfand, S Stoffel, S. Scharf, R Higuchi, G. Horn, K. Mullis, and H. Erlich. Primer-directed enzymatic amplification of dna with a thermostable dna polymerase. Science, 239(4839):487–491, Jan 1988.

[175] R. Saiki, S Scharf, F Faloona, K. Mullis, G. Horn, H. Erlich, and N Arnheim. Enzymatic amplification of beta-globin genomic sequences and restriction site analysis for diagnosis of sickle cell anemia. Science, 230(4732):1350–1354, Dec 1985.

[176] Manuel Salto-Tellez, Suresh G. Shelat, Bernice Benoit, Hanna Rennert, Martin Carroll, Debra G.B. Leonard, Peter Nowell, and Adam Bagg. Multiplex rt-pcr for the detection of leukemia-associated translocations. The Journal of Molecular Diagnostics, 5(4):231–236, Nov 2003.

[177] Carole Samango-Sprouse, Milena Banjevic, Allison Ryan, Styrmir Sigurjonsson, Bernhard Zimmermann, Matthew Hill, Megan P. Hall, Margaret Westemeyer, Jennifer Saucier, Zachary Demko, and et al. Snp-based noninvasive prenatal testing detects sex chromosome aneuploidies with high accuracy. Prenatal Diagnosis, 33(7):643–649, Jun 2013.

[178] Avery A. Sandberg and Aurelia M. Meloni-Ehrig. Cytogenetics and genetics of human cancer: methods and accomplishments. Cancer Genetics and Cytogenetics, 203(2):102–126, Dec 2010.

[179] F. Sanger and A.R. Coulson. A rapid method for determining sequences in dna by primed synthesis with dna polymerase. Journal of Molecular Biology, 94(3):441–448, 1975.

[180] F. Sanger, S. Nicklen, and A.R. Coulson. Dna sequencing with chain-terminating inhibitors. Proc Natl Acad Sci U S A., 74(12):5463–5467, December 1977.

[181] Martin Sauk, Olga Žilina, Ants Kurg, Eva-Liina Ustav, Maire Peters, Priit Paluoja, Anne Mari Roost, Hindrek Teder, Priit Palta, Nathalie Brison, and et al. Niptmer: rapid k-mer-based software package for detection of fetal aneuploidies. Scientific Reports, 8(1), Apr 2018.

[182] Melanie Schirmer, Umer Z. Ijaz, Rosalinda D'Amore, Neil Hall, William T. Sloan, and Christopher Quince. Insight into biases and sequencing errors for amplicon sequencing with the illumina miseq platform. Nucleic Acids Research, 43(6):e37–e37, Jan 2015.

[183] A. Schneider. Untersuchungen über plathelminthen. Jahresberichte der Oberhessischen Gesellschaft für Natur- und Heilkunde in Gießen, 14:69–140, 1873.

[184] C Schoch, S Schnittger, S Bursch, D Gerstner, A Hochhaus, U Berger, R Hehlmann, W Hiddemann, and T Haferlach. Comparison of chromosome banding analysis, interphase- and hypermetaphase-fish, qualitative and quantitative pcr for diagnosis and for follow-up in chronic myeloid leukemia: a study on 350 cases. Leukemia, 16(1):53–59, Jan 2002.

[185] J.P. Schouten, McElgunn C.J., Waaijer R., Zwijnenburg D., and Pals G. Relative quantification of 40 nucleic acid sequences by multiplex ligation-dependent probe amplification. Nucleic Acids Res., 30(12):e57, 2002.

[186] Jonathan A. Scolnick, Michelle Dimon, I-Ching Wang, Stephanie C. Huelga, and Douglas A. Amorese. An efficient method for identifying

gene fusions by targeted rna sequencing from fresh frozen and ffpe samples. PLOS ONE, 10(7):e0128916, Jul 2015.

[187] Virginie Scotet, Ingrid Duguépéroux, Philippe Saliou, Gilles Rault, Michel Roussey, Marie-Pierre Audrézet, and Claude Férec. Evidence for decline in the incidence of cystic fibrosis: a 35-year observational study in brittany, france. Orphanet Journal of Rare Diseases, 7(1):14, 2012.

[188] A. J. Sehnert, B. Rhees, D. Comstock, E. de Feo, G. Heilek, J. Burke, and R. P. Rava. Optimal detection of fetal chromosomal abnormalities by massively parallel dna sequencing of cell-free fetal dna from maternal blood. Clinical Chemistry, 57(7):1042–1049, Apr 2011.

[189] Lisa G Shaffer, Roger A Schultz, and Blake C Ballif. The use of new technologies in the detection of balanced translocations in hematologic disorders. Current Opinion in Genetics and Development, 22(3):264–271, Jun 2012.

[190] Birgit Sikkema-Raddatz, Lennart F. Johansson, Eddy N. de Boer, Rowida Almomani, Ludolf G. Boven, Maarten P. van den Berg, Karin Y. van Spaendonck-Zwarts, J. Peter van Tintelen, Rolf H. Sijmons, Jan D. H. Jongbloed, and et al. Targeted next-generation sequencing can replace sanger sequencing in clinical diagnostics. Human Mutation, 34(7):1035–1042, Apr 2013.

[191] Milena Simioni, François Artiguenave, Vincent Meyer, Ilária C. Sgardioli, Nilma L. Viguetti-Campos, Isabella Lopes Monlleó, Andréa T. Maciel-Guerra, Carlos E. Steiner, and Vera L. Gil-da Silva-Lopes. Genomic investigation of balanced chromosomal rearrangements in patients with abnormal phenotypes. Molecular Syndromology, 8(4):187–194, 2017.

[192] A.F.A. Smit, Hubley R., and Green P. Repeatmasker open-4.0, 2013-2015.

[193] Meagan Smith, Kimberly M. Lewis, Alexandrea Holmes, and Jeannie Visootsak. A case of false negative nipt for down syndrome-lessons learned. Case Reports in Genetics, 2014:1–3, 2014.

[194] S. Snijder, B. Beverloo, C. Mellink, M. Stevens-Kroef, E. van den Berg, Buijs A., and et al. Vkgl v07: Richtlijnen verworven cytogenetica., 2015.

[195] R. J. M. Snijders, K. Sundberg, W. Holzgreve, G. Henry, and K. H. Nicolaides. Maternal age- and gestation-specific risk for trisomy 21. Ultrasound in Obstetrics and Gynecology, 13(3):167–170, Mar 1999.

[196] R.J.M. Snijders, N.J. Sebire, and K.H. Nicolaides. Maternal age and gestational age-specific risk for chromosomal defects. Fetal Diagnosis and Therapy, 10(6):356–367, 1995.

[197] Michał Sobjanek, Magdalena Dobosz-Kawalko, Igor Michajlowski, Rafal Peksa, and Roman Nowicki. Segmental neurofibromatosis. Advances in Dermatology and Allergology, 6:410–412, 2014.

[198] Andrew B. Sparks, Craig A. Struble, Eric T. Wang, Ken Song, and Arnold Oliphant. Noninvasive prenatal detection and selective analysis of cell-free dna obtained from maternal blood: evaluation for trisomy 21 and trisomy 18. American Journal of Obstetrics and Gynecology, 206(4):319.e1–319.e9, Apr 2012.

[199] Andrew B. Sparks, Eric T. Wang, Craig A. Struble, Wade Barrett, Renee Stokowski, Celeste McBride, Jacob Zahn, Kevin Lee, Naiping Shen, Jigna Doshi, and et al. Selective analysis of cell-free dna in maternal blood for evaluation of fetal trisomy. Prenatal Diagnosis, 32(1):3–9, Jan 2012.

[200] Malte Spielmann, Darío G. Lupiáñez, and Stefan Mundlos. Structural variation in the 3d genome. Nature Reviews Genetics, 19(7):453–467, Apr 2018.

[201] Roy Straver, Cees B. M. Oudejans, Erik A. Sistermans, and Marcel J. T. Reinders. Calculating the fetal fraction for noninvasive prenatal testing based on genome-wide nucleosome profiles. Prenatal Diagnosis, 36(7):614–621, May 2016.

[202] Roy Straver, Erik A. Sistermans, Henne Holstege, Allerdien Visser, Cees B. M. Oudejans, and Marcel J. T. Reinders. Wisecondor: detection of fetal aberrations from shallow sequencing maternal plasma based on a within-sample comparison scheme. Nucleic Acids Research, 42(5):e31–e31, Oct 2013.

[203] Markus Stumm, Michael Entezami, Karsten Haug, Cornelia Blank, Max Wüstemann, Bernt Schulze, Gisela Raabe-Meyer, Maja Hempel, Markus Schelling, Eva Ostermayer, and et al. Diagnostic accuracy of random massively parallel sequencing for non-invasive prenatal detection of common autosomal aneuploidies: a collaborative study in europe. Prenatal Diagnosis, 34(2):185–191, Dec 2013.

[204] Peter H. Sudmant, Tobias Rausch, Eugene J. Gardner, Robert E. Handsaker, Alexej Abyzov, John Huddleston, Yan Zhang, Kai Ye, Goo Jun, Markus Hsi-Yang Fritz, and et al. An integrated map of structural variation in 2,504 human genomes. Nature, 526(7571):75–81, Sep 2015.

[205] Anna-Maija Sulonen, Pekka Ellonen, Henrikki Almusa, Maija Lepistö, Samuli Eldfors, Sari Hannula, Timo Miettinen, Henna Tyynismaa, Perttu Salo, Caroline Heckman, and et al. Comparison of solution-based exome capture methods for next generation sequencing. Genome Biology, 12(9):R94, 2011.

[206] W.S. Sutton. On the morphology of the chromosome group in brachystola magna. Biological Bulletin, 4:24–39, 1902.

[207] Bente A. Talseth-Palmer, Denis C. Bauer, Wenche Sjursen, Tiffany J. Evans, Mary McPhillips, Anthony Proietto, Geoffrey Otton, Allan D. Spigelman, and Rodney J. Scott. Targeted next-generation sequencing of 22 mismatch repair genes identifies lynch syndrome families. Cancer Medicine, 5(5):929–941, Jan 2016.

[208] Renjie Tan, Yadong Wang, Sarah E. Kleinstein, Yongzhuang Liu, Xiaolin Zhu, Hongzhe Guo, Qinghua Jiang, Andrew S. Allen, and Mingfu Zhu. An evaluation of copy number variation detection tools from whole-exome sequencing data. Human Mutation, 35(7):899–907, May 2014.

[209] Artem Tarasov, Albert J. Vilella, Edwin Cuppen, Isaac J. Nijman, and Pjotr Prins. Sambamba: fast processing of ngs alignment formats. Bioinformatics, 31(12):2032–2034, Feb 2015.

[210] J.H. Tjio and Levan A. The chromosome number of man. Hereditas, 42(1-2):1–5, 1956.

[211] Synne Torkildsen, Ludmila Gorunova, Klaus Beiske, Geir E. Tjønnfjord, Sverre Heim, and Ioannis Panagopoulos. Novel zeb2-bcl11b fusion gene identified by rna-sequencing in acute myeloid leukemia with t(2;14)(q22;q32). PLOS ONE, 10(7):e0132736, Jul 2015.

[212] Katarzyna Tutlewska, Jan Lubinski, and Grzegorz Kurzawski. Germline deletions in the epcam gene as a cause of lynch syndrome – literature review. Hereditary Cancer in Clinical Practice, 11(1), Aug 2013.

[213] C. Alexander Valencia, Devin Rhodenizer, Shruti Bhide, Ephrem Chin, Martin Robert Littlejohn, Lisa Mari Keong, Anne Rutkowski, Carsten Bonnemann, and Madhuri Hegde. Assessment of target enrichment platforms using massively parallel sequencing for the mutation detection for congenital muscular dystrophy. The Journal of Molecular Diagnostics, 14(3):233–246, May 2012.

[214] E. Van den Berg and Stevens-Kroef M. t(8;14)(q24;q32) igh/myc; t(2;8)(p12;q24) igk/myc; t(8;22)(q24;q11) igl/myc. atlas genet cytogenet oncol heamatol, 2017.

[215] J. M. E. van den Oever, S. Balkassmi, L. F. Johansson, P. N. Adama van Scheltema, R. F. Suijkerbuijk, M. J. V. Hoffer, R. J. Sinke, E. Bakker, B. Sikkema-Raddatz, and E. M. J. Boon. Successful noninvasive trisomy 18 detection using single molecule sequencing. Clinical Chemistry, 59(4):705–709, Jan 2013.

[216] B.L. Van der Waerden. Mathematische Statistik. Springer Verlag, Göttingen: Heidelberg, 1957.

[217] J.J. van Dongen, E.A. MacIntyre, E. Delabesse, V. Rossi, G. Saglio, and et al. Standardized rt-pcr analysis of fusion gene transcripts from chromosome aberrations in acute leukemia for detection of minimal residual disease. report of the biomed-1 concerted action: investigation of minimal residual disease in acute leuekmia.

[218] Aurélie Vasson, Céline Leroux, Lucie Orhant, Mathieu Boimard, Aurélie Toussaint, Chrystel Leroy, Virginie Commere, Tiffany Ghiotti, Nathalie Deburgrave, Yoann Saillour, and et al. Custom oligonucleotide array-based cgh: a reliable diagnostic tool for detection of exonic copy-number changes in multiple targeted genes. European Journal of Human Genetics, 21(9):977–987, Jan 2013.

[219] J. C. Venter. The sequence of the human genome. Science, 291(5507):1304–1351, Feb 2001.

[220] P.-P. Verbeek. Moralizing Technology – Understanding and designing the Morality of Things. The University of Chigago Press, Chicago, 2011.

[221] Lisenka E L M Vissers, Joep de Ligt, Christian Gilissen, Irene Janssen, Marloes Steehouwer, Petra de Vries, Bart van Lier, Peer Arts, Nienke Wieskamp, Marisol del Rosario, and et al. A de novo paradigm for mental retardation. Nature Genetics, 42(12):1109–1112, Nov 2010.

[222] Karl V. Voelkerding, Shale Dames, and Jacob D. Durtschi. Next generation sequencing for clinical diagnostics-principles and application to targeted resequencing for hypertrophic cardiomyopathy. The Journal of Molecular Diagnostics, 12(5):539–551, Sep 2010.

[223] F. von Eggeling, M. Freytag, R. Fahsold, B. Horsthemke, and U. Claussen. Rapid detection of trisomy 21 by quantitative pcr. Hum. Genet., 91:567–570, 1993.

[224] Bateson W, Saunders ER, and Punnett RC. Further experiments on inheritance in sweet peas and stocks: preliminary account. Proceedings of the Royal Society of London. Series B, Containing Papers of a Biological Character, 77(517):236–238, 1906.

[225] W. Waldeyer. Über karyokinese und ihre beziehung zu den befruchtungsvorgängen. Archiv für mikroskopische Anatomie, 32:1–122, 1888.

[226] Jeffrey D. Wall, Ling Fung Tang, Brandon Zerbe, Mark N. Kvale, Pui-Yan Kwok, Catherine Schaefer, and Neil Risch. Estimating genotype error rates from high-coverage next-generation sequence data. Genome Research, 24(11):1734–1739, Oct 2014.

[227] D. G. Wang. Large-scale identification, mapping, and genotyping of single-nucleotide polymorphisms in the human genome. Science, 280(5366):1077–1082, May 1998.

[228] Yanlin Wang, Jiansheng Zhu, Yan Chen, Shoulian Lu, Biliang Chen, Xinrong Zhao, Yi Wu, Xu Han, Duan Ma, Zhongyin Liu, and et al. Two cases of placental t21 mosaicism: challenging the detection limits of non-invasive prenatal testing. Prenatal Diagnosis, 33(12):1207–1210, Aug 2013.

[229] J. D. Watson and F. H. C. Crick. Molecular structure of nucleic acids: A structure for deoxyribose nucleic acid. Nature, 171(4356):737–738, Apr 1953.

[230] P. Wegrzyn, C. Fabio, A. Peralta, C. Faro, M. Borenstein, and K. H. Nicolaides. Placental volume in twin and triplet pregnancies measured by three-dimensional ultrasound at 11 + 0 to 13 + 6 weeks of gestation. Ultrasound in Obstetrics and Gynecology, 27(6):647–651, 2006.

[231] P. Wegrzyn, C. Faro, O. Falcon, C. F. A. Peralta, and K. H. Nicolaides. Placental volume measured by three-dimensional ultrasound at 11 to 13 + 6 weeks of gestation: relation to chromosomal defects. Ultrasound in Obstetrics and Gynecology, 26(1):28–32, Jun 2005.

[232] A. Weismann. Das Keimplasma. Eine Theorie der Vererbung. Gustav Fischer, Jena, 1892.

[233] John S. Welch. Use of whole-genome sequencing to diagnose a cryptic fusion oncogene. JAMA, 305(15):1577, Apr 2011.

[234] Amy B. Wilfert, Arvis Sulovari, Tychele N. Turner, Bradley P. Coe, and Evan E. Eichler. Recurrent de novo mutations in neurodevelopmental disorders: properties and clinical implications. Genome Medicine, 9(1), Nov 2017.

[235] M. H. F. Wilkins, A. R. Stokes, and H. R. Wilson. Molecular structure of nucleic acids: Molecular structure of deoxypentose nucleic acids. Nature, 171(4356):738–740, Apr 1953.

[236] P.J. Willems, H. Dierickx, E.S. Vandenakker, D. Bekedam, N. Segers, Deboulle K., and A. Vereecken. The first 3,000 non-invasive prenatal tests (nipt) with the harmony test in belgium and the netherlands. Facts Views Vis Obgyn, 6(1):7–12, 2014.

[237] Amanda C. Winters and Kathrin M. Bernt. Mll-rearranged leukemias—an update on science and clinical approaches. Frontiers in Pediatrics, 5, Feb 2017.

[238] Daynna J. Wolff, Adam Bagg, Linda D. Cooley, Gordon W. Dewald, Betsy A. Hirsch, Peter B. Jacky, Kathleen W. Rao, and P. Nagesh Rao. Guidance for fluorescence in situ hybridization testing in hematologic disorders. The Journal of Molecular Diagnostics, 9(2):134–143, Apr 2007.

[239] Jianfeng Yang, Xiaofan Ding, and Weidong Zhu. Improving the calling of non-invasive prenatal testing on 13-/18-/21-trisomy by support vector machine discrimination. Nov 2017.

[240] C. Yanofsky. Establishing the triplet nature of the genetic code. Cell, 128(5):815–818, Mar 2007.

[241] E. Yu and S. Sharma. Cystic Fibrosis. [Updated 2018 Mar 20]. In: StatPearls. Treasure Island *FL*: StatPearls Publishing, Available from: https://www.ncbi.nlm.nih.gov/books/NBK493206/, 2018.

[242] H. Zhang, Y. Gao, F. Jiang, M. Fu, Y. Yuan, Y. Guo, Z. Zhu, M. Lin, Q. Liu, Z. Tian, and et al. Non-invasive prenatal testing for trisomies 21, 18 and 13: clinical experience from 146 958 pregnancies. Ultrasound in Obstetrics and Gynecology, 45(5):530–538, Apr 2015.

[243] Wei Zhang, Hong Cui, and Lee-Jun C. Wong. Application of next generation sequencing to molecular diagnosis of inherited diseases. Topics in Current Chemistry, page 19–45, 2012.

[244] Min Zhao, Qingguo Wang, Quan Wang, Peilin Jia, and Zhongming Zhao. Computational tools for copy number variation (cnv) detection using next-generation sequencing data: features and perspectives. BMC Bioinformatics, 14(Suppl 11):S1, 2013.

[245] Zongli Zheng, Matthew Liebers, Boryana Zhelyazkova, Yi Cao, Divya Panditi, Kerry D Lynch, Juxiang Chen, Hayley E Robinson, Hyo Sup Shim, Juliann Chmielecki, and et al. Anchored multiplex pcr for targeted next-generation sequencing. Nature Medicine, 20(12):1479–1484, Nov 2014.

[246] Bernhard Zimmermann, Matthew Hill, George Gemelos, Zachary Demko, Milena Banjevic, Johan Baner, Allison Ryan, Styrmir Sigurjonsson, Nikhil Chopra, Michael Dodd, and et al. Noninvasive prenatal aneuploidy testing of chromosomes 13, 18, 21, x, and y, using targeted sequencing of polymorphic loci. Prenatal Diagnosis, 32(13):1233–1241, Oct 2012.

List of Tables

List of Figures